EDGEWOOD
RESEARCH, DEVELOPMENT & ENGINEERING CENTER
U.S. ARMY SOLDIER AND BIOLOGICAL CHEMICAL COMMAND

ECBC-CR-050

EVALUATION OF THE EFFECT OF PARTICLE SIZE AND PARTICLE SENSING INSTRUMENTS ON THE MEASUREMENT OF MASK PROTECTION FACTORS

Kent C. Hofacre
Aaron W. Richardson

BATTELLE MEMORIAL INSTITUTE
Columbus, OH 43201-2693

June 2001

Battelle

Aberdeen Proving Ground, MD 21010-5424

Disclaimer

The findings in this report are not to be construed as an official Department of the Army position unless so designated by other authorizing documents.

REPORT DOCUMENTATION PAGE

Form Approved
OMB No. 0704-0188

1. AGENCY USE ONLY *(Leave Blank)*	2. REPORT DATE	3. REPORT TYPE AND DATES COVERED
	2001 June	Final; 95 Jun – 97 Aug

4. TITLE AND SUBTITLE

Evaluation of the Effect of Particle Size and Particle Sensing Instruments on the Measurement of Mask Protection Factors

5. FUNDING NUMBERS

C-SPO900-94-D-0002
TA-60
DO-38

6. AUTHOR(S)

Hofacre, Kent C., and Richardson, Aaron W.

7. PERFORMING ORGANIZATION NAME(S) AND ADDRESS(ES)

Battelle Memorial Institute, 505 King Avenue, Columbus, OH 43201-2693

8. PERFORMING ORGANIZATION REPORT NUMBER

ECBC-CR-050

9. SPONSORING/MONITORING AGENCY NAME(S) AND ADDRESS(ES)

DIR, ECBC,* ATTN: AMSSB-RT, APG, MD 21010-5424

10. SPONSORING/MONITORING AGENCY REPORT NUMBER

11. SUPPLEMENTARY NOTES

COR: Paul Gardner, AMSSB-RRT-PR (410) 436-6692

*When this work was conducted, the U.S. Army Edgewood Chemical Biological Center (ECBC) was known as the U.S. Army Edgewood Research, Development and Engineering Center (ERDEC).

12a. DISTRIBUTION/AVAILABILITY STATEMENT

Approved for public release; distribution is unlimited.

12b. DISTRIBUTION CODE

13. ABSTRACT *(Maximum 200 words)*

The current method used by the U.S. military to assess mask performance uses a polydisperse corn oil aerosol of 0.4 to 0.6 micron mass median aerodynamic diameter as a simulant challenge atmosphere. Data are presently lacking regarding the effect of particle size and aerosol sensing instruments on the measured protection factor (PF). Data are also lacking regarding the correlation of PFs measured using an insert aerosol challenge, such as the corn oil, with PFs measured using either a biological aerosol or vapor challenge. The objectives of this task were (1) to evaluate the effect of aerosol detection instruments and aerosol size on measured protection factor, (2) to assess whether inert aerosols are suitable for predicting respirator performance against surrogate biological aerosols, and (3) to assess whether an inert aerosol is a good indicator of respirator performance that is challenged with a vapor. The foremost finding in this study is that the corn oil/photometer test method is a good indicator of PFs that would be experienced by masks challenged with either similar sized aerosols or inert vapors. In addition, use of the corn oil/photometer method used to measure PFs is a conservative estimator of PFs that would be measured against a bioaerosol challenge with a particle size greater than 1 micron.

14. SUBJECT TERMS

Simulant challenge, Protection factor, Photometer, Particle size, Bioaerosol challenge, Aerosol detection, Corn oil

15. NUMBER OF PAGES

110

16. PRICE CODE

17. SECURITY CLASSIFICATION OF REPORT	18. SECURITY CLASSIFICATION OF THIS PAGE	19. SECURITY CLASSIFICATION OF ABSTRACT	20. LIMITATION OF ABSTRACT
UNCLASSIFIED	**UNCLASSIFIED**	**UNCLASSIFIED**	**UL**

NSN 7540-01-280-5500

Standard Form 298 (Rev. 2-89)
Prescribed by ANSI Std. Z39-18
298-102

Blank

EXECUTIVE SUMMARY

The current method adopted by the U.S. Military to assess mask performance uses a polydisperse corn oil aerosol of 0.4 to 0.6 μm mass median aerodynamic diameter as a simulant challenge atmosphere. Data are presently lacking regarding the effect of particle size and aerosol sensing instrument on the measured protection factor (PF). Data are also lacking regarding the correlation of PFs measured using an inert aerosol challenge, such as the corn oil, with PFs measured using a biological aerosol challenge or a vapor challenge. Because a polydisperse aerosol is used as the challenge for mask performance tests, data regarding whether the challenge aerosol is a suitable surrogate for other challenge aerosols of differing sizes and vapors is needed. The effect of particle size is important because bioaerosol threats are likely to be present on larger, polydisperse particulate matter rather than a submicron aerosol as corn oil. The correlation of measured PFs obtained for an aerosol challenge to vapor challenges is important because most chemical warfare threats remain as vapor challenges.

The objectives of the first phase of this task were to evaluate the effect of aerosol detection instruments and aerosol size on measured protection factor, and to assess whether inert aerosols are suitable for predicting respirator performance against surrogate biological aerosols. In the second phase of this study, the objective was to assess whether an inert aerosol is a good indicator of respirator performance that is challenged with a vapor.

PFs of a full facepiece air purifying respirator were measured using the aerosol challenges and aerosol sensing instruments given in Table 1.

Table 1. Aerosol Test Matrix

Aerosol Sensing Instrument	Challenge Aerosol				
	0.17 μm PSL	0.5 μm[a] Corn Oil	0.72 μm PSL	2.0 μm PSL	5.0 μm[a] Silica Powder
M41 (Model 8020M)	X	X	X	--[c]	--[c]
LAS-X	X	X	X	X	--[c]
Aerosizer™	--[c]	X	X	X[b]	X[b]
Laser Photometer (Model 8587)	X	X	X[b]	X[b,c]	--[c]

X = Tested with four controlled leak rates to achieve PFs ranging from 500 to 50,000.
(a) Nominal MMAD.
(b) Low challenge aerosol concentration limited measurement of upper range of PFs.
(c) No tests because of instrument limitations/appropriate operating range.

The mask was mounted to a headform and breathing was simulated at 0.9 ± 0.1 l/breath and 25 breaths/min. The mask was equipped with a fitting into which orifices of 50, 100, 200, and 400 μm diameter were inserted to permit controlled leakage into the mask, or the fitting could be capped to test the mask in a sealed condition. In addition to those aerosol challenges given in Table 1, PFs were measured using sulfur hexafluoride (SF_6) and isoamyl acetate (IAA) as vapor challenges. SF_6 represented an inert vapor that would not interact (e.g., absorb into the mask) with the test system, thus potentially biasing measured PFs. A total of about 425 PF measurements were made.

PF measurements were made by fixing the controlled leak condition and starting simulated breathing. A challenge atmosphere was then generated, and after at least 10 minutes of operation, the concentration of the aerosol or vapor challenge was measured. The aerosol or vapor concentration within the mask was then measured, followed by another measure of the challenge concentration. The ratio of challenge concentration to in-mask concentration was the PF.

The PFs measured using the various aerosol challenges and aerosol sensing instruments were analyzed to obtain correlation equations relating the measurement methods. Similarly, correlation equations were obtained to compare PFs measured using the inert aerosol and aerosol sensing instruments given in Table 1 with PFs measured using a bioaerosol challenge of Bg spores and a bioassay method (Hofacre and Forney, 1995), and with PFs measured using the vapor challenges.

The results indicated that there was no significant or practical difference in measured PFs using aerosol challenges between 0.17 and 0.72 μm. A significant effect on measured PFs was observed when the challenge aerosol size was greater than 2 μm. Typically, the measured PF was 2 to 4 times higher using the 2 μm challenge aerosol and at least 5 times higher using the 5 μm aerosol challenge compared to 0.17 to 0.72 μm challenge aerosols.

Little practical difference was observed in measured PFs for the different instruments at a fixed particle size. Statistically, the PFs measured by the various instruments frequently were different; however, the differences commonly varied by less than a factor of 2.

The PFs measured using the corn oil challenge and photometer were in very good agreement with PFs measured using similar sized inert aerosols and the M41 or LAS-X. The lowest PFs were typically measured using the corn oil aerosol and photometer method, consequently, that method represented the most stringent method regarding the measure of mask protection.

In a related study previously performed, PFs were measured using a nearly identical system and methods, and using Bg spore and 0.72 μm PSL aerosol challenges (Hofacre and Forney, 1995). Those PFs were also in excellent agreement with PFs measured using the inert aerosols. The best agreement between PFs measured using the Bg spore aerosol challenge and

the inert challenge aerosols was with the 2.0 μm PSL challenge and LAS-X. The equation correlating the PFs for those two methods is:
$\log_{10} PF_{Bg,bio} = 0.955 * \log_{10} PF_{2.0\ \mu m\ PSL,LAS\text{-}X} + 0.102$; $r^2 = 0.999$.

Comparison of the corn oil aerosol/photometer PFs to the Bg spore/bioassay method indicated they were in good agreement. The PFs measured using Bg spores and a bioassay counting technique were consistently, on average, ~ 2 times higher than the PFs measured using the corn oil and photometer approach. This is attributed, in part, to the known larger (> 1 μm) particle size of the Bg spore aerosol challenge. The equation correlating the measured PFs is given by: $\log_{10} PF_{Bg,bio} = 1.004 * \log_{10} PF_{CO,Photometer} + 0.177$; $r^2 = 0.997$. Therefore, the corn oil/photometer method is a conservative estimator of PFs measured using a bioaerosol challenge with particle size > 1 μm.

PFs measured using the SF_6 (an inert gas) challenge were in good agreement with the PFs measured using 0.72 μm PSL aerosols and a LAS-X. The equation correlating the PFs is given by: $\log_{10} PF_{SF6} = 0.995 * \log_{10} PF_{0.72\ \mu m\ PSL,LAS\text{-}X} + 0.116$; $r^2 = 0.993$. Significantly poorer agreement was obtained for PFs measured using IAA as a vapor challenge, which is attributed to IAA permeating the rubber of the mask and to surface effects (absorption/desorption) of IAA within the mask and/or test system.

Excellent agreement was observed between PFs measured using the corn oil/photometer method with the SF_6 vapor. The correlating equation is given by:
$\log_{10} PF_{SF6} = 0.996 * \log_{10} PF_{CO,\ Photometer} - 0.020$; $r^2 - 0.996$. Thus, the corn oil/photometer method is an excellent predictor of PFs measured using a vapor challenge.

The foremost finding in this study is that the corn oil/photometer test method is a good indicator of PFs that would be experienced by masks challenged with similar sized aerosols, or inert vapors. Furthermore, use of the corn oil/photometer method to measure PFs is a conservative estimator of PFs that would be measured against a bioaerosol challenge with a particle size greater than 1 μm.

Blank

PREFACE

The work described in this report was authorized under Contract No.: SPO900-94-D-0002, Task No. 60, and Delivery Order No. 38. This work was started in June 1995 and completed in August 1997.

The use of either trade or manufacturers' names in this report does not constitute an official endorsement of any commercial products. This report may not be cited for purposes of advertisement.

This report has been approved for public release. Registered users should request additional copies from the Defense Technical Information Center; unregistered users should direct such requests to the National Technical Information Service.

Acknowledgments

The authors would like to confer a special recognition to Paul Gardner from the U.S. Army Edgewood Chemical Biological Center, U.S. Army Soldier Biological Chemical Command, for his valuable expertise and input, which contributed to the successful conduct of this study.

Blank

CONTENTS

FIGURES

TABLES

EVALUATION OF THE EFFECT OF PARTICLE SIZE AND PARTICLE SENSING INSTRUMENTS ON THE MEASUREMENT OF MASK PROTECTION FACTORS

1.0 INTRODUCTION

1.1 Background

The U.S. Army Edgewood Research, Development and Engineering Center (ERDEC) currently employs a U.S. joint military service standardized method for assessing respirator performance against chemical threats (U.S. DoD, 1992). The method uses a polydispersed corn oil aerosol as the simulant challenge. Data are currently lacking to support the use of the corn oil aerosol as a suitable substitute for predicting respirator performance against bioaerosol challenges. The principal data that are lacking are the effect of particle size and the effect of aerosol sensing instrumentation used to measure the protection factor (PF). Bioaerosol challenges can have particle sizes that range from submicron (viruses) to several microns (bacteria). Since the protection provided by a mask is a function of particle size, it is currently unknown how well the PF measured against the polydisperse corn oil aerosol predicts the mask performance against an aerosol challenge of a different particle size distribution. Also, the aerosol sensing instrumentation used to measure aerosol concentrations may affect the measured PF because of particle size sensitivity and measurement technique.

Few data also exist regarding the correlation of PFs measured using an aerosol challenge with those measured using a gas or vapor challenge. It is not well established whether leakage measured by use of a test aerosol is representative of that of a gas. It is thought that PFs measured using a challenge aerosol may be an overestimate of mask performance because the in-mask aerosol concentration is underestimated. Causes for underestimating in-mask concentration are believed to be due to deposition of aerosol within the mask or respiratory tract of the wearer and due to inefficient sampling of the aerosol.

1.2 Objectives

The objectives of the first phase of this task were to evaluate the effect of aerosol detection instruments and aerosol size on measured protection factor, and to assess whether inert aerosols are suitable for predicting respirator performance against surrogate biological aerosols. In the second phase of this study, the objective was to assess whether an inert aerosol is a good indicator of respirator performance against vapor challenges.

1.3 Scope

The work reported here describes the test system, test aerosols and vapors, aerosol classifying instruments, vapor monitoring systems, and experimental method. Results from this study were compared to results of another study (Hofacre and Forney, 1995) to correlate PFs using inert aerosols to PFs measured using a biological aerosol and bioassay counting technique. The effect of challenge aerosol particle size and sensing instrument on measured PF was assessed. Also, the correlation of PFs measured using an inert aerosol with vapor challenges was made.

2.0 TECHNICAL APPROACH

2.1 Test Design

2.1.1 Test Requirements/Parameters

A full facepiece air-purifying respirator was used in this study. The mask was placed on a test head that was connected to a breathing machine, which simulated respiration. The respiration rate was 25 breaths/min and the tidal volume was 0.9 $\pm$ 0.1 L/breath, which corresponded to a volumetric flow rate of 23 $\pm$ 2.3 L/min. Both the respiration rate and tidal volume, which corresponded to a low to moderate breathing rate (SAE, 1987), were maintained at the stated conditions for all tests.

There was no control of the environmental conditions; temperature was (ambient) 22 $\pm$ 3°C. The challenge aerosol concentration varied depending on the aerosol type being used, and, when possible, was controlled to ensure that a PF of at least 50,000 was measurable. Likewise, the vapor challenge concentration was controlled to ensure that PFs of at least 50,000 could be measured.

2.1.2 Aerosol Test Matrix

The aerosol test matrix completed for this study is provided in Table 1. Four aerosol sensing instruments were used to measure the challenge and in-mask aerosol concentration, which was then used to calculate the PF. The four aerosol sensing instruments represented a broad range of particle counting and sizing techniques, all of which have previously been used to measure PFs.

Table 1. Aerosol Test Matrix

Aerosol Sensing Instrument	Challenge Aerosol				
	0.17 μm PSL	0.5 μm[a] Corn Oil	0.72 μm PSL	2.0 μm PSL	5.0 μm[a] Silica Powder
M41 (Model 8020M)	X	X	X	--[c]	--[c]
LAS-X	X	X	X	X	--[c]
Aerosizer™	--[c]	X	X	X[b]	X[b]
Laser Photometer (Model 8587)	X	X	X[b]	X[b,c]	--[c]

X = Tested with four controlled leak rates to achieve PFs ranging from 500 to 50,000.
(a) Nominal MMAD.
(b) Low challenge aerosol concentration limited measurement of upper range of PFs.
(c) No tests because of instrument limitations/appropriate operating range.

Five different aerosol sizes were used as the challenge (test) aerosols. Three of the aerosols were generated using polystyrene latex (PSL, Duke Scientific Corp., Palo Alto, CA) spheres with nominal diameters of 0.17, 0.72, and 2.0 μm. The fourth aerosol was a polydisperse corn oil with a nominal mass median aerodynamic diameter (MMAD) of 0.4 to 0.6 μm, which is currently used by ERDEC as the test aerosol for fit factor testing of masks using human subjects (U.S. DoD, 1992). Using the LAS-X number distribution to calculate a mass distribution, the MMD of the corn oil aerosol as indicated by the LAS-X was 0.35 μm with a geometric standard deviation of 1.7. The final aerosol challenge used was a polydisperse silica powder with a MMAD of ~5.0 μm. The particle sizes given in the test matrix are nominal target particle sizes. The corn oil and silica powder aerosols were polydisperse aerosols, so the target particle size for these test aerosols was a MMAD, and the geometric standard deviation was less than 2.5.

The 0.17 μm PSL represented particles which could be a viral threat. The 0.72 μm PSL particles were intended to be representative of single bacterium or agglomerates of viruses. The 2.0 and 5.0 μm test aerosols were intended to represent agglomerate and/or large bacteria bioaerosol challenges. The range of particle sizes was intended to permit the measure

of particle size dependency on PFs and cover the range of bioaerosol challenge sizes that may be experienced.

Within each cell of the test matrix, tests were performed with the mask sealed and with a leak created by either a 50, 100, 200, or 400 μm orifice. The orifices were selected so that PFs ranging between 500 and 50,000 were achieved. Previous PF measurements using a similar test system and method indicate that PFs of approximately 500, 2,000, 10,000, and 32,000 would be measured using the 400, 200, 100, and 50 μm orifices to control leakage (Hofacre and Forney, 1995). Five PF measurements for each block of the matrix were completed.

It is important to note that it was difficult to generate the high challenge concentrations of 2.0 and 5.0 μm particles that were required to measure PFs $>10{,}000$. Using a 2.0 μm PSL challenge, it was only possible to measure PFs using the 100, 200, and 400 μm orifices for controlled leaks. Using a 5.0 μm powder challenge, it was only possible to measure a PF using the 400 μm orifice for the controlled leak.

2.1.3 Vapor Test Matrix

In the second phase of this study, PFs were measured using vapor challenges of sulfur hexafluoride (SF_6) and isoamyl acetate (IAA). Each vapor challenge was generated separately for independent PF tests. PF tests using the vapor challenge were conducted in series with tests using the 0.72 μm PSL aerosol challenge.

As in the aerosol test matrix described above, PFs were measured at the same four controlled leak rates and with the mask sealed (no controlled leak). Challenge concentrations were generated to permit measurement of PFs greater than 50,000.

2.2 Aerosol Test Apparatus

2.2.1 Aerosol Test System Description

The test apparatus used to measure PFs of the mask using the aerosol challenges is illustrated in Figure 1. This apparatus was nearly identical to the apparatus used to measure PFs in a prior study (Hofacre and Forney, 1995). In that study, the PFs of an another full facepiece mask were measured using the LAS-X with a 0.72 μm PSL challenge and using a bioassay technique to measure Bg spore aerosol concentration. The test apparatus comprised: an aerosol generator, an aerosol classifier/sampler, a chamber, a breathing machine, a headform, and a mask. The aerosol generator and aerosol classifier/sampler were not specific and depended on the type and size of aerosol used as the challenge. Details regarding the aerosol generators and classifiers are discussed in Section 2.2.2 and 2.2.4.

The schematic depicts a nebulizer used for PSL sphere generation. With this generation scheme, the aerosol passed through a charge neutralizer and mixed with clean dilution air. The aerosol was then transported to the test chamber where it dispersed to form the challenge atmosphere. Because clean air was continuously introduced into the chamber by exhalation, mixing fans were located within the 60 x 53 x 43 cm chamber to ensure a well mixed challenge atmosphere was maintained. All aerosol generators delivered a continuous flow of 35 to 50 lpm of aerosol laden air to the chamber to further ensure that a fresh, stable challenge aerosol was maintained. When corn oil or silica powder was used as the challenge aerosol, the nebulizer and charge neutralizer was replaced with the appropriate generator and all other components remained the same. Excess airflow was vented from the top of the chamber through HEPA filters.

The test chamber contained the challenge atmosphere and housed the headform, onto which a mask was affixed. The headform was mounted on the bottom of the chamber. The headform had a rubber bladder that was inflated to 60 in H_2O to effect a seal between the mask and head form. The bladder was never deflated after a sealed mask was obtained, to

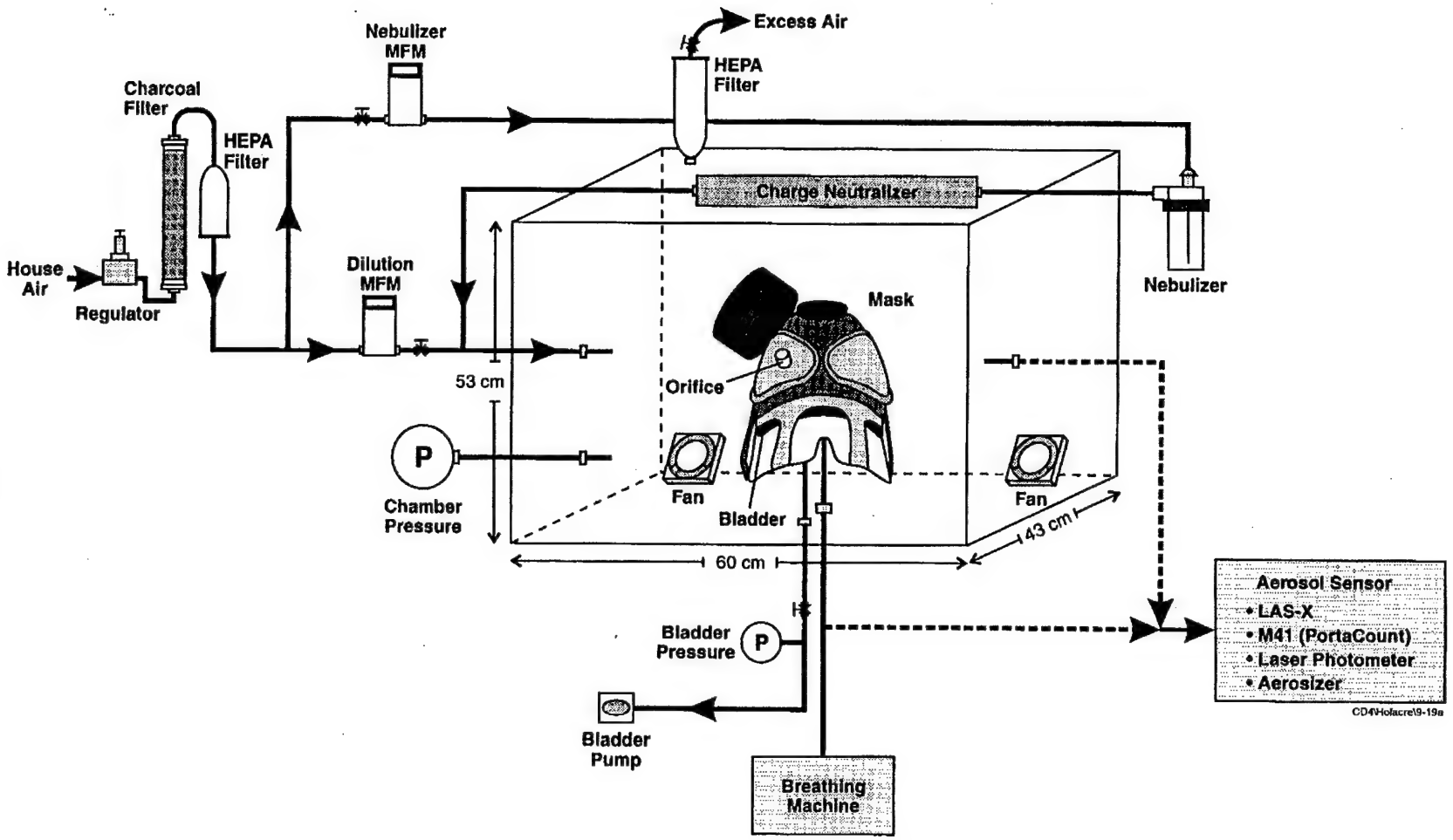

Figure 1. Schematic of the Test Apparatus Used to Measure Mask PFs Challenged with Aerosols

minimize possible leakage at the head form/mask seal. The "throat" of the headform was a 2.5-cm diameter stainless steel tube from the "mouth" which connected to the breathing machine via flexible tubing. The throat was equipped with a sampling port to collect aerosol samples within the mask. The breathing machine, a Battelle fabricated machine, was of a piston/cylinder design. The stroke length was set to produce a tidal volume of 0.9 $\pm$ 0.1 lpm and the stroke rate was adjusted such that the breathing rate was 25 breaths/min.

The mask had a bulkhead (Swagelok®) fitting inserted in the center of the left eye lens (same side as that of the filter canister). A metal disk with a small aperture (orifice) was inserted into the bulkhead fitting to create a leak into the mask. The fitting was capped to test the mask in its "sealed" (best fit) condition. The orifices provided a controllable, reproducible leak so that the PF of the mask was varied in a controlled fashion. Orifices were used as the leak path because they minimize losses of the aerosol due to transport and inlet effects, which are associated with capillaries used as leak paths.

2.2.2 Aerosol Generation

The challenge aerosol generation technique depended on the type of aerosol being produced. The PSL particles were aerosolized using an Airlife® nebulizer. Corn oil aerosol was generated using ERDEC's generator without modification. The ~5 μm silica particles were generated using a pneumatic dust feeder. The aerosol generators were evaluated for each particle size being generated to determine suitable operating conditions that allowed for the challenge concentration to be adequate to calculate PFs $>$50,000. For challenge aerosols greater than 1 μm, the maximum possible challenge concentration was generated to maximize the PF that could be measured. Representative aerosol size distributions and challenge concentrations for each test aerosol are presented in Appendix A.

Suspensions of monodisperse PSL spheres were prepared in deionized water. The deionized water was filtered prior to use with 0.05 μm pore Nuclepore® filters. Suspension concentrations were varied such that the nebulizer could produce an adequate aerosol concentration to measure PFs $>$50,000, as determined by the LAS-X. However, as stated in

Section 2.1.2, it was difficult to generate the high concentrations of 2.0 μm particles needed to measure PFs > 10,000. The 0.17 μm PSL suspension contained 0.1 ml of concentrate in 200 ml of filtered, deionized water. The 0.72 μm PSL suspension contained 5 ml of concentrate per 200 ml of water, and the 2.0 μm suspension contained 10 ml of concentrate per 200 ml of water. The PSL suspension concentrate contained ~10 percent solids. The nebulizer was operated at 40 psig which produced a flow rate of 17 lpm. The aerosol passed through a charge neutralizer (Model 3012, TSI Inc., St. Paul, MN), which was heated to facilitate evaporation of the water droplets. After passing through the neutralizer, 17 lpm of filtered air mixed with the aerosol-laden stream to prevent water vapor from condensing on the PSL spheres.

The corn oil generator was operated such that the MMAD of the particle size distribution was between 0.4 and 0.6 μm, and the geometric standard deviation was less than 2.5. Those characteristics of the corn oil aerosol challenge were consistent with those used by ERDEC in the human subjects test and the requirements of the United States Joint Service Standardization Agreement for Fit Factor Testing of Military Masks (U.S. DoD, 1992). The modified Laskin nozzle design that is used in ERDEC's corn oil aerosol generator was used. The operating pressure was 20 psig. The mass rate of aerosol generation was excessive for the low flow system used. Therefore, the output from the generator was split and a portion diluted with filtered air in a small chamber.

The silica powder used was Syloid 244™ (WR Grace Corp., Baltimore, MD) which has an average particle size of 6.0 μm, as reported by the manufacturer. The silica was dispersed using a pneumatic dust feeder (Model MF2, MDA Scientific Inc., Glenview, IL) and passed through a cyclone to remove large agglomerates. Results showed the desired particle size could be generated; however, the particle concentration was not adequate to measure PFs >10,000.

2.2.3 Aerosol Sampling

The aerosol sampling technique depended on the instrument used to classify the aerosol. The challenge sampling probe was either a 0.2 or 0.4 cm ID stainless steel tubing that extended

15 cm beyond the chamber wall. The sampling rate and probe depended on the instrument being used for the analysis. The LAS-X sampled at a flow rate of 0.1 lpm, the photometer 2 lpm, the Aerosizer® 2 lpm, and the M41 0.7 lpm. Sampling probe diameters were varied to reduce the difference in inlet velocity between different instruments. The LAS-X and M41 sampled through a ~0.2 cm ID stainless steel probe; the photometer and Aerosizer® sampled through the 0.4 cm ID probe.

The in-mask aerosol concentration was sampled from the "throat" of the test fixture. The "throat" being the 2.5 cm ID tubing that connected the breathing machine to the headform. The sampling probe entered through a tee and had a 90° bend so the probe inlet was parallel to the "throat" along its centerline. The sampling probe diameter was the same as that used for sampling the challenge. The length of all sampling lines was as short as possible to minimize transport losses. The sample lines used for in-mask and challenge samples were either the same or of matched length.

2.2.4 Aerosol Classification

Four types of aerosol sensing instruments: Aerosizer™, LAS-X, M41 and a laser photometer, were used to classify the challenge and in-mask aerosol to measure PFs as shown in the test matrix.

The Aerosizer™ (Amherst Process Instruments, Hadley, MA) classifies particles based on their aerodynamic behavior. The instrument measures the time-of-flight as particles are accelerated through the sensing zone of the instrument. The time-of-flight is then in proportion to particle size and density. The density of the aerosol material is then used to determine the particle size distribution either on a number, surface, or volume (mass) basis. The Aerosizer™ can classify particles ranging from 0.5 to 200 μm. Data reducing software that accompanies the instrument permits user selected size ranges to be analyzed. Thus, polydisperse aerosols, especially the 5 μm challenge, were analyzed within selected size ranges. For this study, the particle size range of 4 to 6 μm was used.

The LAS-X is a laser aerosol spectrometer (Particle Measuring Systems, Boulder, CO) which classifies particles from 0.09 to 3.0 μm. The LAS-X provides a measure of the particle

size based on the light scattering properties of the aerosol. Particles are focused into the sensing region by the pneumatic system such that particles pass through one at a time. The light from a He-Ne laser is scattered by the particle, which is then collected by receiving optics. The signal intensity produced is proportional to the particle size, and the number of signals is a measure of the number of particles counted, which is processed into 16 size specific channels. Thus, the LAS-X gives a number distribution of the aerosol and size specific channels of interest can be selected for data analysis. This was important when polydisperse aerosols were used as the test aerosol because the target particle size of interest was selected for data analysis.

The M41 mask tester is commercially known as the PORTACOUNT™ Plus (Model 8020M; TSI Inc., St. Paul, MN), and is a condensation nucleus counter (CNC). Aerosol enters the M41 into a chamber of saturated isopropanol vapor, which then condenses onto the particle. The particles then "grow" to ~10 μm and pass through the sensor region one at a time. The particles scatter light and each pulse of light scattered is a measurement of the number of particles. Thus, the M41 can provide only a number concentration of the aerosol, and no information about particle size. The largest particle size that can be used with a M41 is ~5 μm; the M41 can detect particles as small as 10 nm.

The laser photometer is a Model 8587 (TSI Inc., St. Paul, MN) instrument. Aerosol enters into the sensing chamber and a laser passes through the chamber. The intensity of the total light scattered by the aerosol cloud is measured. The intensity of the light scattered is a function of particle concentration and particle size. Because the total light scatter of an aerosol cloud is measured, the photometer provides no direct information of particle size or concentration. Discussions with technical representatives of TSI indicated that the photometer has been designed for use with ~0.3 μm particles (Beck, 1996). The photometer is used for aerosol penetration testing of filters using 0.3 μm particles. The photometer was not used with the 5.0 μm particles because it is not designed for use with particles of that size.

2.2.5 Aerosol System Characterization

Shakedown tests of the system were conducted to characterize the system and establish proper operating conditions. First, the system was operated to ensure the mask was well sealed and that results similar to previous mask studies could be duplicated. These tests were conducted by donning the mask onto the test head and initiating simulated breathing. The seal of the mask was demonstrated by capping the bulkhead fitting so there was no controlled leakage into the mask. The PF was measured using the LAS-X and a 0.72 μm aerosol challenge. The mask was considered sealed if a PF of greater than 50,000 was obtained. The only manipulation of the mask after it was sealed was to change the orifices. This could be performed with little stress applied to the mask/head form seal; therefore, changing of the orifices did not create uncontrolled leaks at the mask/head form interface.

A leakage test was conducted of the entire system (inside and outside of test chamber) by locally exposing the system to 0.17 μm PSL and monitoring the in-mask concentration with the LAS-X. A sudden spike in the in-mask concentration would indicate the location of a leak. This test indicated no leakage into the system. A test was then performed to determine whether particles were being generated in the system. A PF test was performed using both the M41 and LAS-X with a HEPA filtered air challenge or 'zero' challenge. A 'zero' challenge consisted of fewer than 50 total counts as measured by the LAS-X. Since it had been verified there was no leakage into the mask and the challenge concentration was "zero", it was concluded the in-mask particle concentration was due to particle generation within the system. This was classified as a background and subtracted from in-mask concentrations in the calculation of the PF. The effect on PF calculations is discussed in Section 2.5.1.

Tests were performed to characterize aerosol challenge concentrations and size distribution. The ~0.5 μm corn oil challenge was generated with ERDEC's generator, without modification. The generator was operated at a pressure of 20 psig. The output of the generator was so large that a portion was vented and the remainder transported to the test chamber. Since the four aerosol sensing instruments rely on different operating principles to

classify the aerosol, different corn oil aerosol challenge concentrations were used, depending on the instrument being used. The photometer required a relatively high aerosol concentration to accurately measure the PF. For this reason, the photometer reading was maintained ~ 0.5 V when monitoring the challenge. However, the LAS-X, M41, and Aerosizer could not properly count and/or size at such a high concentration. The challenge was reduced to a photometer reading of 0.1 V when the M41 and Aerosizer™ were used to determine PFs. PF tests using the LAS-X were initially conducted with an aerosol at a challenge corresponding to a photometer reading of 0.01 V. However, it was noted the resulting PFs were significantly lower than those measured by the other instruments. To determine the LAS-X was properly counting the challenge aerosol, PF tests were performed with a decreased challenge concentration (photometer reading of 0.005 V). The resulting PFs increased and more resembled PFs measured by other instruments. Further reduction of the challenge did not lead to larger PFs; therefore, the LAS-X was considered to be counting particles properly.

It is important to note the operating conditions of the corn oil aerosol generator were not changed (the operating air pressure and airflow rate were constant) for all tests, only the amount of aerosol fed to the test chamber is varied. The aerosol size distribution was therefore assumed to remain unchanged, even though the concentration did change.

2.3 Vapor Test Apparatus

2.3.1 Vapor Test System Description

The test apparatus used to measure PFs with a SF_6 challenge is illustrated in Figure 2. This apparatus is very similar to that used for the aerosol tests, except the challenge vapor system, air sampling system, and location of the filter canister were modified. The basic test system remained unchanged, however. To ensure that SF_6 did not penetrate the filter,

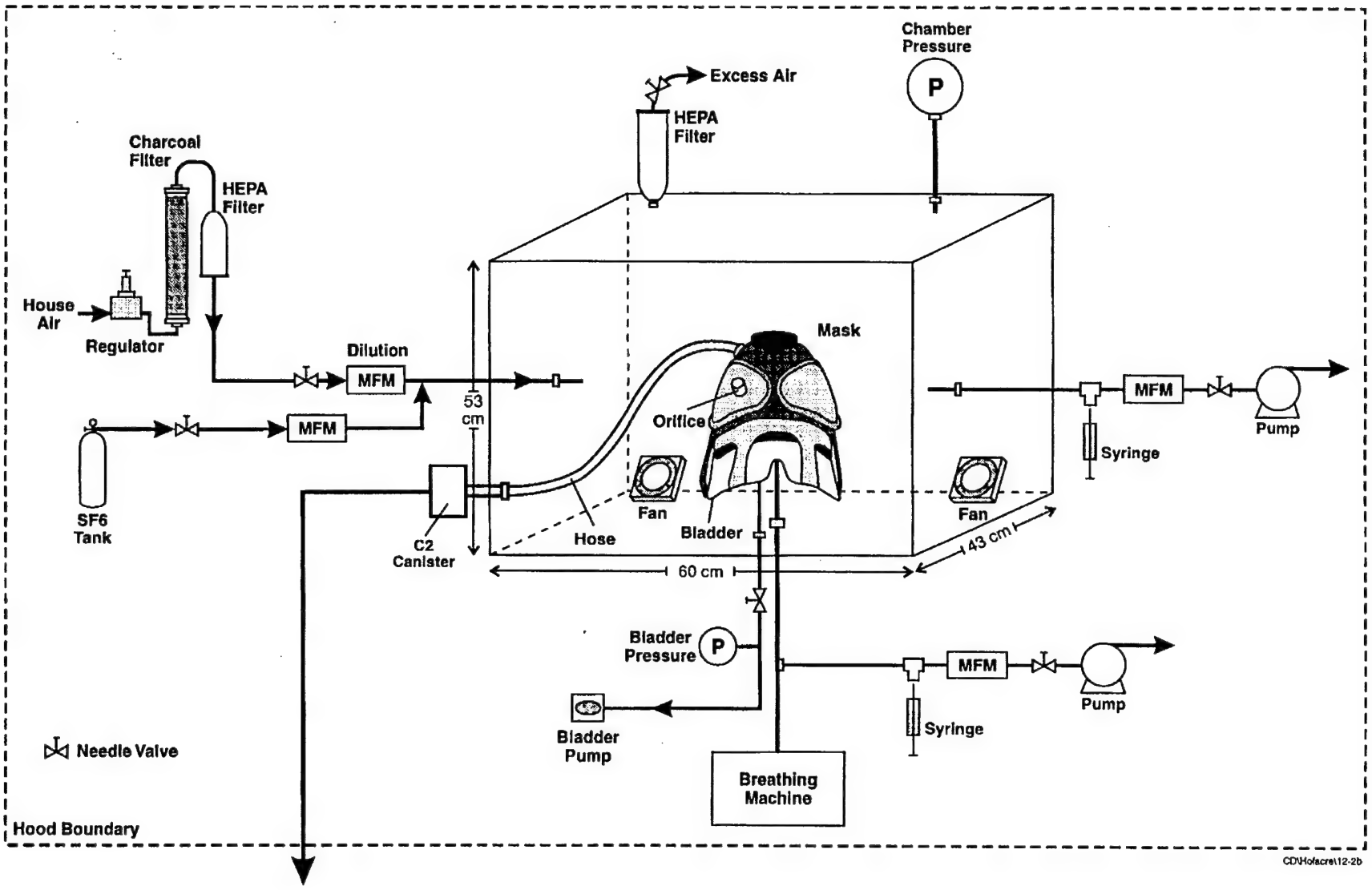

Figure 2. Schematic of the Test Apparatus Used to Measure Mask PFs Challenged with SF_6

room air entered the filter canister through a 1-in-diameter hose that extended approximately 5 feet away from the hood. Also, the filter canister was mounted remotely by connecting a hose from the mask to the filter canister located outside of the test chamber. This configuration was used for all tests with vapor challenges and with the corresponding 0.72 μm PSL tests. Although the placement of the filter outside the chamber was not required for the aerosol tests, it was unchanged to ensure that it would not affect measured PFs.

2.3.2 SF_6 Vapor Generation

The SF_6 challenge was generated by releasing a controlled flow from a compressed cylinder containing 1.5 percent SF_6 in air and diluting by 30 lpm (plus ~ 25 lpm of clean, exhaled air) of filtered house air prior to entering the test chamber. The SF_6 challenge concentration was adjusted to ensure an adequate concentration of SF_6 in the mask for direct measurement. The challenge concentration was determined based on the optimal detection range of the GC and the approximate PF expected for the selected leak condition. The challenge concentration was typically 150 to 250 ppm for the sealed, 50, and 100 μm leak rates and 50 to 60 ppm for the 200 and 400 μm leak rates. The concentration was controlled by the rate at which SF_6 was bled from the compressed cylinder. SF_6 was released at a flow rate of 0.3 lpm to generate a 150 to 250 ppm challenge and 0.1 lpm to generate a 60 ppm challenge. The SF_6 was introduced into the test chamber through the same inlet as the aerosol. The challenge was given at least 10 minutes to reach steady state before samples were obtained.

2.3.3 SF_6 Vapor Monitoring

The SF_6 challenge was sampled through a 0.4 cm ID stainless steel tube which extended 10 cm beyond the chamber wall. Initially, multiple sampling locations were used to verify the chamber was well mixed. The SF_6 concentrations measured at all locations were within 10 percent. A pump pulled 250 cc/min through the sampling probe to ensure the sample was representative of the challenge. A 10 cc challenge sample was collected from the probe using

a syringe, and then injected into a Tedlar bag containing 1000 cc of clean air. This diluted sample (by a factor of 1000) was then injected into the GC to quantify the challenge concentration. Two challenge samples were obtained at five minute intervals after the system had reached steady state (after at least 10 min of operation) and while the in-mask air samples were collected.

The in-mask SF_6 concentration was measured by sampling directly from the throat of the test head. The sample was collected using a 60 cc syringe. A pump pulled 250 cc/min through the throat port to ensure a representative sample was collected. A sample was obtained prior to each SF_6 test to verify no residual SF_6 in the mask. When the SF_6 challenge had reached steady state, two in-mask samples were taken separated by five minutes. A sample of the air supplied to the filter canister was also collected to verify there was no uncontrolled SF_6 penetrating into the mask through the filter.

The SF_6 challenge and in-mask concentrations were measured using a gas chromatograph (GC) with an electron capture detector (ECD). Both pairs of challenge and in-mask samples were analyzed. The average challenge and in-mask concentrations were used to calculate the PF. The results were analyzed to identify any potential significant variations in challenge ($\pm$ 20%) and to ensure consistent results.

2.3.4 IAA Generation/Monitoring

The test apparatus used to measure PFs with a vapor challenge of isoamyl acetate (IAA) is illustrated in Figure 3. This test apparatus is the same as the depicted for SF_6 in Figure 2, except that a different vapor generation and monitor system are needed.

The vapor challenge was generated by sparging 2 lpm of filtered house air through IAA liquid. The vapor generator temperature was 20°C. The vapor stream exiting the generator entered a "trap" where entrained liquid and any condensate was removed. The vapor stream was diluted with 28 lpm of filtered house air prior to entering the test chamber. The challenge

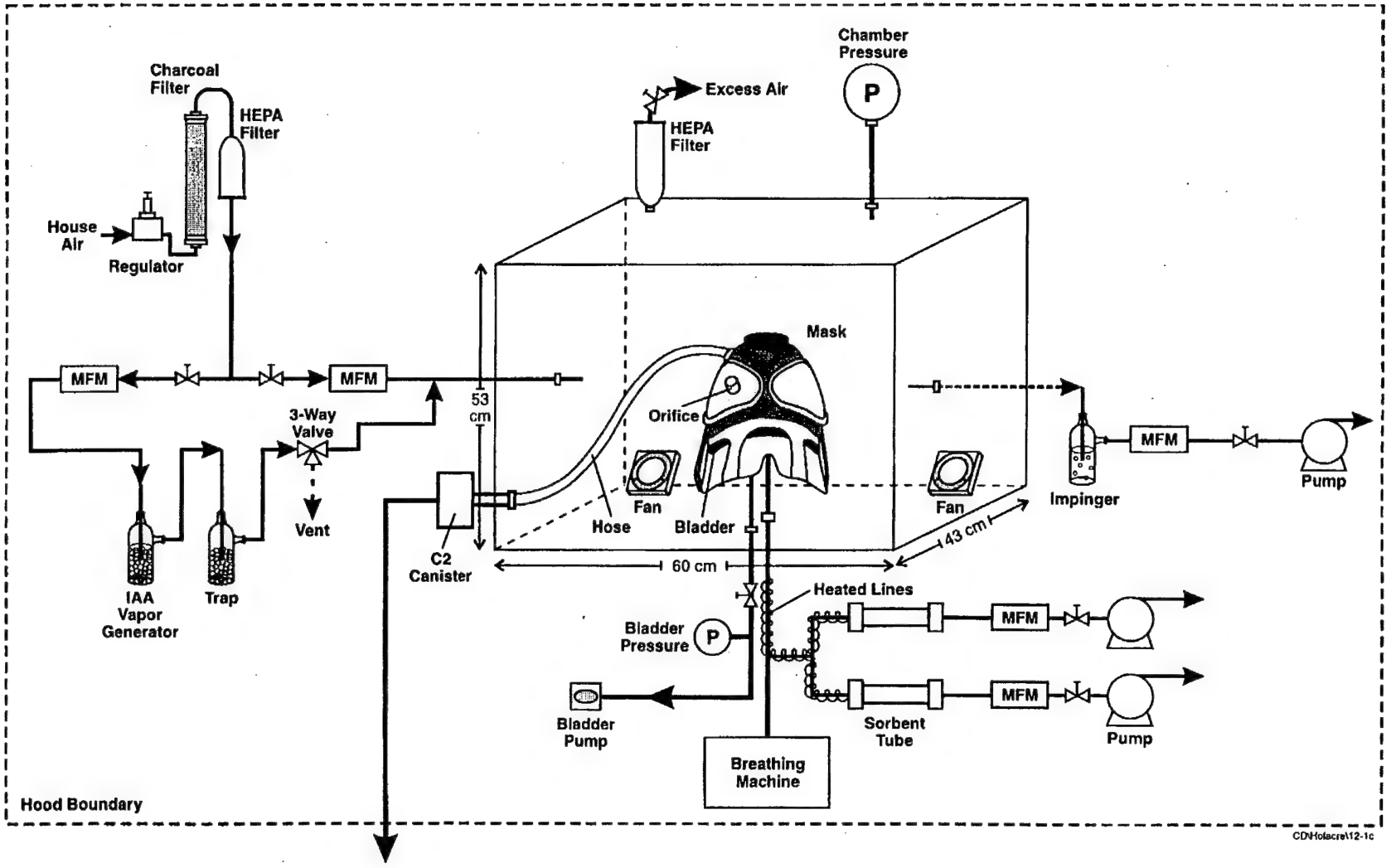

Figure 3. Schematic of the Test Apparatus Used to Measure Mask PFs Challenged With IAA

atmosphere was sampled through the same port as SF_6; however, the challenge was collected using an impinger filled with 10 ml of ethanol. A pump was used to pull 250 cc/min through the impinger. Two consecutive 10 min challenge samples were collected per test, after 15 min of challenge generation. Typical challenge concentrations were 750 - 1000 mg/m^3, which agreed well with predicted concentration of ~ 1000 mg/m^3.

The air inside the mask was sampled from the throat with Tenax sorbent tubes. Two in-mask samples were collected in parallel for each test. The sampling line was heated to 40°C to reduce any IAA adsorption on the sampling lines. A sample from the throat was collected prior to each IAA test for an in-mask background. This background was subtracted from in-mask samples to determine the actual amount of IAA in the mask due to leakage. In-mask sample duration and flow rate were selected to ensure the IAA collected was within the operating range of the GC. Lower sampling flows and shorter sampling durations were used when low PFs were expected to ensure that the mass of IAA collected on the sorbent tubes did not saturate the GC detector. In-mask sample collection was initiated 15 minutes after start up of the vapor generator. Table 2 lists flow rates and sampling duration for each of the leak rates.

Table 2. IAA Challenge and In-Mask Sampling Flow Rates and Durations

	Background		In-mask Sample	
Leak Rate	Flow (cc/min)	Duration (min)	Flow (cc/min)	Duration (min)
sealed	1000	15	1000	15
50 mm	1000	10	1000	10
100 mm	1000	5	500	5
200 mm	500	10	500	5
400 mm	500	5	250	5

The IAA collected in the challenge and in-mask samples was quantified using a GC with flame ionization detection (FID). Liquid samples of the challenge were injected directly into the GC. Samples collected on sorbent tubes were thermally desorbed and automatically

injected into the GC. When analyzing the IAA samples, both pairs of sorbent tubes and challenge samples were analyzed. Average challenge and in-mask concentrations were used to calculate PFs.

2.4 PF Measurement Test Procedure

2.4.1 Aerosol Tests

With the mask donned to the headform and an effective seal demonstrated, testing commenced. The general test procedure, regardless of type of aerosol, was conducted as follows.

The specified orifice was placed in the bulkhead fitting and the specified aerosol generator and classifier were connected to the test chamber. (The order of orifice selected and of aerosol sensing instrument used was random and is discussed later in this section.) The breathing machine was started. The challenge aerosol generator was started and permitted to operate ~15 min to allow the aerosol to reach a steady state concentration.

When steady state was reached, a sample of the challenge aerosol was collected for 2 min. A purge sample was then recorded if testing with either the photometer or Aerosizer™. This was accomplished by operating the photometer in the 'purge' mode and by sampling through a HEPA filter with the Aerosizer™. Next, the sampling line was switched to sample within the mask. Adequate time (2 to 5 min, depending on the aerosol concentration) was given to allow the instrument response to stabilize. In mask sample durations were varied to provide adequate time for the different instruments to count a sufficient number of particles within the mask. The M41 sampled for 5 min and collected concentrations based on 15 sec averages. Data were recorded electronically. The photometer sampled for 5 min and the response was captured on a strip chart recorder. The LAS-X sample duration for the sealed and 50 μm orifice was 5 min with three consecutive samples collected over a 15-min sampling period. For the 100, 200, and 400 μm orifices, LAS-X sample duration was 1 min with five consecutive samples. Three consecutive 1-min sampling durations were recorded by the

Aerosizer™. A second sample of the challenge aerosol was then recorded after sampling in-mask. If the two challenge samples were not within 20 percent of each other, the test was voided because the challenge aerosol was not stable. After sampling with the specified instruments, the aerosol generated was stopped and the system flushed with clean air for 5 min.

To reduce the potential of disturbing the system, the changing of orifices was minimized. With a fixed leak rate, the aerosol challenge was selected and each aerosol classifying instrument used with the selected test aerosol was used prior to shutdown of the aerosol generator. The test aerosol was then changed and the procedure was repeated. After all test aerosols had been used, the orifice was changed and testing continued. When the LAS-X was one of the instruments to be used, it was used first and its results used as an indicator of how well the system was operating. If an unexpected result was obtained using the LAS-X, it could have been an indication that there was a problem with the system. Tests with the 0.17, 0.5, 0.72 μm PSL aerosol challenges were performed in the same trials. Tests using the 2.0 μm PSL aerosol challenge were conducted separately due to difficulties in obtaining high challenge concentrations. Syloid tests were conducted last due to the possibility of fouling the system. The order of leak rates was random. The order of aerosol sensing instrument was random, except for the LAS-X as discussed.

2.4.2 Vapor Tests

The same basic test procedure as described for the aerosol tests in Section 2.4.1 was followed. The same orifices were used for controlled leaks and the same breathing conditions were simulated. For a given leak condition, tests were performed as a group. In that manner, each of the three challenges (0.72 μm PSL, IAA, and SF_6) were used to measure PFs without disturbing the mask fit or controlled leak. The resulting PFs could therefore be treated as matched pairs for analyses. Although not possible for the sealed condition, because of vapor permeation resulting in high backgrounds, all PFs were measured for a given leak condition

before proceeding to the next leak condition. The orifice was removed and replaced into its fitting after each test.

The general procedure executed was to install the selected orifice for the controlled leak. The PF was then measured using 0.72 μm PSL aerosol challenge and LAS-X to measured aerosol concentration. This ensured that the system was operating properly as the aerosol PFs were very consistent.

After the aerosol tests, the chamber was flushed and the SF_6 generation and monitoring equipment was installed. With the clean air challenge, the in-mask SF_6 background was measured along with the air at the filter canister inlet. These measurements ensured that no residual SF_6 was present in the mask. The SF_6 challenge was then generated, and after 15 min (aerosol test demonstrated that the chamber challenge concentration reach steady state within 10 min), the in-mask and challenge samples were collected as previously described.

The test system was then flushed with clean air and fitted with the IAA vapor generation and monitoring equipment. Background IAA concentration within the mask was measured with a clean air challenge (the orifice was capped to ensure no leakage into the mask during the background measurements.) The IAA challenge was generated, and after 15 min, the challenge and in-mask air samples collected.

The orifice was removed and replaced in the system and the entire procedure repeated.

2.5 Data Analysis

2.5.1 Calculation of PFs

The PF is the ratio of the challenge aerosol concentration (C_{chal}) to the in-mask aerosol concentration (C_{mask}):

$$PF = \frac{C_{chal}}{C_{mask}}$$

The concentrations were the average concentrations measured by each instrument or method. The challenge concentration was the average of the challenge measurements made before and after the in-mask sample. The number concentration was used for calculation of the

PFs when the M41, LAS-X, and Aerosizer™ were used, mass concentration was used for IAA, and molar concentration was used for SF_6.

The LAS-X indicates the number of particles in 16 size specific channels, over a range from 0.09 to 3.0 μm. Thus, the LAS permitted the particle number concentration to be determined within a selected size range and the other channels excluded. The three consecutive channels with the largest particle counts were used to determine the aerosol number concentration. For example, channels with midpoint diameters of 0.13, 0.18, and 0.23 μm were used to determine the 0.17 μm PSL concentration. The aerosol concentration was calculated by summing the number of particles in the selected size range and dividing by the volume of air sampled (the product of sampling flow rate and sampling duration).

The Aerosizer™ also indicates the number of particles in size specific channels. The size range of interest varied depending on the particle size. For the 0.72 μm PSL trials, the upper and lower size limits were $\pm$0.1 μm from the peak. For the 2.04 μm PSL, the selected size range was $\pm$0.2 μm from the peak. The size range 0.4 to 1.4 μm was used for the 0.5 μm corn oil because the peak was not well defined. The 0.5 μm corn oil was near the 0.4 μm lower size limit of the Aerosizer's detection capabilities. The size range selected for the 5.0 μm powder was 4.0 to 6.0 μm. By selecting those ranges for PF calculation, typically more than 90 percent of the particles counted were used in the calculation.

Instrument backgrounds were subtracted from in-mask concentrations obtained from the Aerosizer™ and photometer. These corrected responses were then used to calculate the PF. Instrument backgrounds had negligible effect on challenge concentrations. When the Aerosizer™ was used, a background was recorded during each PF test by sampling through a HEPA filter (done after sampling challenge and prior to sampling in-mask). When the photometer was used, the instrument's background was measured while operating in the 'purge' mode. The purge measurement set a limit on the maximum PF obtainable. This limit was determined by defining the minimum mask concentration which could be differentiated from the purge as 5×10^{-7} V higher than the purge. The maximum PF was then determined by taking the challenge concentration and dividing by 5×10^{-7} V.

Backgrounds to account for particle generation or pin-hole leaks (discussed earlier in system characterization) were subtracted from in-mask concentrations when PFs were

calculated from M41 or LAS-X data. Occasionally, very low particle concentrations were detected by the LAS-X and M41 that were near 0.2 μm in size that were not detected by the photometer or Aerosizer™. Therefore, the test system background was not distinguishable from instrument background for the photometer or Aerosizer™. When the LAS-X was used, the background noise was limited to channels with midpoint diameter ranging from 0.13 to 0.45 μm. Therefore, backgrounds were only subtracted from PF tests using 0.17 and 0.5 μm aerosol challenges. Since the M41 was not size specific, backgrounds were subtracted from PF tests using all aerosol challenges. For both instruments, backgrounds were subtracted from PF tests with sealed, 50, and 100 μm orifices. The background was small enough to have negligible effect on PF tests with the 200 and 400 μm orifices.

For the vapor challenges, the in-mask background vapor concentration was subtracted from the in-mask vapor concentration during a PF test. Residual IAA was present within the test system and mask, so finite in-mask IAA vapor concentrations were measured. SF_6 backgrounds were measured initially with the mask sealed and a challenge present. This permitted correction of SF_6 that was permeating the mask system, which occurred when the mask was sealed with clay (see Section 5.3).

2.5.2 Statistical Analyses

Statistical analyses were performed to assess: (1) the effect of challenge aerosol size on measured PF for each instrument, (2) the effect of instrument on measured PF (comparison of indicated PF by instrument), (3) the correlation of PFs measured using a Bg spore aerosol challenge and bioassay counting method to PFs measured using inert aerosol challenges and electronic aerosol sensors, and (4) to correlate PFs measured with vapors and inert aerosols.

To determine whether the size of the aerosol challenge affected the measured PF, a Full Two Factor Analysis of Variance (ANOVA) model was fitted to the logarithmic (base 10) transformed PF for each of the four devices. The two factors in the ANOVA model are Aerosol type (A), Leak rate (L), and their interaction term (A*L). The above model was used to test the following sets of statistical hypotheses:

Set 1

H_0: The average PF for the various combination of aerosols and leak rates are equal.
H_1: The average PF for the various combination of aerosols and leak rates are not equal.

Set 2

H_0: The average PF for the aerosols are equal.
H_1: The average PF for the aerosols are not equal.

First, the hypothesis in Set 1 was tested using the F-test for the interaction term (A*L) from the ANOVA model. If the null hypothesis (H_0) in Set 1 was rejected, then the interaction term in the model was declared significant, implying that the average PF for various aerosol challenges might be different within leak rates. To determine which aerosol challenges were different, Bonferroni multiple comparisons procedure was used, which compare the average PFs for various aerosols within each leak rate at 5 percent overall error rate. If the F-test for the interaction term does not reject H_0 in Set 1, then the interaction term is declared insignificant in the model.

The hypotheses in Set 2 were then tested using F-test for the aerosol term (A) in the ANOVA. If H_0 is rejected in Set 2, then factor A is declared to be a significant factor in the model. Tukey's multiple comparisons procedure is performed to compare the PFs for the aerosol challenges at 5 percent error rate. If H_0 is not rejected in Set 2, then the average protection factor for the various aerosols are declared equal.

The same analysis described above was applied to determine whether the PFs measured for vapor challenges correlated with the PFs measured for 0.72 μm PSL.

To compare PFs measured using the four different instruments, linear regression lines were fitted to the data. A Full Two Factor ANOVA model was then fitted to compare the average PF for the various devices. The regression lines were fitted to the logarithmic (base 10) transformed PF for the four instruments and the 0.5 μm corn oil and 0.72 μm PSL challenges (excluding PFs for the mask sealed). The fitted regression line coefficient of determination (R^2 adj.), and 95 percent confidence interval for the slope of the line of various pools of data were determined. Those two challenge aerosols were used for the analysis

because all instruments were tested with those challenges and the challenges were of sufficient concentration to measure PFs over the range of all leak rates.

The two factors in the ANOVA model are Device type (D), Leak rate (L) and their interaction term (D*L). The above model is used to test the following sets of statistical hypotheses:

Set 1

H_0: The average PF for the various combination of instruments and leak rates are equal.

H_1: The average PF for the various combinations of instruments and leak rates are not equal.

Set 2

H_0: The average PF for the instruments are equal.

H_1: The average PF for the instruments are not equal.

The same method for the ANOVA model for particle size effect was used to compare instruments. In this analysis, however, the interaction term (D*L) was used.

To correlate PFs measured in this study to those measured for Bg spores/bioassay method, linear regression lines were fitted to three sets of data. The first was to compare the current PF data from Photometer/0.5 μm corn oil to the LAS-X/0.72 μm PSL PFs. The second was to compare LAS-X/0.72 μm PSL PFs from current study to LAS-X/0.72 μm PSL PFs measured using the same method in a previous study (Hofacre and Forney, 1995). The third was to compare the current PF data from Photometer/0.5 μm corn oil to the Bioassay/BG PF data measured by Hofacre and Forney. This approach was necessary because of the two independent studies. Both studies were linked by the common test using the LAS-X and the 0.72 μm PSL challenge. By demonstrating that the LAS-X/0.72 μm PSL results are the same, one can compare the results from this study to the results of the previous study.

The general form of the regression line fitted to the logarithmic transformed protection factor data is:

$$\text{Model 1: } \text{Log}_{10}(PF) = \beta + \beta_1 * \text{Leak rate} + \beta_2 \text{ Treatment Type}$$

where:

Leak rate (L) range between 40 and 400, and

Treatments Type (T) equals 0 or 1.

The regression lines fitted to the PF data in this comparison is different than the one fitted earlier because the Bg/bioassay PF data were collected at slightly different leak rates than the current data thus the factor leak rate had to be used in the model to account for the variation, and the data were not collected as matched pairs.

3.0 LITERATURE SEARCH AND REVIEW

3.1 PFs Measured Using Aerosol Challenges

A literature review was conducted to help define the test matrix presented in Table 1. An on-line computer search of Chemical Abstract Services Scientific and Technical Information Network (STN) was performed. The purpose of the search was to identify literature regarding the effect of test aerosol (size and type) and the types of instruments used to classify aerosols.

Six databases of STN were searched: (1) National Technical Information Services (NTIS), (2) Engineering Index (EI) COMPENDEX, (3) BIOSIS, (4) Pollution Abstracts (POLLUAB), (5) Health and Safety (HEALSAFE), and (6) MEDLINE. These databases were considered to most likely contain information regarding mask protection factor measurements. The databases encompass Government reports as well as commercial publications and they emphasize industrial hygiene and health and safety.

The search strategy implemented comprised the following keywords and hiarchy:

L1	Mask OR respirator	(20,572 records)
L2	Protection factor OR fit factor	495 records)
L3	L1 AND L2	(83 records)
L4	L1 AND (aerosol and penetration)	(94 records)

The records in L3 and L4 were screened to remove duplicate records (total of 73), leaving 104 unique records. The title, author, and source of these records were printed to review and identify potentially useful articles. Of these 104 records, 29 were obtained for review, and 12 were specific to particulate size and instrument effects on measurement of PFs.

Much of the literature reviewed pertained to the evaluation of half-face, disposable respirators. For such respirators, the PF is typically 100 or less and the respirator serves as the filter, rather than the air being filtered by a canister with a HEPA filter. Thus, for filtering

respirators, the effect of particle size on aerosol penetration follows that of aerosol penetration through the filtration media, rather than through a leak site. When leaks were created (either by holes or by capillaries), the diameter of the leak path was relatively large, greater than 0.5 mm. Thus, very low protection factors were achieved. Because of the type of respirator and of the low PFs, those studies were not considered useful indicators for the effect of particle size on aerosol penetration.

The most relevant work was that performed by Myers, et al. (1990) and by Holton, et al. (1987).

In the Myers' study, the test aerosols were all PSL spheres with diameters of 0.36, 0.62, 1.0, and 2.56 μm, and the capillary sizes that were used to control leakage into the mask were 0.25, 0.275, 0.3, 0.33, and 0.51 mm ID, all 19 mm long. The capillaries were placed between the mask and test head and sealed into place with silicone. The PSL aerosol concentration was measured using a parts per million (ppm) Incorporated Aerosol Scanner® Model S-0.2/2. The Scanner® has a sizing range capability from nominally 0.2 to 5 μm in eight size specific ranges. The Scanner® sampling flow rate is adjustable between 6 lpm and 60 lpm. For this study, the flow rate was adjusted to sample the entire inspired airflow rate. This was performed to minimize sampling bias that may be associated with the collection of a representative sample of lesser volume. Breathing was simulated using a constant breathing rate of 18 breaths/min and the tidal volume was either 600 or 1500 ml/breath.

Myers found no consistent effect of the apparent fit factors (AFF) as a function of particle size. Inconsistencies were also observed regarding the AFF within a specific particle size. That is, the AFF did not always increase with decreasing capillary diameter used to control the leak rate into the mask for the 1.0 and 2.5 μm PSL aerosol challenges. This may be due to the extremely low particle concentrations that were likely present within the mask. Even with some inconsistencies, the general trend that AFF is decreasing with increasing diameter of capillary was observed, as expected. The aerosol penetration results were compared to the penetration of acetone vapor, and in all cases the aerosol penetration was lower than the vapor penetration. The upshot from Myers' work is that no discernible trends could be identified regarding dependency of challenge aerosol particle size on AFF, over the range of particle sizes studied.

Holton's results were a little clearer. In this study, smoke and corn oil aerosol were used to generate small size aerosol challenges and a limestone powder was used for large particles to cover a range from 0.07 to 4.4 μm. Circular holes of 0.57, 1.07, and 1.68 mm diameter were used for the leak sites. (Other leak paths were created, such as slits and capillaries, to study their effects, but they are not considered relevant for this discussion.) The holes were located at the bottom of a half-face mask, near the exhalation valve and another set at the nose. Sampling ports were located in the center of the mask and adjacent to the holes at the nose. The mask was worn by human subjects for this study. An electrostatic aerosol classifier (EAC)/condensation nucleus counter (CNC), active scattering aerosol spectrometer (ASAS), and aerodynamic particle sizer (APS) were used to measure fit factors (FF) over the range of particle sizes.

Fit factors ranged from 20 to 5,000, an order of magnitude lower than those targeted in this study. Over the range of particle sizes from 0.2 to 2 μm, there was no discernible dependency of FF with particle size. When the particle size was greater than ~2 μm, and certainly at 5 μm, the FF was higher, upwards of an order of magnitude. Below 0.2 μm there was also an apparent increase in FF with decreasing particle size.

There was discontinuity of measured FF for the three instruments used to cover the range of particle sizes. The ASAS counting method yielded a lower FF than the EAC/CNC counting method for test aerosols of the same size (~0.2 μm). The APS counting method yielded a lower PF than the ASAS counting method for test aerosols of the same size (~1 μm). The relative differences between measured PFs for the instruments is small (factor of two).

In previous work performed by Battelle (Kuhlman and Hofacre, 1990) similar instruments to those being evaluated in this study were used to measure PFs. The instruments included a CNC, an early version M41, (TSI Model 8010) an ASAS, and a white light photometer. A range of particle sizes was investigated: 0.17, 0.32, 0.72, 1.24, and 2.0 μm and 0.9 μm AMMD corn oil. Capillaries were used for the leak path and the mask was mounted on a test head, which was connected to a breathing machine.

Results from that study indicated good agreement when the leak rate was high (PF $<$5,000) but significant deviation of PF $>$5,000. The photometer was not very sensitive and

a good correlation over a range of PFs was not achieved. Over the range of particle sizes used as challenge aerosols, no significant dependency of PF on particle size was evident. This is consistent with other published work.

Based on the literature findings, significant particle size dependency of PF is not expected until the challenge aerosol is greater than ~2 μm. Differences may be observed depending on the instrument used to measure aerosol concentration. The test matrix in Table 1 should permit the effects, if present, of particle size to be observed. None of the literature contains a wide range of particle sizes, types of instrument, controlled leaks with orifices, and a controlled mannequin test that was performed for this study.

3.2 PFs Measured Using Vapor Challenges

The databases searched for the aerosol PFs in Section 3.1 were also searched to identify publications regarding measured PFs using vapor challenges. The search strategy was as follows:

L1 (Mask OR Respirator) AND (Vapor or Gas)	(2,059 Records)
L2 AND L1 (Protect* OR Fit OR Penetrat*)	(34 Records)

After removing duplicate citations, 23 records were identified. The abstracts of those 23 records were reviewed and only 3 were considered applicable for further review for this study. These findings supplemented three relevant references in Myers' (1990) study.

In the study by Myers, et al. (1990) the AFF of masks were measured using an acetone vapor challenge and compared to AFF measured using aerosol challenges, as discussed in Section 3.1. Capillaries were used as controlled leak paths. Myers' study showed that the gas penetrated through the capillary significantly more than the aerosols, regardless of aerosol size and capillary size. The reported AFF for the masks was typically two to four times lower than the corresponding AFF measured using the aerosol challenge. Myers' results were comparable to those results of Schwabe (1980), who reported that sodium chloride (NaCl) aerosols penetrated less efficiently than methane gas. In contrast, Hounam, et al. (1964) and Griffin and Webb, as cited by Myers (1990), reported similar penetration of NaCl compared to either difluorodichloromethane or argon vapors.

In Hounam, et al. (1964) the aerosol and vapor penetrations were nearly the same when the measured penetration was greater than 1 percent. The minimum penetration that could be measured using the vapor challenge was 0.2 percent (equivalent to the PF of 500). Much of the reported penetration data were below the minimum detectable by the vapor method. Hounam's results are therefore limited to relatively low (<500) PFs.

In a study by da Roza, et al., (1988) the leak rate of corn oil aerosol was compared to that from Freon 12 and SF_6. A mask was fitted to a headform and the mask manipulated to create leaks using a Model TDA 104 mask leakage detector. The measured leakage of Freon 12 is, on average, 1.99 times higher that that measured for the corn oil. The SF_6 results also indicated a higher leak rate for the gas compared to the corn oil aerosol as, on average, the measured leak rate for SF_6 was 2.47 times that of corn oil aerosol. It is important to note that the leakage into the mask was not controlled in this study. Leaks were random due to the mechanical manipulation of the mask. Therefore, the results of da Roza's study cannot be compared directly to the results of others who used controlled leaks.

The findings reported in the literature regarding comparison of vapor leakage versus aerosol leakage are therefore contradictory. It has been reported that there is no difference in aerosol leakage compared to vapor leakage, and that vapors penetrate more readily.

4.0 AEROSOL TEST RESULTS

4.1 Data Summary

A summary of the measured PFs for each instrument by challenge particle size is presented in Table 3. The summary includes the number of PFs measured (n), the average PF (x), and the sample standard deviation (s). The individual PFs (350 PFs were measured) for which this summary is based are presented in Appendix B.

The sample size was typically four to six. There were instances however, where the sample size was only one or two. In those cases, PFs exceeding the maximum that could be measured (instrument background could not be distinguished from in-mask aerosol concentration) were excluded from the summary. The maximum PFs are indicated in the data in Appendix B. When all of the tests indicated a PF greater than the maximum, the upper limit of the PF is reported in Table 3. Because there were instances where it was known that a PF could not be measured (e.g., at a leak rate lower than a leak rate that yielded a PF exceeding the maximum measurable) no PFs were measured.

4.2 Effect of Particle Size

The effect of particle size on measured PFs is illustrated in Figures 4 through 7. The measured PF is plotted versus the challenge aerosol diameter on a log-log scale. PFs were not measured using all instruments and all particle sizes due to instrument sizing limitations and the ability to generate adequate challenge concentration of the larger particles.

In Figure 4, the effect of particle size in measured PF is illustrated using the LAS-X. For particles between 0.17 and 0.72 μm, there was no discernible effect of particle size on measured PF. However, the PFs measured using a 2.0 μm PSL challenge aerosol indicate that the apparent PF is beginning to increase. On average, the PFs measured using the 2.0 μm PSL challenge were about two to four times higher than those PFs measured using the 0.17 and

Table 3. Summary Statistics of Measured PF by Aerosol Challenge, Aerosol Sensing Instrument, and Leakage Condition

Challenge Aerosol	Device	Statistic	Leak Condition				
			Sealed	50 μm	100 μm	200 μm	400 μm
0.173 μm PSL	LAS-X	n	5	5	6	5	5
		$\bar{x}$	86300	30200	9780	1480	390
		s	26900	5540	2930	280	40
	M41	n	2	5	5	5	5
		$\bar{x}$	184000	112000	15300	1920	510
		s	7070	27300	1890	170	30
	Photometer	n	2	2	4	5	5
		$\bar{x}$	>4000	>4000	>4000	1530	400
		s	-(a)	-(a)	-(a)	150	50
0.5 μm Corn Oil	LAS-X	n	4	5	5	5	5
		$\bar{x}$	85100	48600	9650	1680	460
		s	17200	12200	1600	270	40
	M41	n	5	5	5	5	5
		$\bar{x}$	82100	37600	9490	1740	400
		s	10400	4710	550	150	40
	Photometer	n	3	5	5	5	5
		$\bar{x}$	>100000	61900	11700	2060	460
		s	-(a)	21800	1110	200	60
	Aerosizer™	n	5	5	5	5	5
		$\bar{x}$	>100000	34100	9580	1670	420
		s	-(a)	5760	2590	650	110
0.72 μm PSL	LAS-X	n	4	5	6	5	5
		$\bar{x}$	132000	37600	10600	1710	440
		s	31800	8470	1140	180	50
	M41	n	5	5	5	5	5
		$\bar{x}$	>200000	74400	14000	1860	490
		s	-(a)	13000	1470	210	50
	Photometer	n	3	5	5	5	5
		$\bar{x}$	>100000	43400	11500	1980	500
		s	-(a)	14900	1650	360	100
	Aerosizer™	n	3	5	5	5	5
		$\bar{x}$	>100000	48700	10500	1840	490
		s	-(a)	26400	2450	350	130
2.0 μm PSL	LAS-X	n	0	1	5	5	4
		$\bar{x}$		>100000	29000	3260	770
		s		-(a)	8700	480	40
	Photometer	n	0	0	1	5	5
		$\bar{x}$			>20000	2820	640
		s			-(a)	640	60
	Aerosizer™	n	0	1	5	5	5
		$\bar{x}$		79000	26200	4340	860
		s		-(a)	7240	1280	180
5.0 μm Syloid	Aerosizer™	n	0	0	0	0	5
		$\bar{x}$					2460
		s					1470

(a) Sample standard deviation could not be calculated because measured PF exceeded maximum value measurable, or sample size 1.

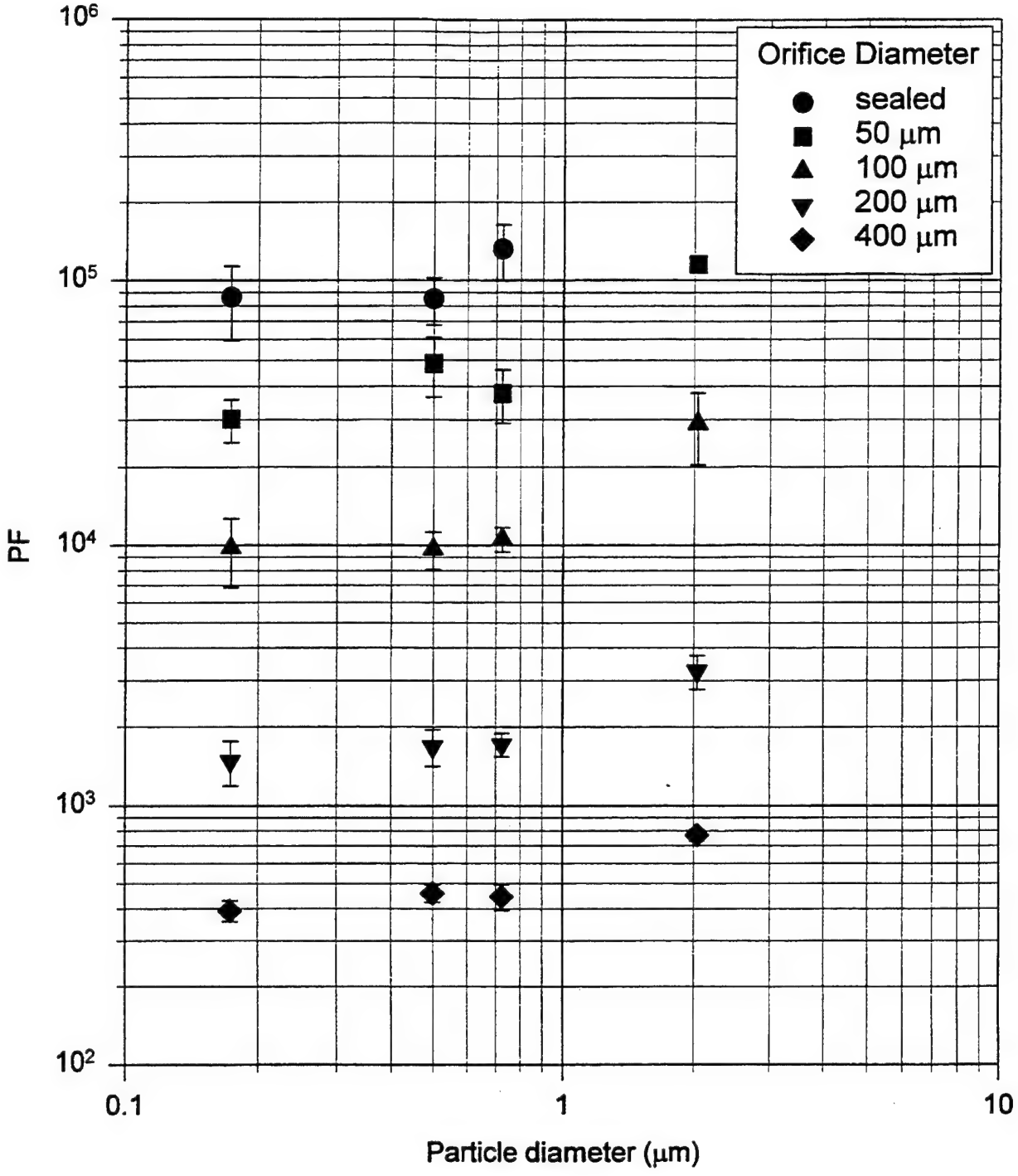

Figure 4. Measured PF as a Function of Challenge Aerosol Particle Size for the LAS-X

0.72 μm PSL challenge or the 0.5 μm corn oil aerosol challenge. The statistical analyses performed indicated that there was no significant difference in PFs using particles between 0.17 and 0.72, but significantly higher PFs using 2.0 μm challenge aerosol.

Similar trends are observed for the M41, photometer, and Aerosizer™, as illustrated in Figures 5, 6, and 7.

In Figure 5, the M41 indicates a consistently lower PF using the corn oil aerosol challenge than for either the 0.17 or 0.72 μm PSL. Statistical analyses indicated the 0.5 μm corn oil aerosol PFs were significantly lower than the 0.17 or 0.72 μm PSL. However, the practical difference in measured PF (typically less than a factor of two) is considered insignificant, especially for those PFs exceeding 20,000.

In Figure 6, the results for the photometer also indicate no appreciable effect of particle size on measured PF for challenge particles between 0.17 and 0.72 μm. Because of challenge concentration limitations and limitations of the photometers sensitivity, PFs could not be measured for the 100 and 50 μm orifice leak condition for the 0.17 and 2.0 μm PSL. A quick-look test was performed using a ~1.5 μm corn oil aerosol challenge (particle size as indicated by the Aerosizer™). PFs measured in that test were not different than those measured for the nominal 0.5 μm corn oil aerosol challenge.

In Figure 7, the results for the Aerosizer™ further illustrate the increase (approximately a factor of 2) in measured PF as the challenge aerosol size exceeds 2 μm. The 2 μm PSL challenge and nominal 5 μm silica powder challenge indicate significant increase in measured PF. Because of the limited particle concentration that could be achieved for the 5 μm challenge, only PFs for the 400 μm orifice leak condition could be measured. There was significant spread in the measured PF using the 5 μm silica powder challenge because of the relatively low challenge concentration. On average, though, the measured PF for the 5 μm aerosol challenge and 400 μm orifice leak condition were 5 times higher than PFs measured using 0.5 μm corn oil and 0.72 μm PSL aerosol challenges.

The fact that there is little dependence of measured PF on particle size in the range of 0.2 to 0.7 μm is consistent with what one would expect based on filtration theory. Liu and Lee (1976) measured the penetration of particles through various nuclepore filters and found that

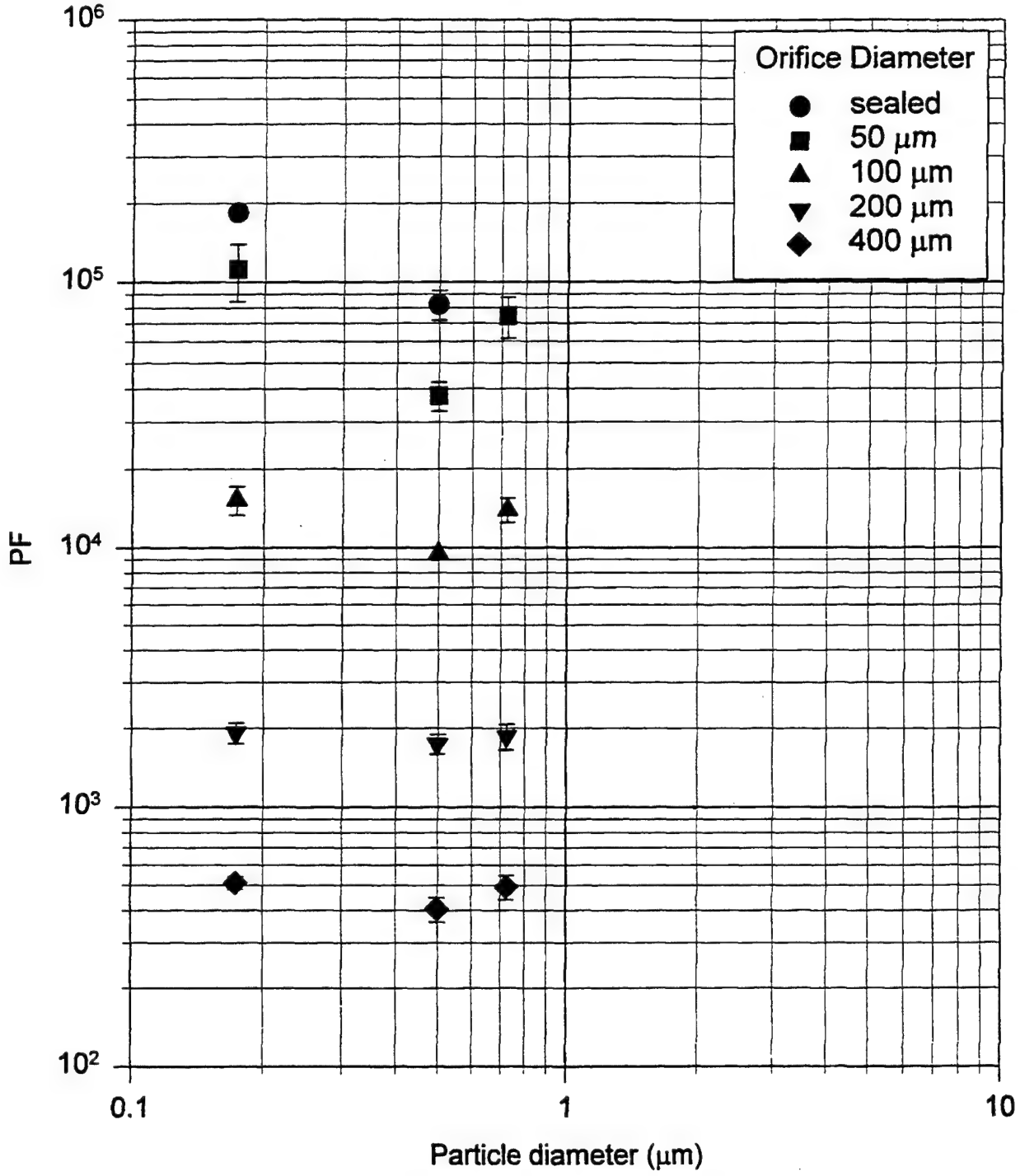

Figure 5. Measured PF as a Function of Challenge Aerosol Particle Size for the M41

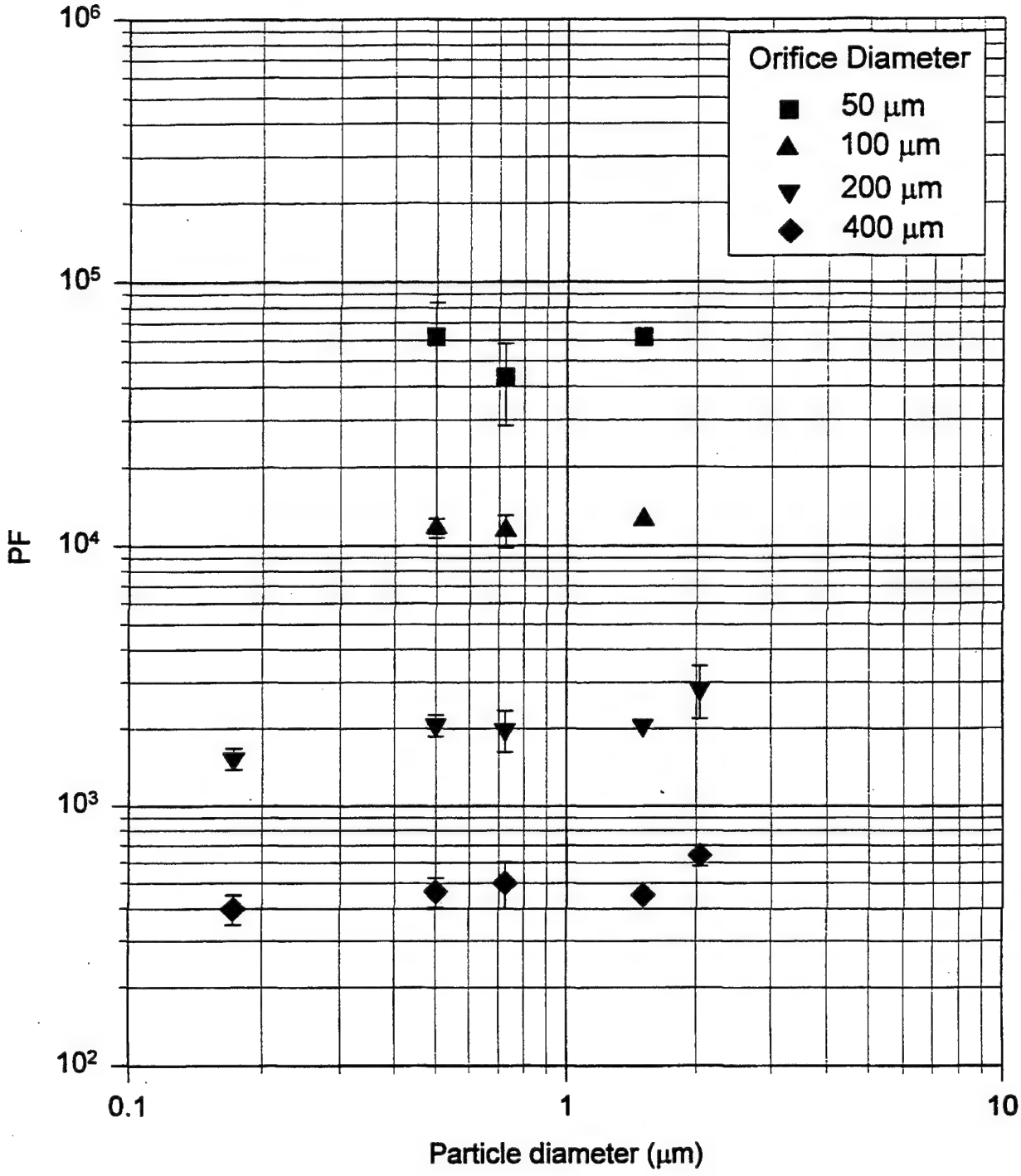

Figure 6. Measured PF as a Function of Challenge Aerosol Particle Size for the Photometer

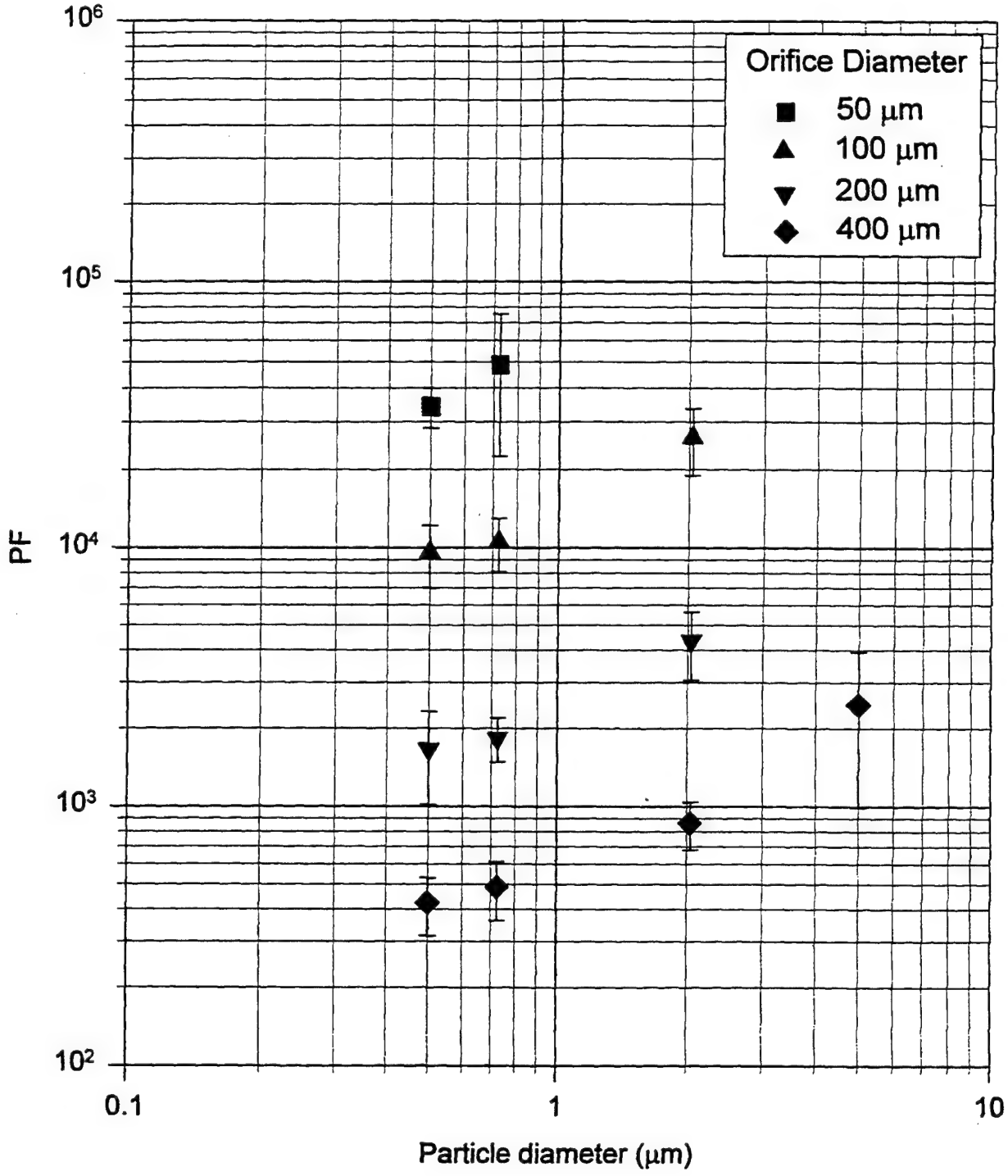

Figure 7. Measured PF as a Function of Challenge Aerosol Particle Size for the Aerosizer™

penetration is a maximum for particles in the 0.1 to 0.7 μm range. Nuclepore filters are polycarbonate membranes with straight-through holes. Therefore, the filters are physically comparable to the controlled leaks in this study. Filtration theory of the nuclepore filter predicts decreasing penetration (increasing PF) for particles greater than 1 μm.

The results obtained in this study are consistent with those reported in the literature (Myers et al., 1990; Holton et al., 1987). The upshot is that there is no significant dependence of measured PF on size of challenge aerosol (and phase, solid or liquid) for particles between 0.17 and 0.72 μm. The measured PFs did begin to increase significantly until the challenge aerosol diameter was 2 μm or higher and, with the limited data available for the 5.0 μm aerosol challenge and Aerosizer™, continued to increase with increasing particle size. The 0.17 to 0.72 μm particles, therefore, present a harsher challenge for PF measurement than 2 μm or greater particles.

4.3 Comparison of PFs by Instrument

The PFs measured by the instruments were compared by correlating their responses. Selected comparisons were made focusing on comparisons of the photometer with the LAS-X, M41, and Aerosizer, all for the corn oil aerosol challenge. Similar comparisons were made of the instruments using the 0.72 μm PSL challenge. Correlation of instrument responses are given by a best-fit linear regression of the general equation:

$$\mathrm{Log}_{10}\, Y = \alpha\, \mathrm{Log}_{10}\, X + \beta$$

where X is the measured PF for a specific instrument/aerosol combination and Y is the same for another instrument/aerosol combination.

A summary of linear regressions for selected instrument/aerosol combinations are presented in Table 4. Figures 8 through 11 illustrate the correlation graphically for selected combinations noted in Table 4. Because the standard PF measurement method uses the corn oil aerosol challenge and the photometer, comparisons to those measured PFs were emphasized. It is

Table 4. Correlation of PFs Measured Using the Various Instruments for 0.5 μm Corn Oil (CO) Aerosol and 0.72 μm PSL Aerosol Challenges

Method Comparison		Regression Statistics $\log_{10} Y = \alpha * \log_{10} X + \beta$			
Y	X	α	β	r^2	95% CI
0.5 μm CO, Photometer	0.5 μm CO, LAS-X	1.031	-0.044	0.98	(0.966, 1.097)
0.5 μm CO, Photometer	0.5 μm CO, Aerosizer™	1.061	-0.089	0.97	(0.963, 1.158)
0.5 μm CO, Photometer	0.5 μm CO, M41	1.062	-0.117	0.998	(0.948, 1.177)
0.5 μm CO, LAS-X	0.5 μm CO, M41	1.021	-0.039	0.995	(0.847, 1.195)
0.5 μm CO, LAS-X	0.5 μm CO, Aerosizer™	1.043	-0.097	0.995	(0.864, 1.222)
0.5 μm CO, Aerosizer	0.5 μm CO, M41	0.978	-0.055	0.999	(0.978, 1.035)
0.72 μm PSL, LAS-X	0.72 μm PSL, M41	0.882	0.327	0.99	(0.824, 0.939)
0.72 μm PSL, LAS-X	0.72 μm PSL, Photometer	1.036	-0.167	0.99	(0.960, 1.112)
0.72 μm PSL, LAS-X	0.72 μm PSL, Aerosizer™	0.954	0.086	0.99	(0.871, 1.038)
0.72 μm PSL, M41	0.72 μm PSL, Photometer	1.163	-0.515	0.97	(1.017, 1.308)
0.72 μm PSL, M41	0.72 μm PSL, Aerosizer™	1.080	-0.263	0.99	(0.991, 1.168)
0.72 μm PSL, Photometer	0.72 μm PSL, Aerosizer™	0.915	0.265	0.98	(0.821, 1.01)
0.5 μm CO, Photometer	0.72 μm PSL, LAS-X	1.081	-0.202	0.997	(0.99, 1.17)
0.5 μm CO, Photometer	0.72 μm PSL, M41	0.959	0.117	0.998	(0.84, 1.07)

important to note that the PF correlation in Figure 10 for the CO/Photometer versus the 0.72 μm PSL/LAS-X was used to obtain the correlation of the CO/Photometer PFs to Bg spore PFs presented in Section 4.4. The comparison to Bg spore PFs is possible because the 0.72 μm PSL/LAS results obtained in this study and the previous study (Hofacre & Forney, 1995) are the same.

The correlations provided in Table 4 and illustrated in Figure 8 through 11 were determined without the PFs measured for the mask in its sealed condition. Those PFs were not included because they were frequently reported as a maximum PF, so an accurate measure of the PF was not obtained nor could a standard deviation be calculated. Inclusion of the PFs measured for the mask sealed would therefore bias the correlation.

The results of the correlations indicate very good agreement for the different measurement methods. Perfect agreement would be a line that coincides with the 1:1 line (i.e., α of 1 and a β of 0). On average, the PFs measured using the different instruments were

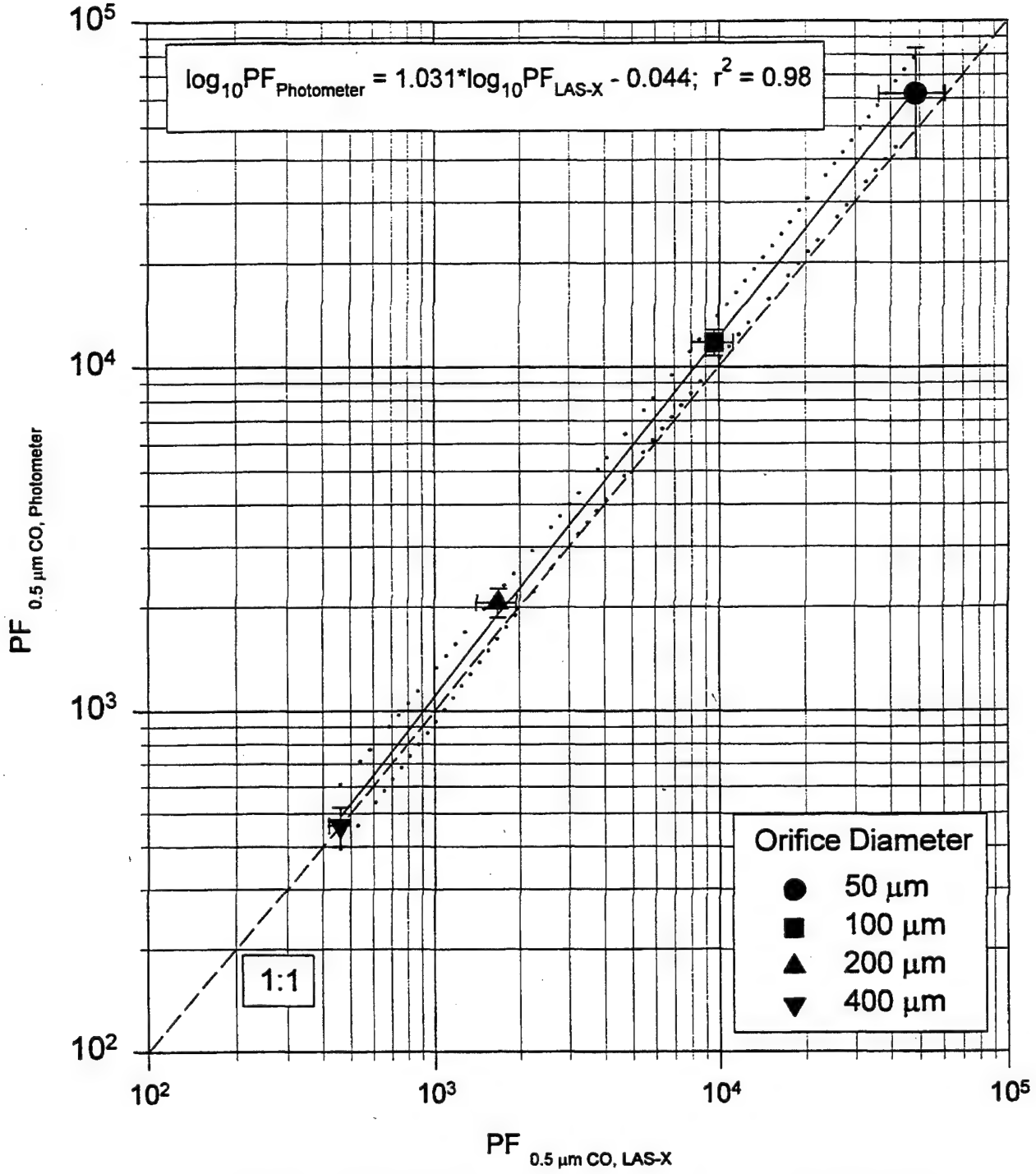

Figure 8. Correlation of Measured PF Using the Photometer and the LAS-X for a 0.5 µm CO Aerosol Challenge

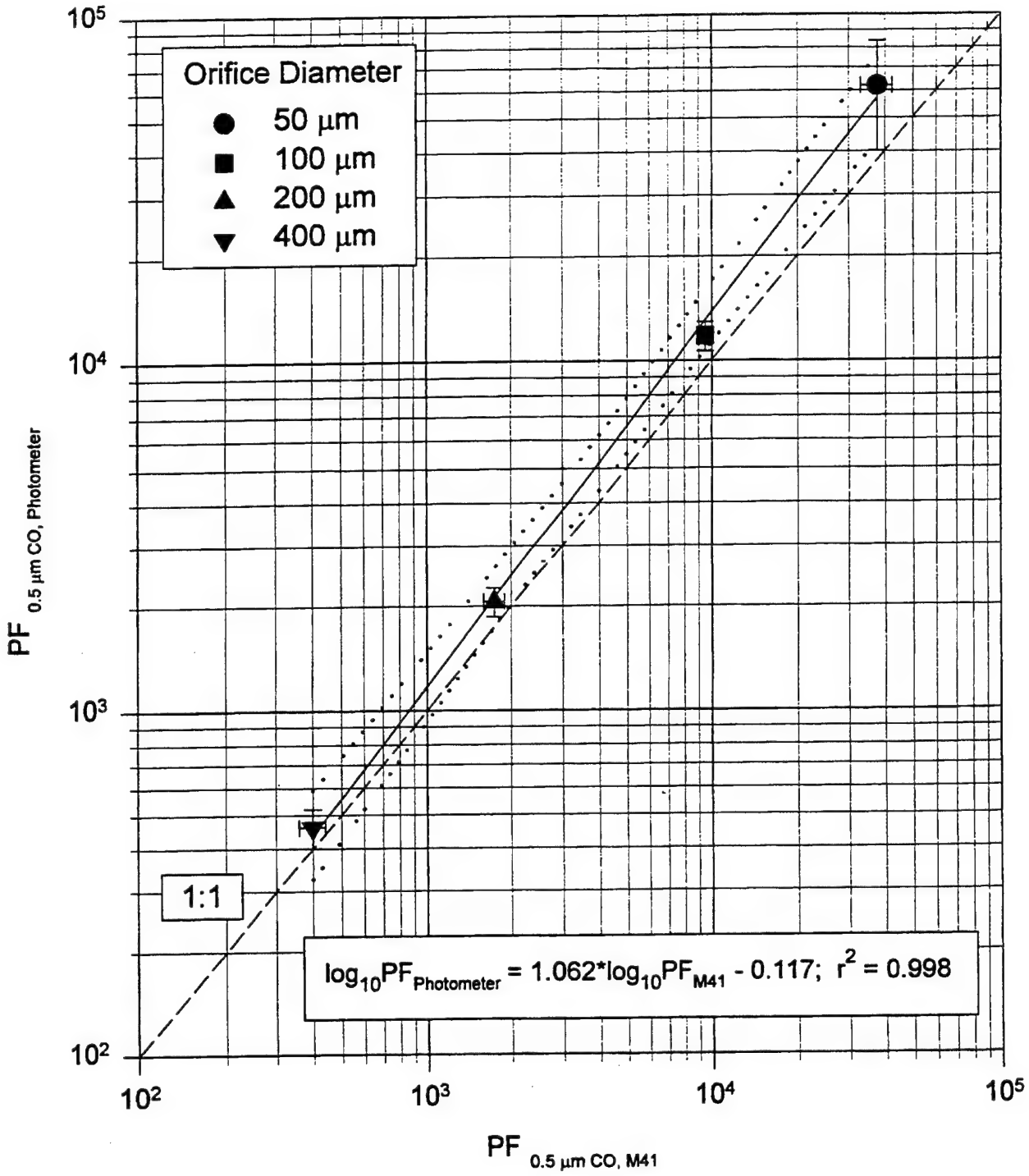

Figure 9. Correlation of Measured PFs Using the Photometer and the M41 for a 0.5 µm CO Aerosol Challenge

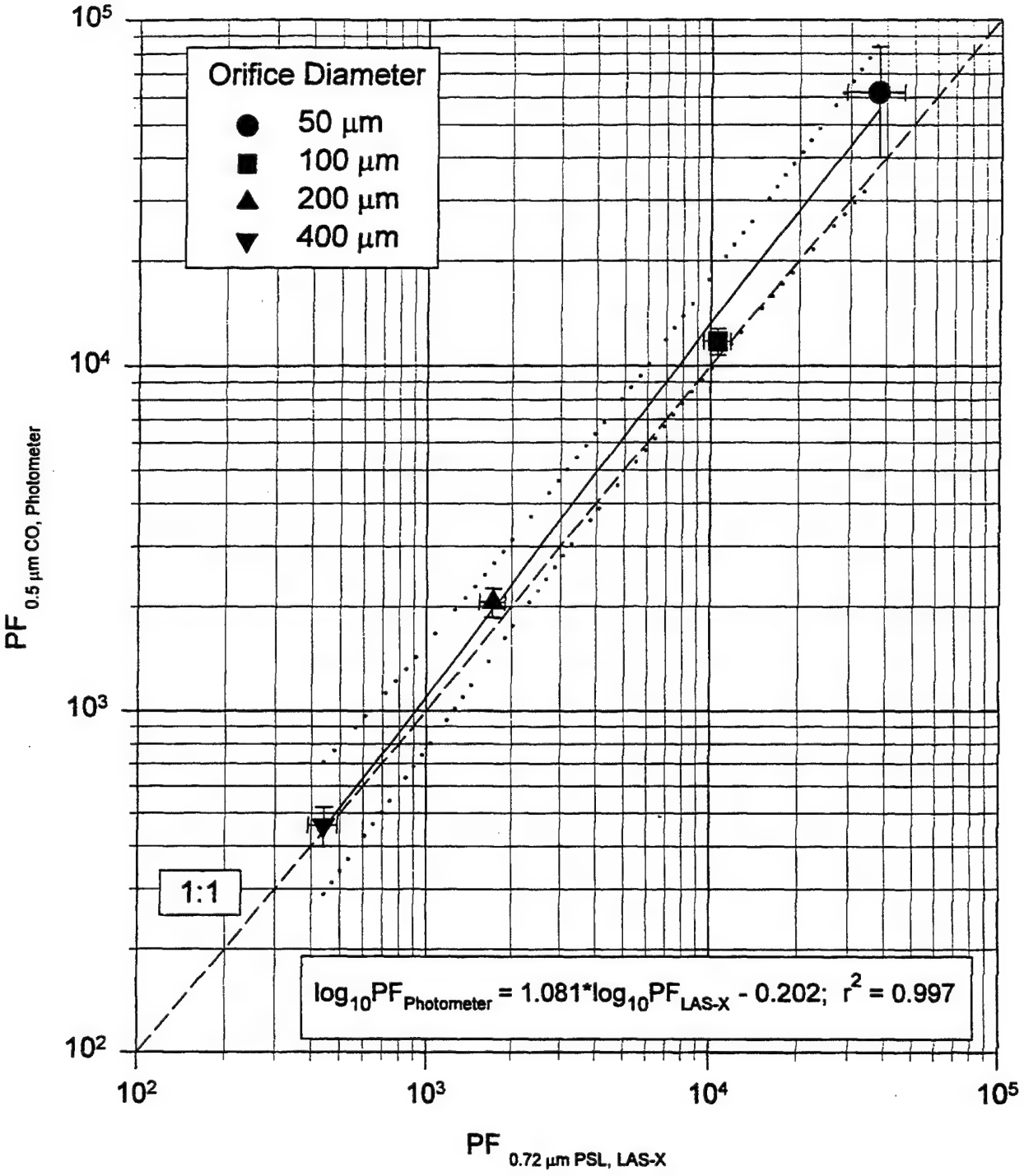

Figure 10. Correlation of Measured PF Using the Photometer and 0.5 µm CO Aerosol and the Measured PF Using the LAS-X and 0.72 µm PSL Aerosol

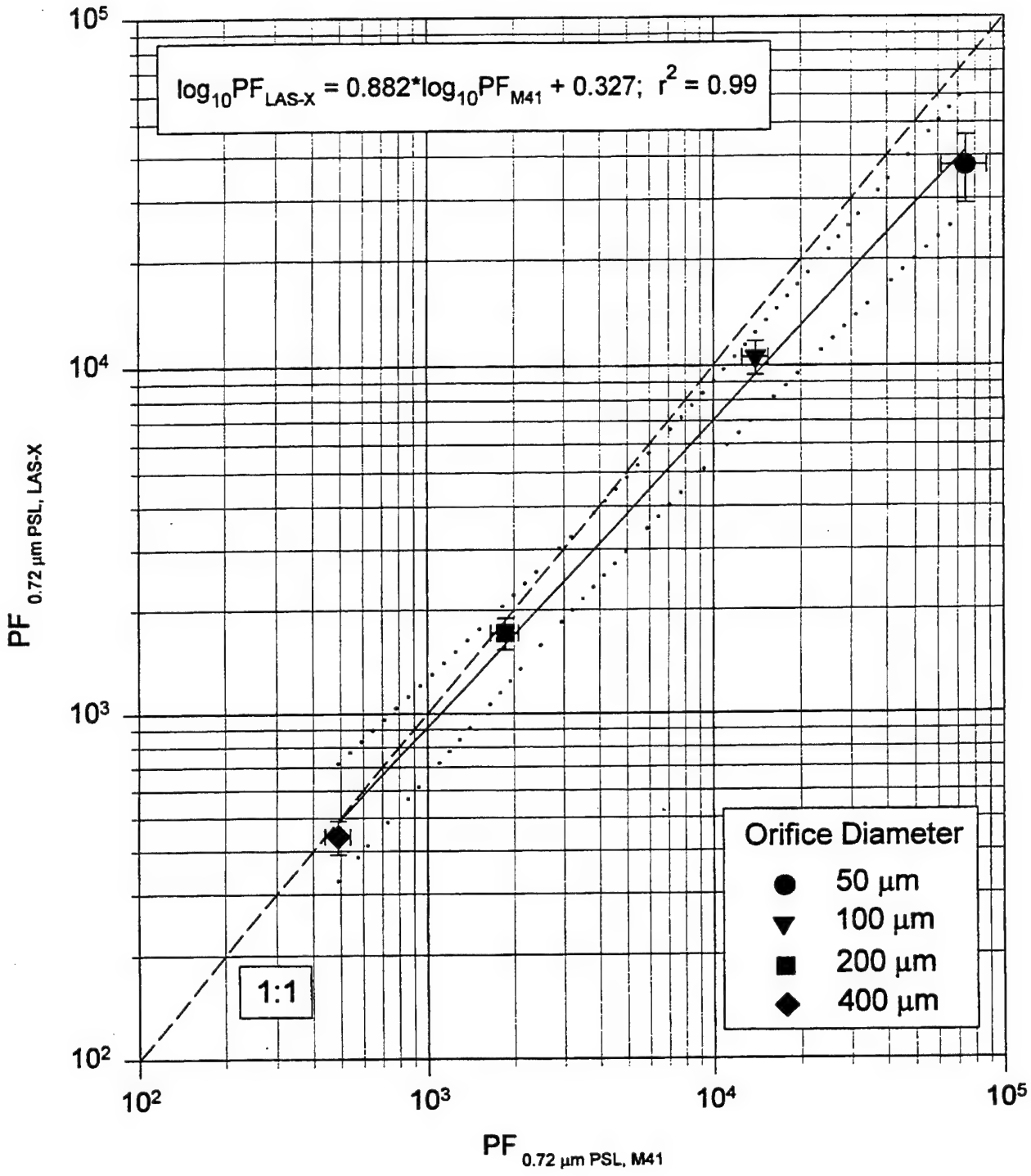

Figure 11. Correlation of Measured PFs Using the LAS-X and M41 for a 0.72 µm PSL Aerosol Challenge

always within a factor of two, and typically differ by less than 25 percent. Statistically, the ANOVA models indicate that the PF measured using the photometer and corn oil aerosol is larger than those measured using the M41 or Aerosizer™.
Additional plots depicting the correlations are presented in Appendix C.

4.4 Comparison of Inert Aerosol PFs to Bg Spore PFs

For an earlier study (Hofacre and Forney, 1995), PFs were measured using a Bg spore challenge and a bioassay counting method (and the LAS-X counting method). In that study, an identical test system (using another mask with orifices of 40, 100, 200, and 330 μm to control leakage) were used to measured PFs. The PFs measured using the Bg spore challenge aerosol were correlated to PFs measured using the 0.72 μm PSL and
LAS-X method. The correlation, like those illustrated in Figures 8 through 11, is depicted in Figure 12.

The PFs measured using 0.72 μm PSL and the LAS-X in this current study were compared to the PFs of the same method obtained in the earlier study (Hofacre and Forney, 1995). The PFs measured in both studies were statistically equivalent. (Because a 40 and 330 μm diameter orifice was used in the previous study, the PFs associated with a 50 and 400 μm orifice leak were predicted from a log-log plot of PF versus orifice diameter.) The measured PF using Bg spores could therefore be compared directly to those PFs measured in this study.

Correlations of the PF data from this study were then made with the PFs measured using Bg spores in a fashion identical to that in Section 4.3. The best fit linear regression constants are given in Table 5. Illustrated in Figure 13 are a series of curves that depict the PFs measured using a photometer and the various aerosol challenges compared to the PFs measured using the Bg spore/bioassay method. Because the correlation curves all reside above the 1:1 line, the PFs measured using the Bg spores/bioassay was always higher than PFs measured by the photometer. The PFs, on average, agreed within a factor of two. Only when the Bg spore PFs were compared with PFs measured with the 0.17 μm PSL and photometer was the Bg spore PF about three times higher. Although statistically the measured Bg spore

Table 5. Correlation of PFs Measured Using the Various Instruments and Aerosol Challenges With PFs Measured Using a Bg Spore Challenge and Bioassay Counting Method

Method Comparison		Regression Statistics $\log_{10} Y = \alpha * \log_{10} X + \beta$		
X	Y	α	β	r^2
0.5 μm CO, Aerosizer™	Bg, Bioassay	1.107	-0.069	0.999
0.72 μm PSL, Aerosizer™	Bg, Bioassay	1.063	0.005	0.997
2.0 μm PSL, Aerosizer™	Bg, Bioassay	1.071	-0.353	0.996
0.17 μm PSL, LAS-X	Bg, Bioassay	1.104	-0.024	0.999
0.5 μm CO, LAS-X	Bg, Bioassay	1.049	0.086	0.996
0.72 μm PSL, LAS-X	Bg, Bioassay	1.090	-0.040	1
2.0 μm PSL, LAS-X	Bg, Bioassay	0.955	0.102	0.999
0.17 μm PSL, M41	Bg, Bioassay	0.900	-0.480	0.991
0.5 μm CO, M41	Bg, Bioassay	1.081	0.017	0.999
0.72 μm PSL, M41	Bg, Bioassay	0.965	0.290	0.997
0.17 μm PSL, Photometer	Bg, Bioassay	1.111	-0.063	1
0.5 μm CO, Photometer	Bg, Bioassay	1.004	0.177	0.997
0.72 μm PSL, Photometer	Bg, Bioassay	1.092	-0.107	0.999
2.0 μm PSL, Photometer	Bg, Bioassay	1.007	0.008	1

PF is greater than all PFs measured using the photometer, except for the 2.0 μm PSL challenge, there is very little practical difference in the measured PFs. These results indicate that the PF measured using the 0.5 μm CO and Photometer is a conservative estimator of the PF that would be measured against a Bg spore aerosol challenge. This, in part, is likely due to the Bg spore aerosol challenge size being greater than 1 μm. Results in Section 4.1 indicate that the measured PF would be relatively higher for challenge aerosols greater than 1 μm.

A similar plot illustrating the correlation of Bg spore PFs with PFs measured using the LAS-X and various inert challenges is given in Figure 14. This plot illustrates the Bg spores PFs were typically two to three times higher than PFs measured using the LAS-X and inert

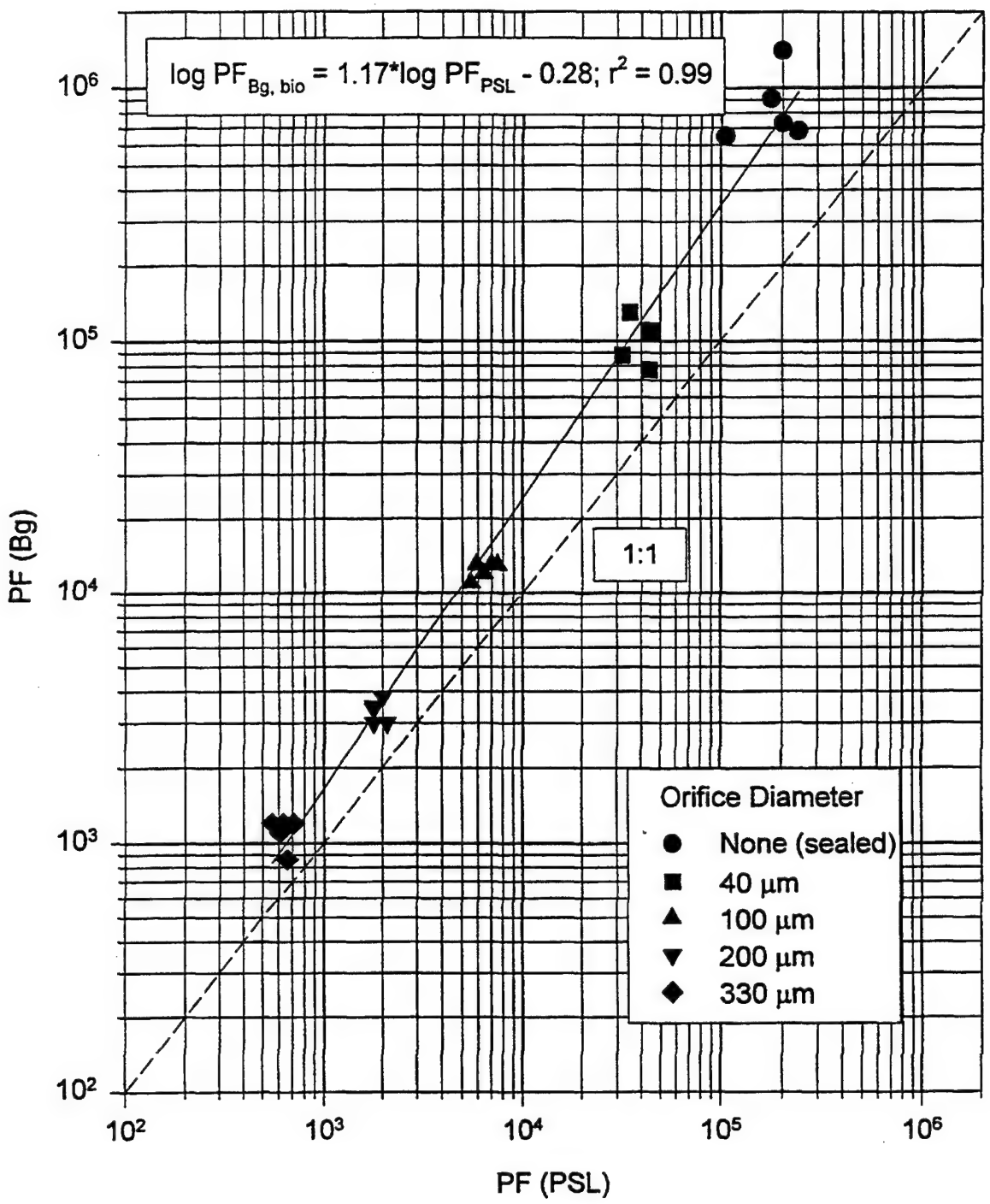

Figure 12. Correlation of PFs Measured Using Bg Spore Challenge and Bioassay Counting Method and PFs Measured Using 0.72 µm PSL Challenge and LAS-X Counting Method (Hofacre and Forney, 1995)

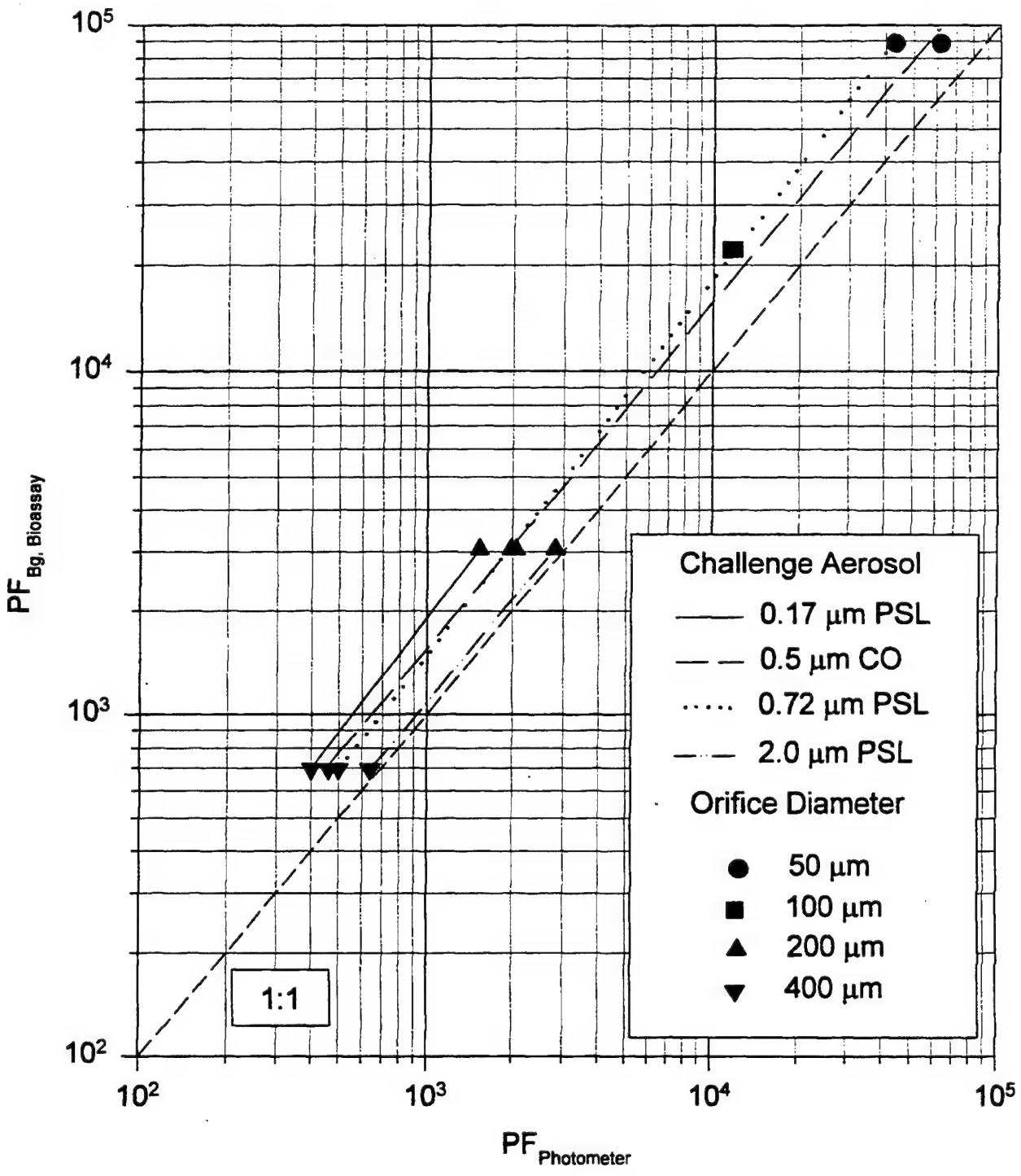

Figure 13. Comparison of PFs Measured Using the Photometer and 0.17, 0.72, and 2.0 µm PSL and 0.5 µm CO Aerosol to PFs Measured Using Bg Spores and Bioassay Method

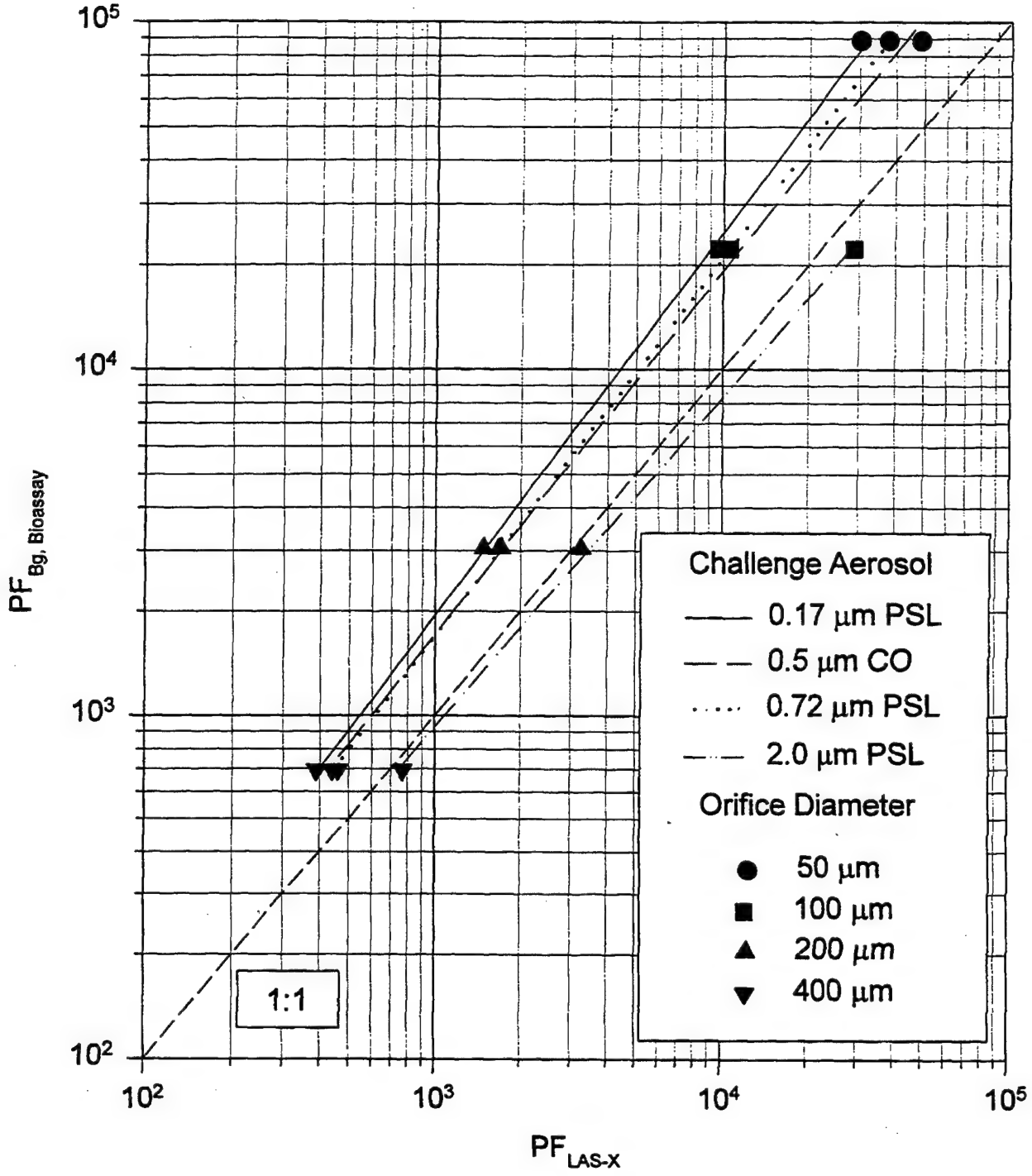

Figure 14. Comparison of PFs Measured Using the LAS-X and 0.17, 0.72, and 2.0 μm PSL and 0.5 μm CO Aerosol to PFs Measured Using Bg Spores and Bioassay Method

aerosols, except when 2.0 μm PSL was used as the challenge. The Bg spore PFs agree nearly perfectly with the PFs measured using the LAS-X and 2.0 μm PSL. In fact, the LAS-X/2.0 μm PSL combination is the best predictor of measured PFs for the Bg spore aerosol challenge of all the instrument and inert aerosol combinations investigated.

The observation that the 2.0 μm PSL challenge best represents the PF that would be measured using a Bg spore challenge is attributed to the fact that the Bg spores can be present in a distribution of particle sizes. Agglomerates of spores or spores and inert material > 1 μm are likely present in the aerosol challenge. Thus, when PFs are measured using the bioassay method (which uses water soluble filters to collect the Bg spores) the entire distribution of particles contribute to the measurement. The results indicate that the Bg spores were most likely present, in part, as agglomerates, and thus best represented by the 2.0 μm PSL particles for PF measurements.

Similar plots for the other instruments and aerosol challenges are presented in Appendix D. In those plots, it is apparent that the PFs for the Bg spore/bioassay method are consistently higher (up to a factor of two times), but still in good agreement. Inspection of those plots indicate that the best agreement of measured PFs was with the 2.0 μm PSL and LAS-X. The correlation line was nearly coincident with the 1:1 line.

To further illustrate the comparison of inert aerosol challenge and aerosol sensing instrument on measured PFs compared to Bg spore PFs, the PF data were plotted with each plot containing a set of curves for each of the four instruments per aerosol challenge. Those plots are also presented in Appendix D. The correlation curves in those plots indicate that the PFs measured with Bg spore/bioassay method are typically two to three times those of PFs measured using the submicron inert aerosol challenges. When the Bg spore PFs are compared to those using the 2.0 μm PSL challenge, they differ by less than a factor of 2.

5.0 VAPOR RESULTS

5.1 Methyl Salicylate Findings

Initially, methyl salicylate (MeS) was selected as a vapor challenge; however, problems associated with vapor permeation and carry-over made it unacceptable as a vapor challenge for this study. A complete discussion of the problems encountered and trouble shooting efforts performed with MeS are given in Appendix E. In summary, MeS was permeating the mask and causing high, dynamic background concentrations within the mask. The MeS is readily absorbed by the mask and once contaminated, continually off gases. The off-gassing of MeS was significant in that it was not readily flushed from the mask, and the in-mask background concentration could not be differentiated from the in-mask concentration during controlled leakage. Thus, PFs could not be accurately measured. MeS was replaced with IAA as a vapor challenge because IAA was more volatile; it was less likely to be retained (because of surface effects) in the mask once it entered the mask and it is commonly used as a challenge for qualitative mask fit tests.

5.2 Vapor PF Summary Data

Table 6 presents a summary of the measured PFs using IAA, SF_6, and 0.72 μm PSL spheres as challenge atmospheres for four controlled leaks into the mask. The PFs are matched pair data because the PFs were measured in sequence, without a change to the mask. Thus, changes in measured PF were attributed to the measurement method, not a change in the test system.

Table 6. Measured PFs for IAA, PSL, and SF_6 Challenges

		Challenge		
Leak Condition (Orifice Size)	Trial	IAA	0.72 μm PSL	SF_6
Sealed	- (a)	> 100000	77500	- (a)
	- (a)	> 100000	48900	- (a)
	1	40700	138000	99700
	2	71100	>383000	>156000
	3	62500	>496000	>166000
	4	- (b)	>550000	>164000
	5	36400	>447000	>172000
	$\bar{x}$	52700	403000	152000
	s	16800	160000	29500
50 μm	1	25300	17800	20900
	2	16200	22500	27500
	3	30000	22400	23800
	4	- (c)	22200	26100
	5	31600	40700	35100
	6	28100	39700	46400
	$\bar{x}$	26200	27600	30000
	s	6080	9960	9360
100 μm	1	- (d)	5830	9900
	2	21300	6480	11100
	3	5550	7280	10300
	4	14300	6930	9400
	5	7320	4740	7260
	6	11000	5000	9350
	$\bar{x}$	11900	6040	9550
	s	6250	1030	1300
200 μm	1	1810	1260	1220
	2	1260	1250	1550
	3	2080	1110	1420
	4	3200	1320	1390
	5	3260	1240	1430
	$\bar{x}$	2320	1240	1400
	s	880	80	120
400 μm	1	870	290	300
	2	1290	300	380
	3	990	290	350
	4	- (e)	300	410
	5	920	280	380
	$\bar{x}$	1020	290	360
	s	190	10	40

(a) IAA shakedown tests; no SF_6 test performed; PFs not used in final analysis
(b) no test performed, background IAA concentration too high
(c) background IAA concentration indistinguishable from in-mask sample
(d) breathing machine not functioning during test
(e) insufficient challenge to measure PF; generator exhausted

5.3 IAA and SF_6 Findings

PF tests were initiated with the mask sealed to the headform using clay rather than the headform's bladder. Clay was used in an effort to eliminate possible IAA permeation through the headform bladder. After three tests with the mask sealed (no controlled leak), IAA was permeating the test system (the mask). It was then decided to begin controlled leak tests using the 200 μm orifice, so that the leakage of IAA was significantly greater than that permeating. Next, PFs were measured using the 400 μm orifice for controlled leakage. By increasing the controlled leak rate, residual IAA within the mask (mask background) from previous tests and permeation would be relatively insignificant.

After the tests with the 400 μm orifice for controlled leakage, the IAA background concentration was considered too high to permit accurate measurement of PFs much greater than 5,000. Therefore, the mask was removed and replaced with another mask, and the remainder of the system was cleaned (thermal desorption and/or solvent rinse) and purged with clean air. In addition to IAA permeating, SF_6 was also permeating the test system in the above tests. With the mask sealed, the PF measured using the SF_6 challenge was 4,000; the corresponding PF with the PSL challenge was >50,000, so SF_6 was not leaking into the mask. It was believed that the SF_6 was permeating the clay seal. Therefore, when the mask was resealed to the headform, the bladder was used rather than the clay.

Tests were then reinitiated with the mask sealed. After the first test, the IAA background in the mask began increasing, indicating the IAA was permeating the mask test system. SF_6 was not detected in the in-mask samples with the mask sealed, which indicated that SF_6 was not permeating the mask/headform seal (the bladder). The results thus confirmed that SF_6 was permeating the clay seal in the 200 and 400 μm orifice controlled leak tests discussed above. Because IAA was permeating the mask, it was decided to proceed with the 100 μm orifice controlled leak rate before the mask background concentration increased such that accurate PFs could not be measured. It should be noted that the background concentration of simulant within the mask is subtracted from the in-mask concentration during leakage when the PF is calculated.

After the tests with the 100 μm orifice leak condition, the system was cleaned and a cleaned mask (cleaned by thermal desportion) was sealed to the headform using the bladder and clay.

The next test was performed with the mask sealed. The in-mask background concentration of IAA before the initial exposure was 10 ng/l, and after the test (before the second exposure), 55 ng/l. The in-mask IAA concentration during the sealed mask tests was 36 ng/l. The challenge IAA concentration for the test was 940,000 ng/l. Therefore, after subtracting the pretest background from the in-mask IAA concentration, the PF was 36,400. This result indicates that IAA was permeating the test system and affecting the measured PF. Because the IAA was permeating rather than leaking into the mask, the measured PF was artificially low. Because there is no detectable leakage into the mask when it was sealed based on the PSL and SF_6 results yielding a PF > 100,000, the increased IAA concentration within the mask was attributed to permeation.

Tests were then performed with the 50 μm orifice leak condition. Only three tests could be performed before the IAA mask background concentration was nearly equal to that in the mask with a controlled leak. Therefore, the system had to be cleaned before completing the final two tests with the 50 μm orifice.

Although IAA was a better surrogate vapor challenge than MeS because it was not as sticky, vapor permeation and carryover in the mask remained a problem. These results indicate the significant effort that is needed to measure PFs accurately when using an organic vapor challenge.

5.4 Comparison of Vapor and Aerosol PFs

Figures 15 and 16 illustrate the correlation of PFs measured for the SF_6 versus the PSL challenge and for the IAA versus PSL challenge. The average PF is plotted with error bars of one standard deviation about the mean. Also the best fit linear regression with 95% confidence interval is shown.

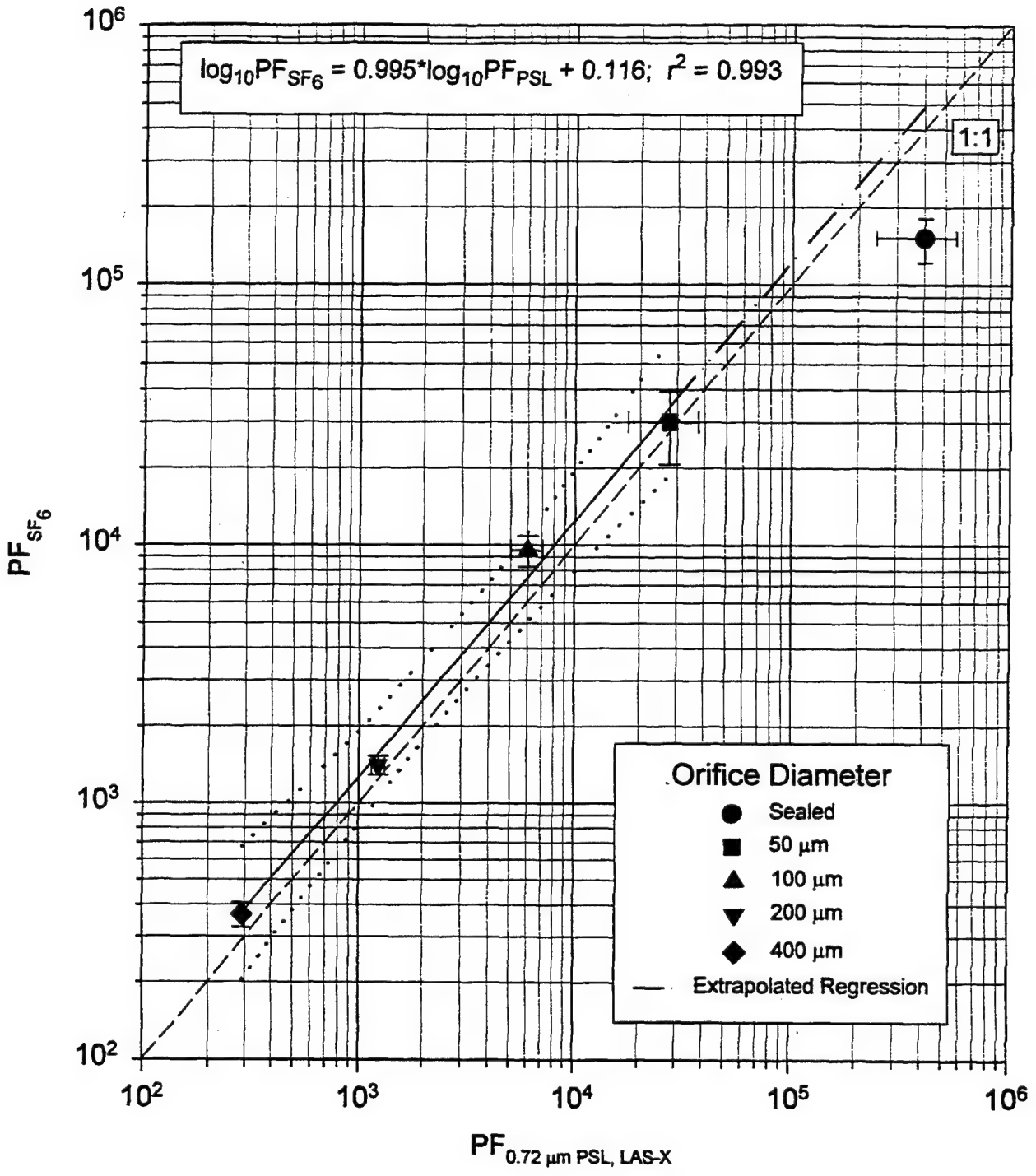

Figure 15. Correlation of PFs Measured Using SF_6 and 0.72 µm PSL Challenges

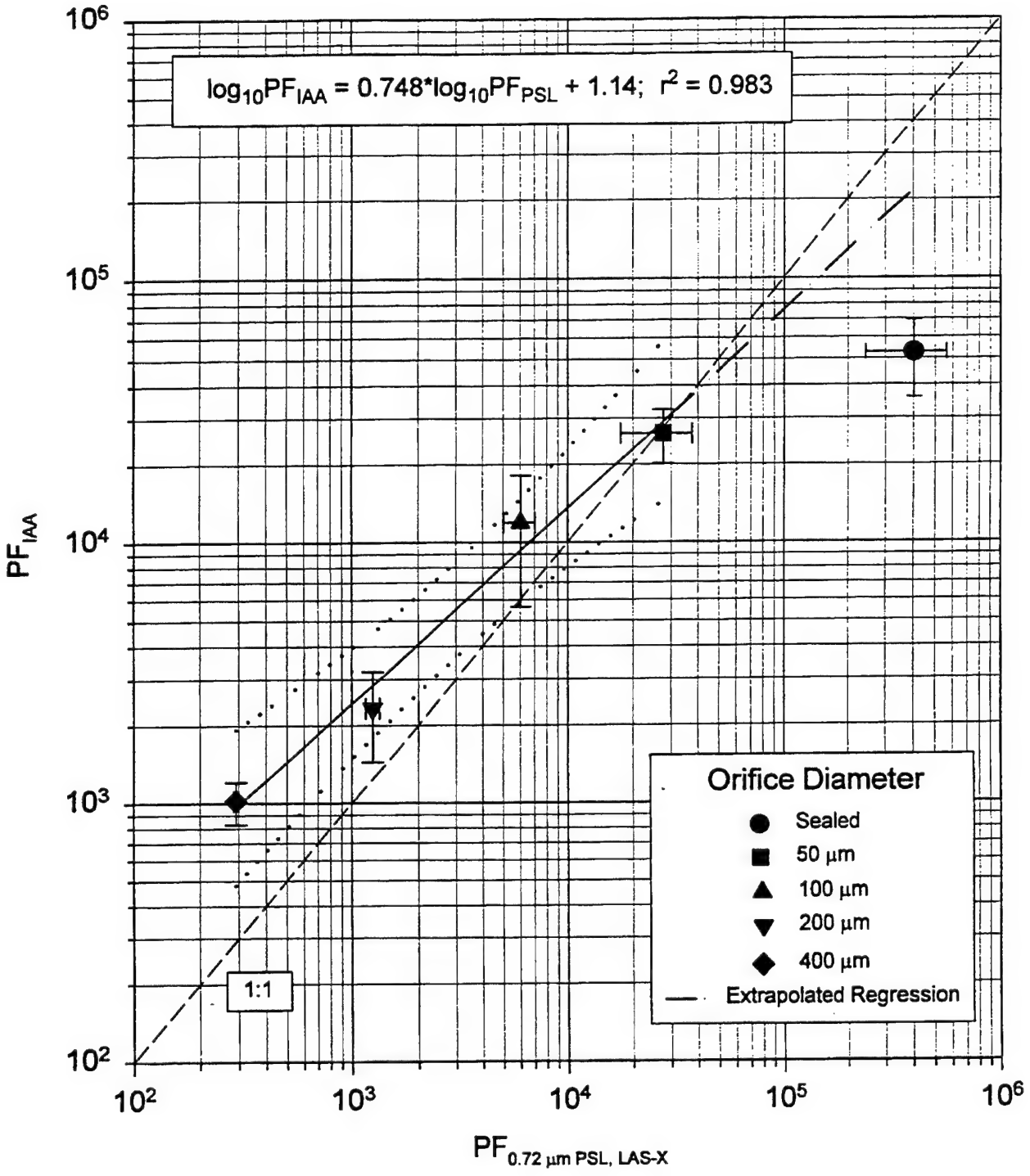

Figure 16. Correlation of PFs Measured Using IAA and 0.72 µm PSL Challenge

The PFs measured using the SF_6 and PSL challenge were in excellent agreement. The PFs measured using SF_6 were, on average, within 50 percent (higher) of the PFs measured using PSL. A linear regression of log transformed average PFs yielded a correlation equation of:

$$\log_{10} PF_{SF6} = 0.995 \times \log_{10} PF_{PSL} + 0.116; r^2 = 0.993$$

The correlation equation is based on the data for the controlled leak rates of the 50, 100, 200, and 400 μm orifices. The measured PFs for the sealed mask condition have been excluded from the regression analysis because those PFs were typically greater than a maximum PF measurable for the SF_6 and PSL challenges, and therefore were not necessarily an accurate measure of the PF. Because a maximum PF had to be reported, the actual PF was underestimated. Since the PF was known to be underestimated when the mask was sealed, those maximum PFs would therefore potentially bias the correlation. For reference, however, the average PF for the sealed condition is presented.

The r^2 value of 0.993 indicates that an excellent correlation was obtained. The best fit line nearly coincides with the one-to-one line. If the PFs for the two challenges agreed perfectly, the slope of the line would be 1.0 and the intercept 0 and the PFs would be on the one-to-one line. Because the best fit line correlating the PFs is nearly coincident with the one-to-one line, the PF measured using the 0.72 μm PSL aerosol is a good indicator of the PF that would be measured with SF_6.

The ANOVA model applied to the PF data indicate that the average PF measured using the SF_6 challenge is significantly higher than the average PF measured using the 0.72 μm PSL challenge. As the case for comparison of PFs for the various aerosol challenges, the practical difference in measured PFs between the SF_6 and 0.72 μm PSL challenges, however, is insignificant. The PFs measured using the SF_6 challenge were, on average, only about 25 percent higher than the PFs measured using the 0.72 μm PSL challenge.

The agreement of PFs measured using IAA and PSL was not as good as that for the SF_6 and PSL PFs, yet a reasonably strong correlation ($r^2 = 0.983$) was obtained and is given by:

$$\log_{10} PF_{IAA} = 0.748 \times \log PF_{PSL} + 1.14; r^2 = 0.983$$

The slope (0.748) and intercept (1.14) of the best fit regression, however, deviate significantly from that required for perfect agreement between the measured PFs. For PFs < 20,000, the PF measured for the IAA challenge (PF_{IAA}) was higher than the corresponding PF measured for the PSL challenge (PF_{PSL}). The PFs deviated, on average, a factor of three when PF_{PSL} was ~ 300 (400 μm orifice leak condition). Near PFs of 20,000, PF_{IAA} and PF_{PSL} were in good agreement, on average. For measured PFs > 20,000, the average PF_{PSL} was higher than the average PF_{IAA}. The deviation between PFs became more pronounced as the PFs increased above 20,000.

The reason for the relatively poor agreement between PFs (compared to the SF_6 and PF_{PSL} correlation) is attributed to IAA vapor interaction with system materials. As discussed in Section 5.3, the IAA was clearly permeating the mask and/or portions of the test system (e.g. the headform bladder), partly causing the in-mask background concentration to increase with time. The fact that in-mask background IAA concentration increased after performing a test with the mask sealed (see discussion in Section 5.3) indicates that IAA is permeating during the tests. When the mask is sealed or the leak rate is very low (with the 50 μm orifice), the quantity of IAA that permeates is relatively significant. Therefore, the apparent leakage into the mask is higher than actual leakage, and thus, the apparent low PF. Simply subtracting the IAA background concentration in the mask is not adequate to correct for the IAA that does not leak because IAA is permeating into the mask during that test. An estimate of the amount of IAA permeating into the mask during a test cannot be made accurately, thus it cannot be used to correct the measured in-mask IAA concentration. The masks and test system were frequently cleaned; however, it was not a sufficient condition to prevent permeation during a test.

When the PFs are relatively low, < 10,000, leakage into the mask was significantly greater than that which permeates the mask. Therefore, the bias of underestimating PFs was no longer observed. As the leakage into the mask was further increased (lower PFs) there was an

apparent underestimation of the IAA concentration within the mask. The underestimation of IAA within the mask is likely attributed to interactions with the interior surface of the mask and/or the test system (i.e., teflon line from breathing machine to the headform.) Any surface adsorption would reduce the IAA concentration within the mask and therefore the indicated PF would be artificially high.

These results indicate that vapor challenges that interact with the mask system materials, either by permeating the materials or adsorbing to surfaces, greatly affect measured PFs.

The PFs measured using the corn oil aerosol challenge and the photometer, as reported in Section 4.1, were compared to PFs measured using the SF_6 vapor challenge. The PFs for the corn oil/photometer and the SF_6 method were predicted for selected 0.72 μm PSL/LAS PFs, using the correlation equations given in Figure 10 and 15, as shown in Table 7.

Table 7. Predicted PFs for the Corn Oil Aerosol and Photometer Method and the SF_6 Vapor Method for Selected 0.72 μm PSL/LAS PFs

PF		
0.72 μm PSL/LAS	SF_6[(a)]	CO/Photometer[(a)]
500	520	630
2,000	2,510	2,320
8,000	9,990	10,400
32,000	39,700	46,600

(a) Predicted PF based on correlation equation with 0.72 μm PSL/LAS

A plot of the CO/Photometer vs. SF_6 PFs is shown in Figure 17. This figure illustrates that there is excellent agreement in PFs for the two methods, as the correlation line nearly coincides with the one-to-one line. The correlation equation is given by:

$$\log_{10} PF_{SF6} = 0.996 \times \log_{10} PF_{CO,\ Photometer} - 0.020;\ r^2 = 0.996$$

This correlation indicates that the corn oil aerosol and photometer method to measure PFs is an accurate estimator of PFs measured using an inert gas.

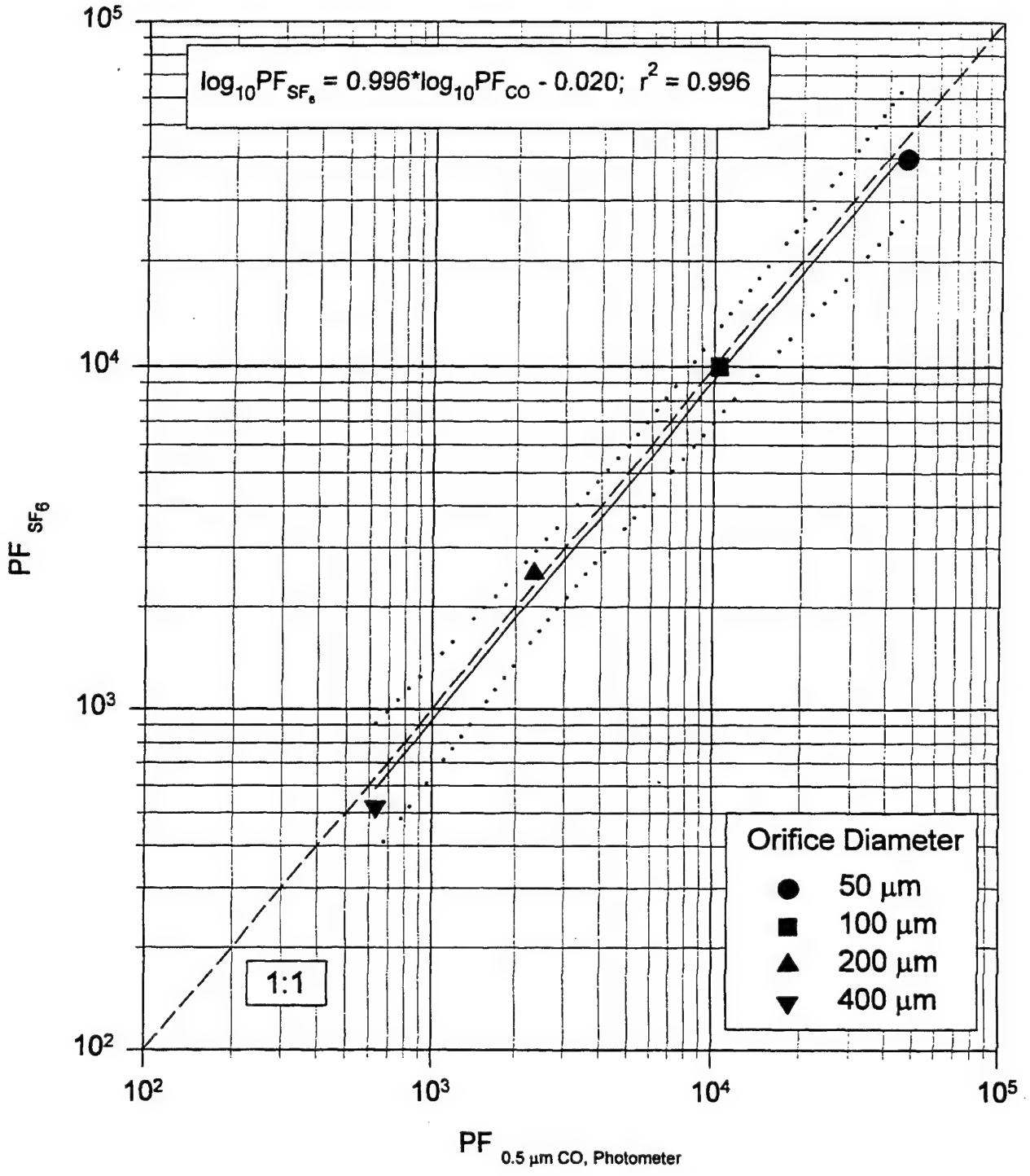

Figure 17. Correlation of PFs Measured Using SF_6 Vapor With Corn Oil Aerosol and Photometer

6.0 CONCLUSIONS

PFs were measured using aerosol challenges of 0.17, 0.72, and 2.0 μm PSL, 0.5 μm corn oil, and 5.0 μm silica powder using all or some of four aerosol sensing instruments: the Aerosizer™, LAS-X, M41, and laser photometer. PFs were measured for a mask affixed to a testhead with simulated breathing. Leakage into the mask was controlled using orifices with 50, 100, 200, and 400 μm diameter holes to produce PFs that typically ranged from 500 to 50,000. Typically, five PFs were measured for each combination of instrument/aerosol challenge for a given leak rate. A total of 350 PFs were measured.

In the second phase of the study, PFs were measured using the same basic test system and test procedures, except vapor challenges of IAA and SF_6 were used. IAA represented an organic vapor that may interact with mask materials and is used as a qualitative fit test challenge. SF_6 represented an inert gas that would not exhibit material interaction effects.

The particle size of the challenge aerosol was not found to significantly affect measured PF for aerosol challenges between 0.17 and 0.72 μm. Measured PFs began to increase significantly for a given leak condition for aerosol challenges >2 μm in diameter. Measured PFs were 2 to 4 times higher for the 2.0 μm PSL challenge and at least 5 times higher for the 5 μm aerosol challenge compared to PFs measured for the 0.17 to 0.72 μm aerosol challenges.

There is good agreement of PFs measured for the four aerosol sensing instruments. Best fit linear regressions of log-transformed PFs had correlation coefficients typically >0.95. The correlation equations were very close to the 1:1 line (a perfect correlation). For a specific challenge aerosol, the measured PF for the various instruments was almost always within a factor of 2, and over half the time within 50 percent. Although the PFs indicated by the instruments were statistically different in some comparisons, there was little practical difference in indicated PF for the instruments tested.

PFs measured using the corn oil aerosol challenge and the photometer method were in very good agreement with PFs measured using similar sized aerosol challenges and either the M41 or LAS-X. The measured PFs using the corn oil/photometer method were typically 20 to 50 percent higher than PFs measured using the corn oil/LAS-X or corn oil/M41 method.

Also, the PFs measured using the corn oil/photometer method were 10 to 50 percent higher than PFs measured using the 0.72 μm PSL/LAS-X method.

The PFs measured using the inert aerosol challenges in this study were in good agreement with PFs measured using Bg spores as a challenge and a bioassay method to assess penetration, performed using a similar test method for another study (Hofacre and Forney, 1995). The PFs for the various methods typically agreed with the Bg spore/bioassay method within a factor of 3 (the Bg spore PFs being higher than the inert aerosol PFs); the best agreement was with PFs measured using 2.0 μm PSL and the LAS-X. In that case, the measured PFs using the Bg spore/bioassay method were in nearly one-to-one agreement with the 2.0 μm PSL/LAS-X method. This finding was attributed to the particle size of the Bg spore being at least 1 μm. Note that it was shown that for a challenge aerosol with a diameter of 2 μm or greater, the measured PF was at least twice that of PFs measured with a submicron challenge aerosol.

It was also found that the PFs measured using the corn oil aerosol challenge and photometer method were consistently lower than the PFs measured using the Bg spore and bioassay method. Thus, the corn oil and photometer method represent a conservative estimator of the PF that would be measured with the Bg spore challenge. This finding is also attributed to the particle size of the Bg spore challenge being at least 1 μm, as described above.

PFs measured using an inert vapor challenge of SF_6 were consistent with PFs measured using a submicron aerosol challenge. Excellent agreement between PFs measured using the SF_6 challenge and 0.72 μm PSL and LAS-X was obtained. The measured PFs differed by only 25 percent over the range of PFs measured. In addition, the correlation derived for PFs measured using corn oil aerosol and photometer versus the PFs for the SF_6 vapor challenge was excellent. The measured PFs differed by less than 20 percent for the two methods.

In contrast, organic vapors that can permeate and/or adsorb onto mask materials and subsequently off-gas are not as useful challenges as an inert vapor. The measured PF using IAA challenge was not a good indicator of PF measured using the 0.72 μm aerosol challenge. At high (>20,000) PFs, the indicated IAA PF was significantly lower than that of the aerosol PF. This was attributed to IAA permeating the mask, which contributes to the apparent

leakage. At PFs lower than 20,000, the IAA PFs were higher than the aerosol PFs. The higher IAA PF was attributed to the IAA adsorbing to surfaces within the mask; therefore, decreasing the measured IAA concentration within the mask.

These results indicates that the use of a submicron aerosol challenge is a good indicator of the leakage that would be measured for an inert vapor. Specifically, the corn oil aerosol and photometer method to measure PFs is an accurate estimator of PFs measured using an inert vapor. It also indicates that interaction of the challenge vapor with the test system (i.e., mask, hoses, seals) must be considered, much like aerosol deposition, when interpreting measured PFs.

The foremost finding in this study is that the corn oil/photometer test method is a good indicator of PFs that would be experienced by masks challenged with similar sized aerosols, or inert vapors. Furthermore, use of the corn oil/photometer method to measure PFs is a conservative estimator of PFs that would be measured against a bioaerosol challenge with a particle size greater than 1 μm.

Blank

REFERENCES

Beck, Tyler, Personal communication with Kent Hofacre of Battelle regarding performance characteristics of the TSI Model 8587 photometer, February 23, 1996.

da Roza, Robert A. and Foiles, Linda G., "Gas Phase Leakage Testing of Protective Masks," Final report to U.S. Army AMCCOM, Aberdeen Proving Ground, MD, January 11, 1988.

Griffin, O.G. and Longson, D.J., The Hazard Due to Inward Leakage of Gas into a Full Facemask. Annals of Occupational Hygiene 13: 1147-151 (1970)

Hofacre, Kent C. and Forney, Traci L., Battelle Memorial Institute, Columbus, OH, "Test Method for Mask Protection Factor Measurements Using a Bioaerosol Simulant," presented at the Scientific Conference on Chemical and Biological Defense at ERDEC, Aberdeen Proving Grounds, MD, October 14-17, 1995.

Holton, Patricia M., Tackett, Denise Lynne, and Willeke, Klaus, University of Cincinnati, Cincinnati, OH, "Particle Size-Dependent Leakage and Losses of Aerosol in Respirators," *American Industrial Hygiene Association Journal*, 48(10): 848-854, October 1987.

Hounam, R.F., Morgan, D.J., O'Connor, D.T.,and Sherwood, R.J. The Evaluation of Protection Provided by Respirators. Annals of Occupational Hygiene 7: 353-364 (1964).

Kuhlman, Michael R. and Hofacre, Kent C., Battelle Memorial Institute, Columbus, OH, "Comparison of Several Aerosol Detectors as Indicators of Respirator Performance," presentation at the American Association for Aerosol Research 1990 Annual Meeting, June 18-21, 1990.

Liu, B.Y.H. and Lee, K.W. "Efficiency of Membrane and Nuclepore Filters for Submicrometer Aerosols." Environmental Science and Technology 10: 345-350 (1976).

Myers, Warren R., Kim, Hyunwook, and Kadrichu, Nani. "Effect of Particle Size on Respirator FaceSeal Leakage," USAFSAM-TE-90-34, Final Report (period June 1986-January 1990) prepared for USAF School of Aerospace Medicine, Brooks Air Force Base, TX, and National Institute for Occupational Safety and Health, Morgantown, WV, December 1990.

SAE Technical Report, "Dynamic Testing Systems for Oxygen Breathing Equipment," Aerospace Recommended Practice, Society of Automotive Engineers, Inc., issued April 1, 1969, revised April 1987.

Schwabe, P.H. The Measurement of Face-Seal Leakage of Respirators by Gases and Aerosols. International Symposium on Air Pollution Abatement Filtration and Respiratory Protection, Copenhagen, 1980.

APPENDIX A

REPRESENTATIVE PARTICLE SIZE DISTRIBUTIONS OF CHALLENGE AEROSOLS

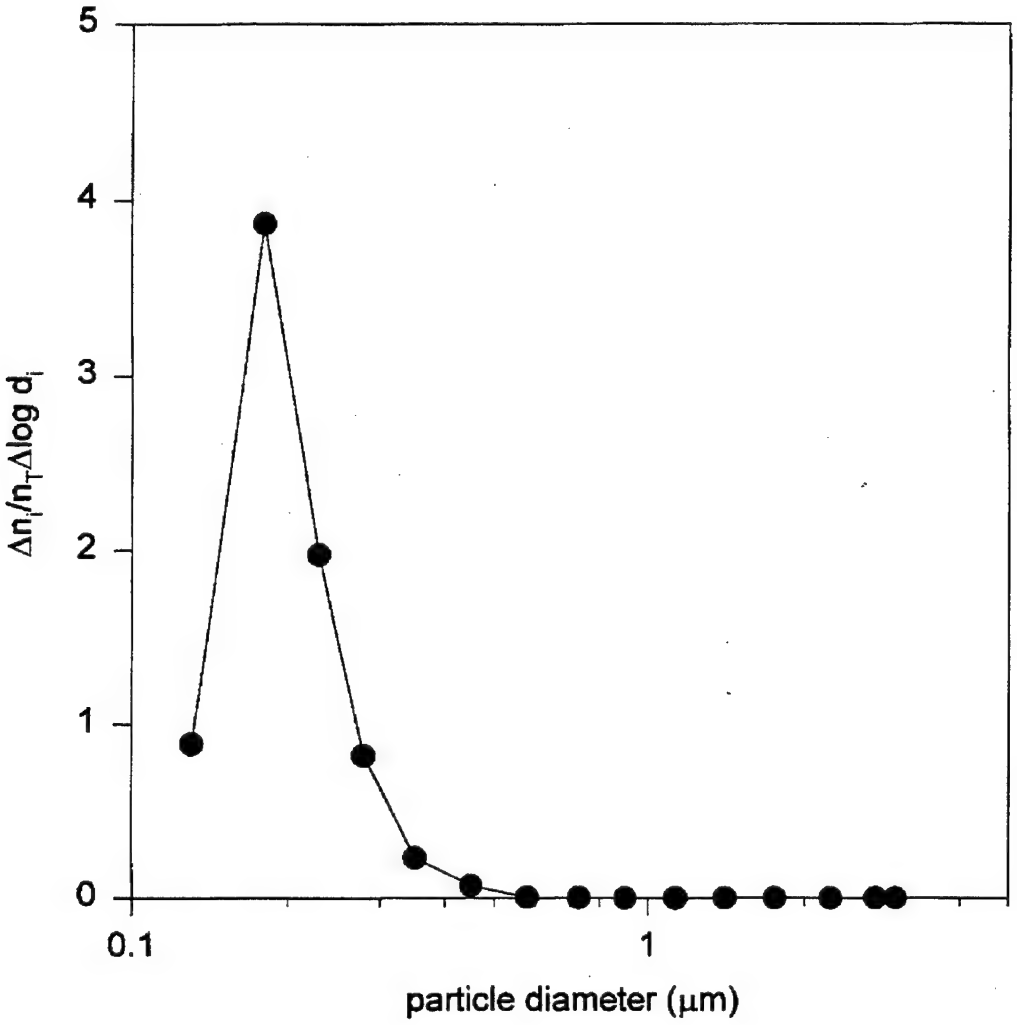

Figure A-1. 0.17 μm PSL Aerosol Number Distribution as Determined by the LAS-X

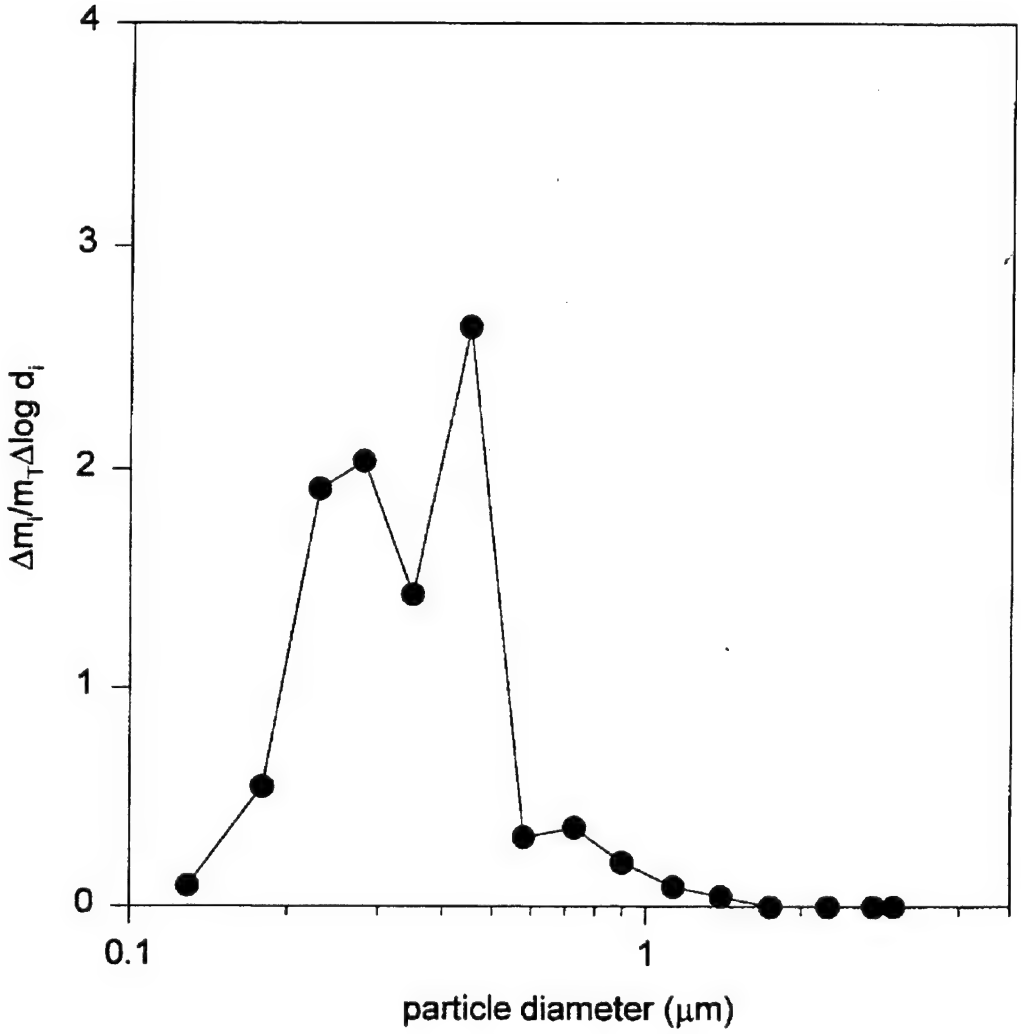

Figure A-2. 0.5 μm CO Aerosol Mass Distribution as Determined by the LAS-X

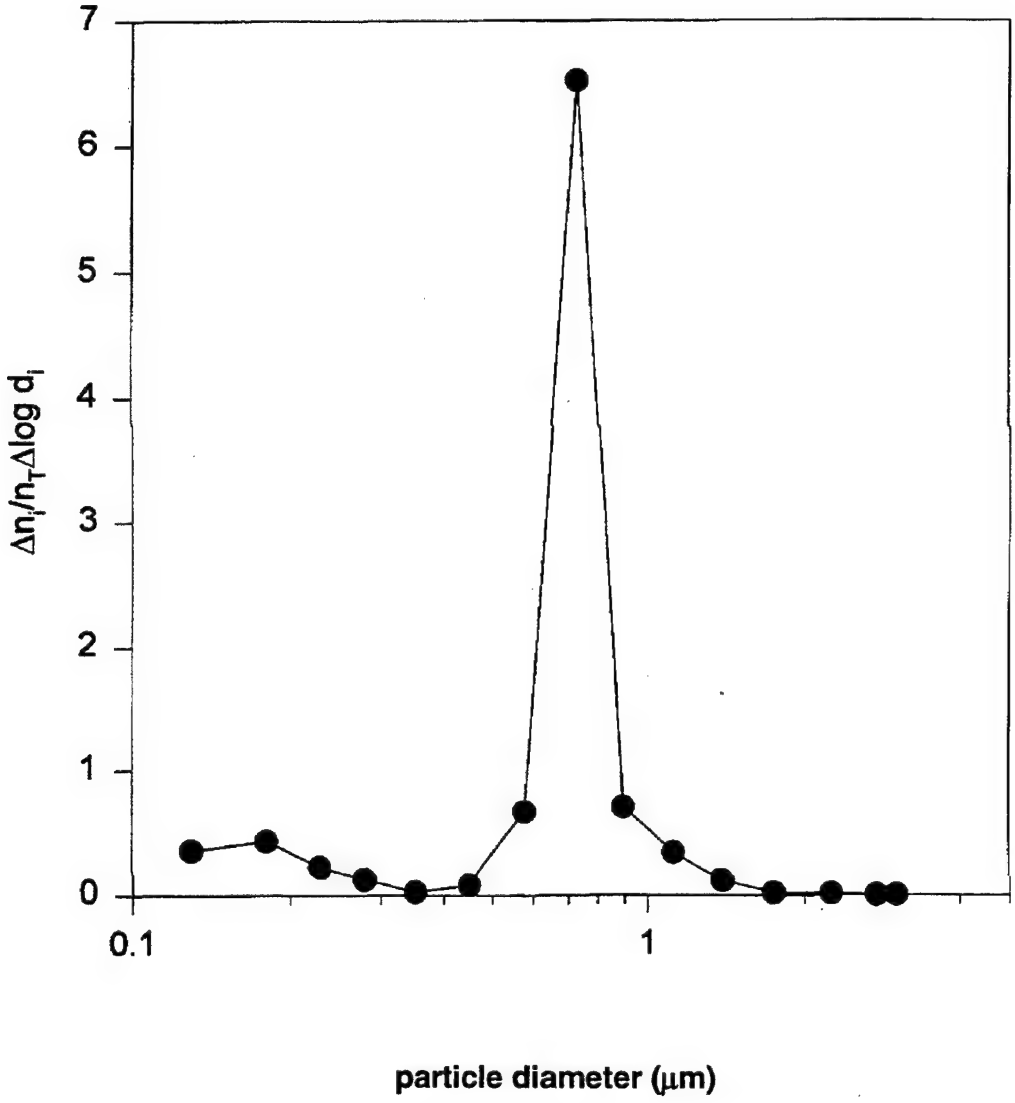

Figure A-3. 0.72 μm PSL Aerosol Number Distribution as Determined by the LAS-X

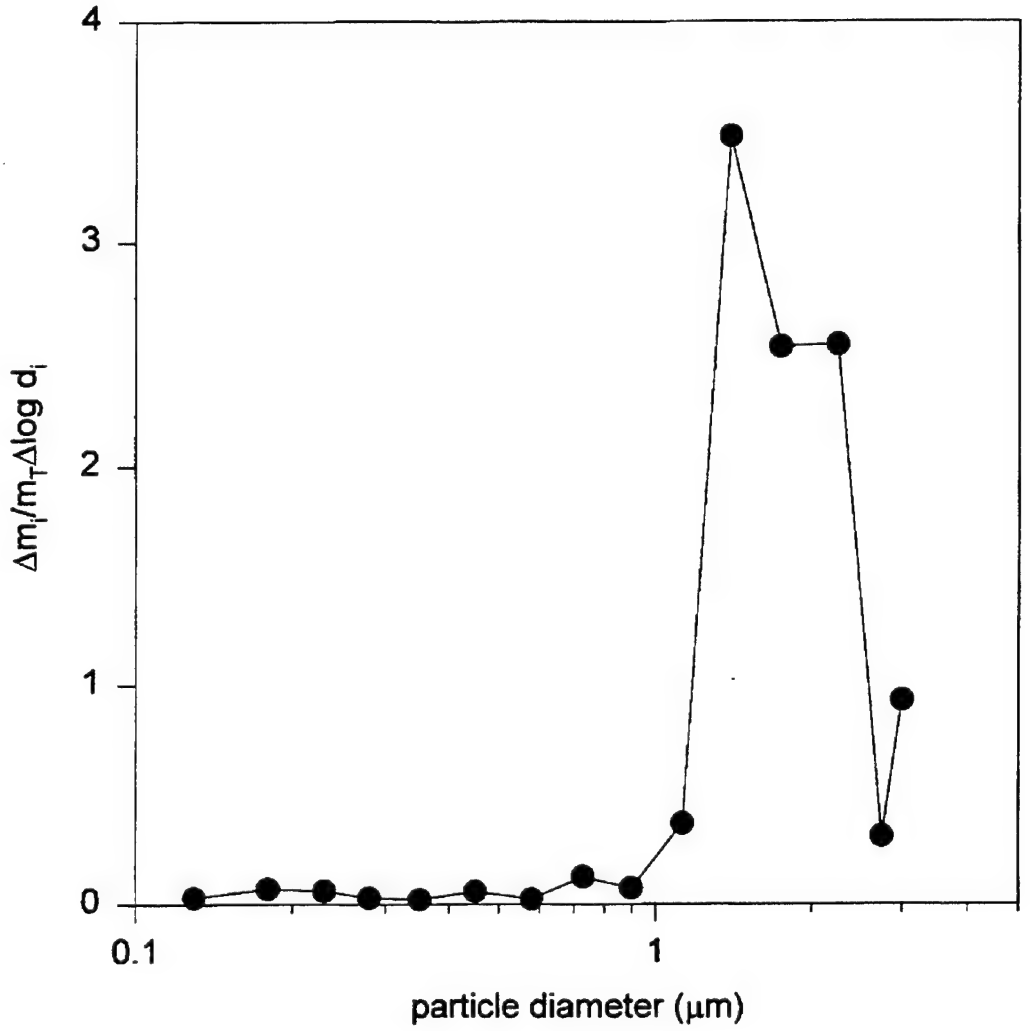

Figure A-4. 2.0 μm PSL Aerosol Mass Distribution as Determined by the LAS-X

Table A-1. Summary of Typical Aerosol Challenge Concentration

Challenge Aerosol	Range (particles/cc)
0.17 μm PSL	4500 - 6500
0.5 μm CO	1400 - 2000
0.72 μm PSL	1200 - 2200
2.04 μm PSL	40 - 70
5.0 μm Syloid	10 - 30

Blank

APPENDIX B

MEASURED PROTECTION FACTORS USING AEROSOL CHALLENGES

Table B-1. Summary of Measured PF Organized by Aerosol Sensing Device, Aerosol Challenge, and Leakage Condition

		LEAKRATE				
Device	Aerosol	Sealed	50 µm	100 µm	200 µm	400 µm
LAS-X	0.17 µm PSL	79300	26300	10900	1510	340
		94400	27200	8400	1120	390
		64300	39500	8100	1910	420
		64400	26800	10900	1450	430
		129000	31000	14400	1400	380
				6000		
LAS-X	0.5 µm corn oil	69200	55300	11400	1550	490
		73800	63700	10100	1870	500
		90200	31200	8030	1380	430
		107000	48700	10800	2040	420
		>200000	44300	7930	1570	450
LAS-X	0.72 µm PSL	126000	39600	11000	1650	480
		96900	32900	11200	1580	400
		174000	35600	10300	1580	380
		130000	28800	12000	2000	490
		>200000	51000	10300	1760	470
				8640		
LAS-X	2.0 µm PSL		115400	28000	3400	760
				24000	3000	770
				43000	3200	800
				20000	2700	790
				30000	3980	710
M41	0.17 µm PSL	>200000	86900	17800	1730	510
		>200000	80000	15800	1750	500
		189000	122000	13600	2000	550
		>200000	144000	16000	2010	520
		179000	126000	13200	2120	470
M41	0.5 µm corn oil	77800	39800	9860	1600	370
		98300	34300	8750	1870	450
		84900	42000	9600	1600	440
		70400	31000	9140	1930	410
		78900	40800	10100	1700	350
M41	0.72 µm PSL	>200000	54800	16300	2000	490
		>200000	71000	14400	1980	480
		>200000	80600	12900	1500	420
		>200000	76100	13800	1950	570
		>200000	89700	12600	1860	500

Table B-1. Summary of Measured PF Organized by Aerosol Sensing Device, Aerosol Challenge, and Leakage Condition (Continued)

		LEAKRATE				
Device	Aerosol	Sealed	50 µm	100 µm	200 µm	400 µm
Photometer	0.17 µm PSL	>4000	>4000	>4000	1480	480
		>4000	>4000	>4000	1780	370
				>4000	1400	400
				>7000	1480	340
					1500	400
Photometer	0.5 µm corn oil	>100000	44000	11800	2400	490
		>100000	77500	11300	2000	360
		>100000	54600	13100	1900	470
			91600	12200	2000	500
			42000	10100	1990	500
Photometer	0.72 µm PSL	>100000	57000	9130	1840	530
		>100000	26000	10400	1560	420
		>100000	29000	13000	1780	370
			56000	12300	2370	590
			48800	12500	2340	590
Photometer	2.0 µm PSL			>20000	3000	640
					2700	540
					3600	690
					2720	670
					2100	660
Aerosizer™	0.5 µm corn oil	>100000	25400	12000	2600	420
		>100000	37000	9500	1500	590
		>100000	41000	7700	1000	440
		>100000	33000	6400	1200	320
		>100000	34200	12300	2030	340
Aerosizer™	0.72 µm PSL	>100000	56000	9100	1590	430
		>100000	85700	11200	2400	600
		>100000	55000	12000	1890	640
			19100	13300	1500	390
			27600	7100	1800	370
Aerosizer™	2.0 µm PSL		79000	35400	3040	540
				29400	4000	970
				28000	4600	850
				17000	6400	940
				21000	3650	970
Aerosizer™	5.0 µm syloid					2800
						4850
						1060
						1810
						1800

Blank

APPENDIX C

COMPARISON OF PFs BY INSTRUMENT

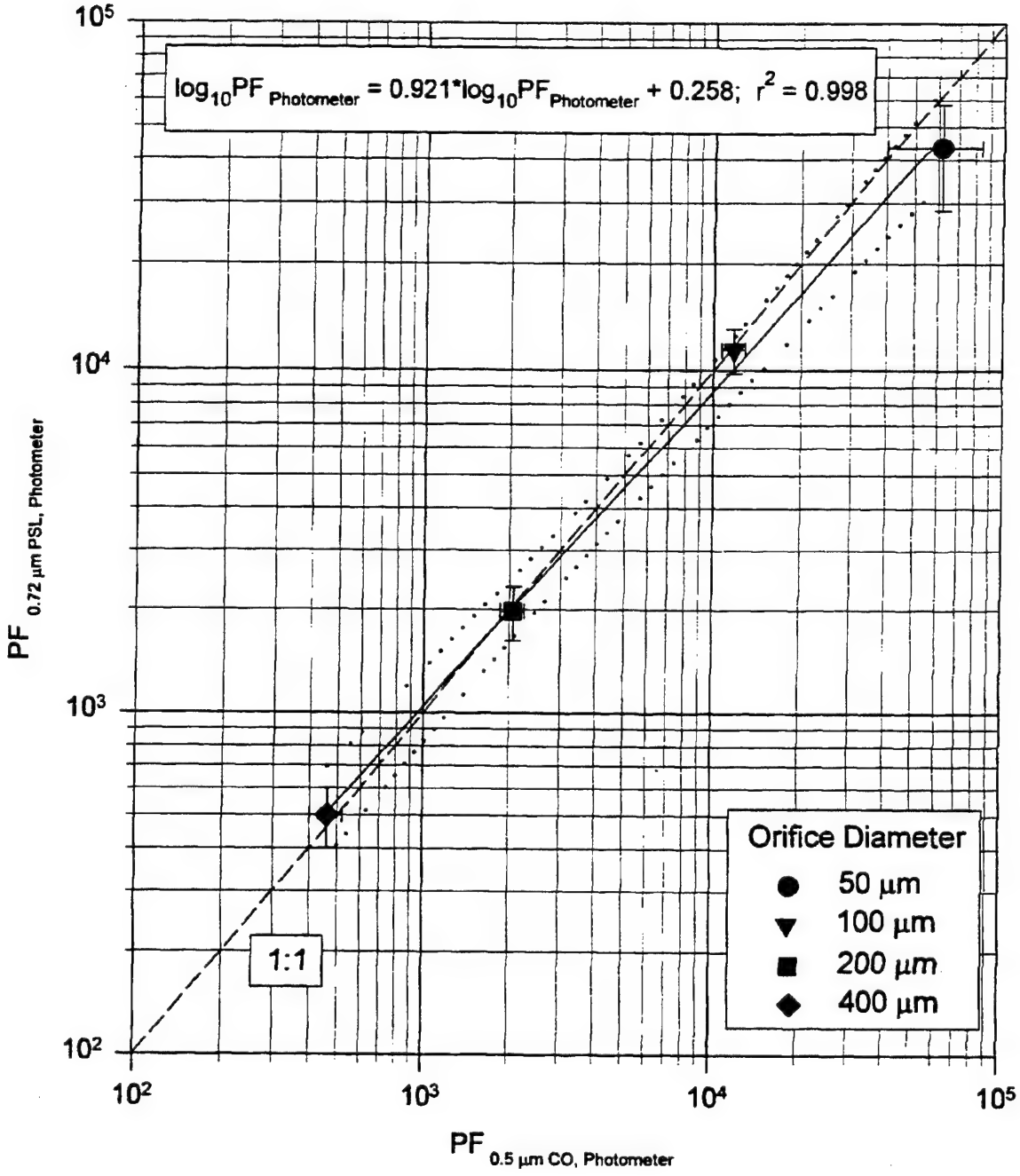

Figure C-1. Correlation of Measured PF Using the Photometer for a 0.72 µm PSL Aerosol Challenge Versus a 0.5 µm CO Aerosol Challenge

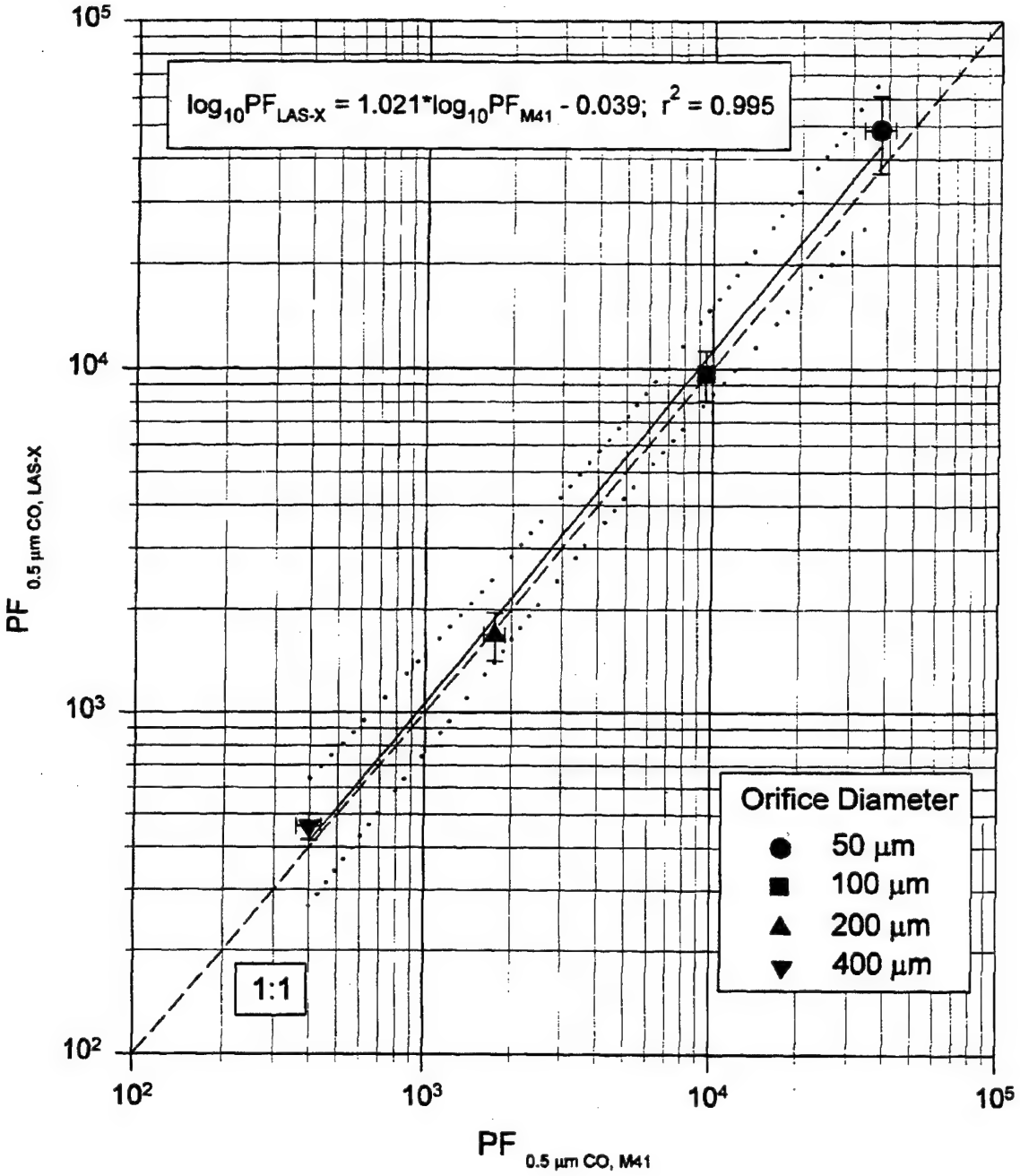

Figure C-2. Correlation of Measured PF Using the LAS-X Versus the M41 for a 0.5 µm CO Aerosol Challenge

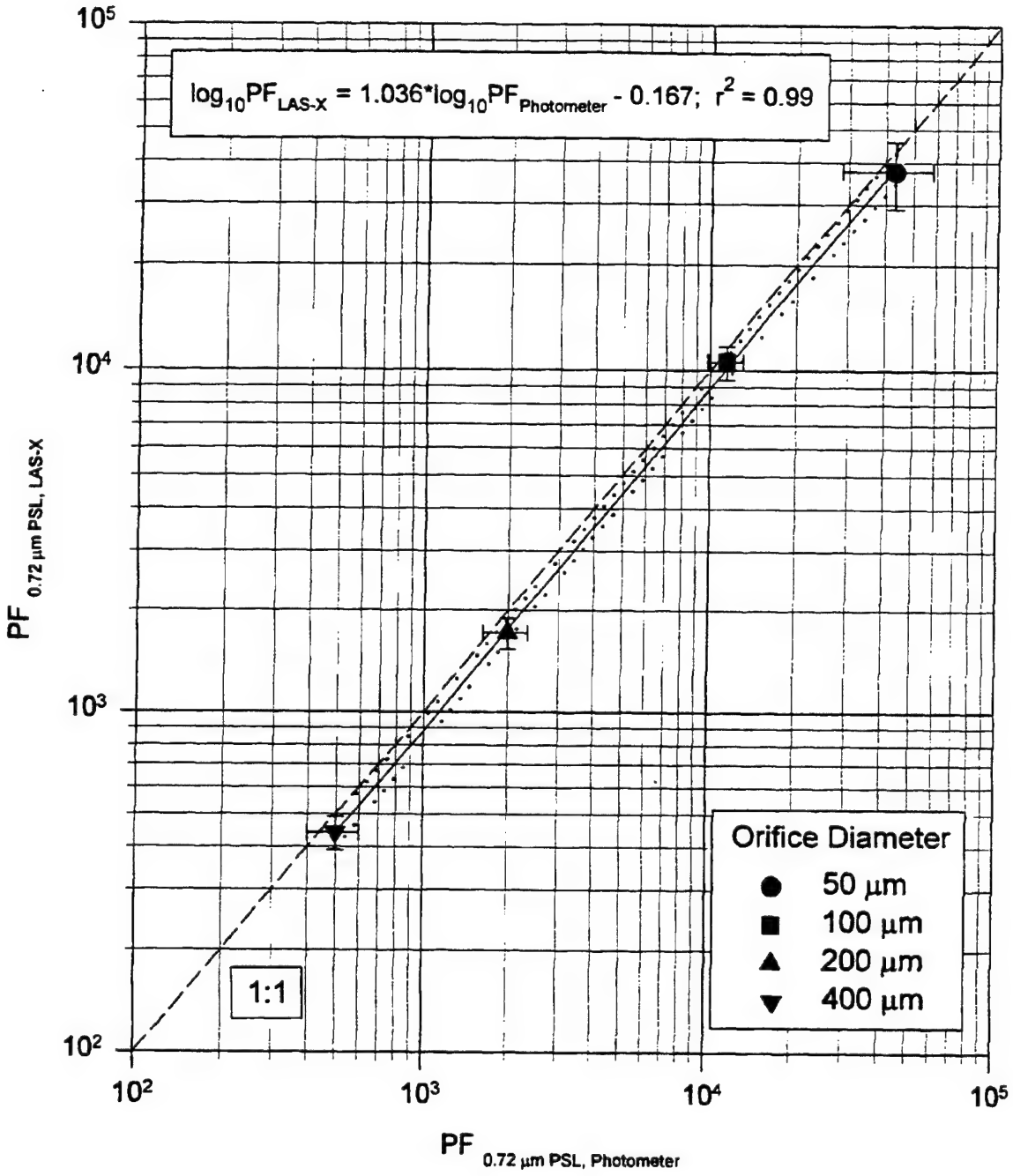

Figure C-3. Correlation of Measured PF Using the LAS-X Versus the Photometer for a 0.72 µm PSL Aerosol Challenge

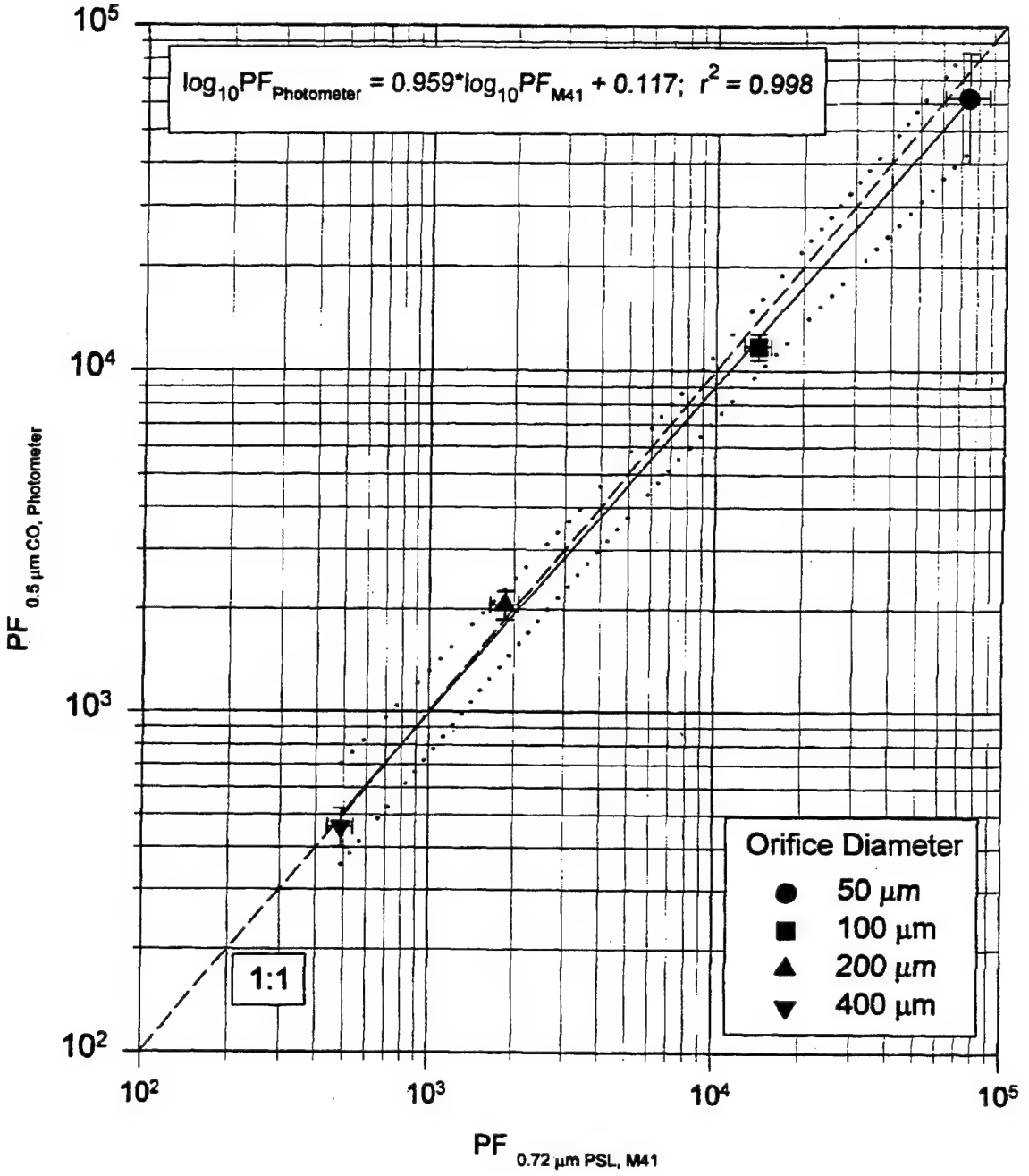

Figure C-4. Correlation of Measured PF Using the Photometer for a 0.5 µm CO Aerosol Challenge Versus the M41 for a 0.72 µm PSL Aerosol Challenge

Blank

APPENDIX D

COMPARISON OF PFs TO Bg SPORE PFs

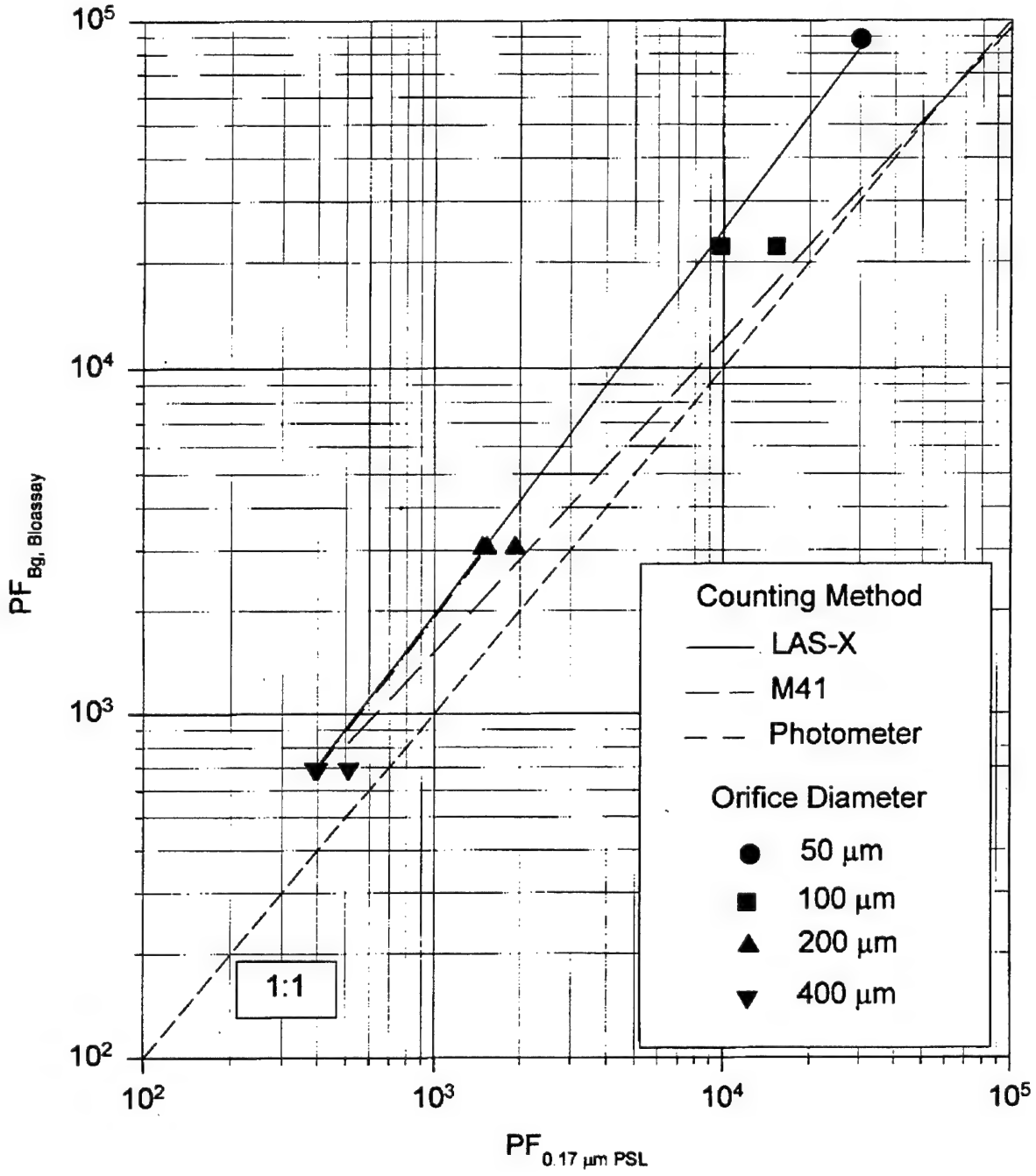

Figure D-1. Comparison of PFs Measured Using the Bioassay Counting Method and a Bg Spore Challenge to PFs Measured Using the LAS-X, M41, and Photometer and a 0.17 µm PSL Aerosol Challenge

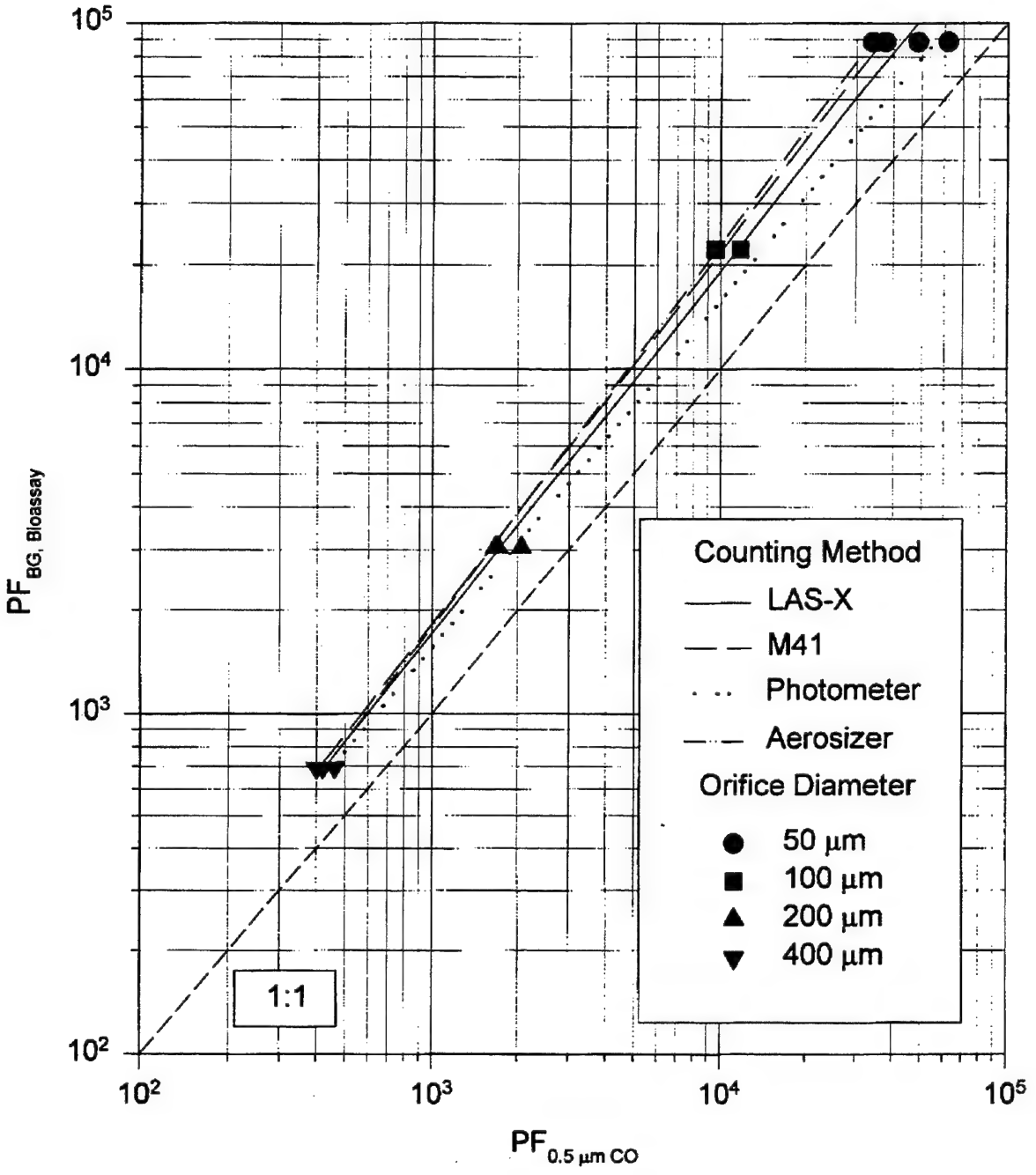

Figure D-2. Comparison of PFs Measured Using the Bioassay Counting Method and a Bg Spore Challenge to PFs Measured Using the LAS-X, M41, Photometer, and Aerosizer and a 0.5 µm CO Aerosol Challenge

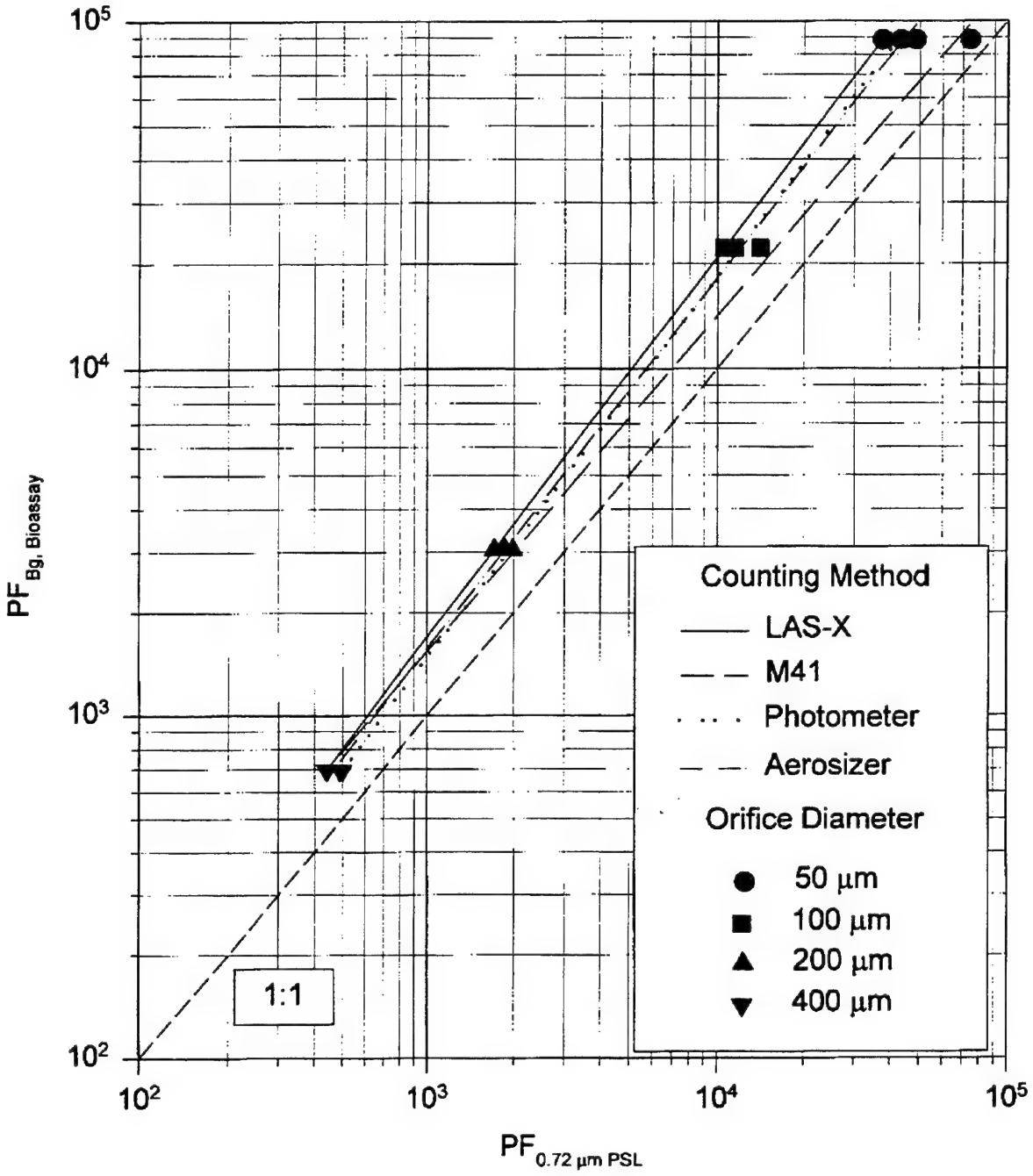

Figure D-3. Comparison of PFs Measured Using the Bioassay Counting Method and a Bg Spore Challenge to PFs Measured Using the LAS-X, M41, Photometer, and Aerosizer and a 0.72 µm PSL Aerosol Challenge

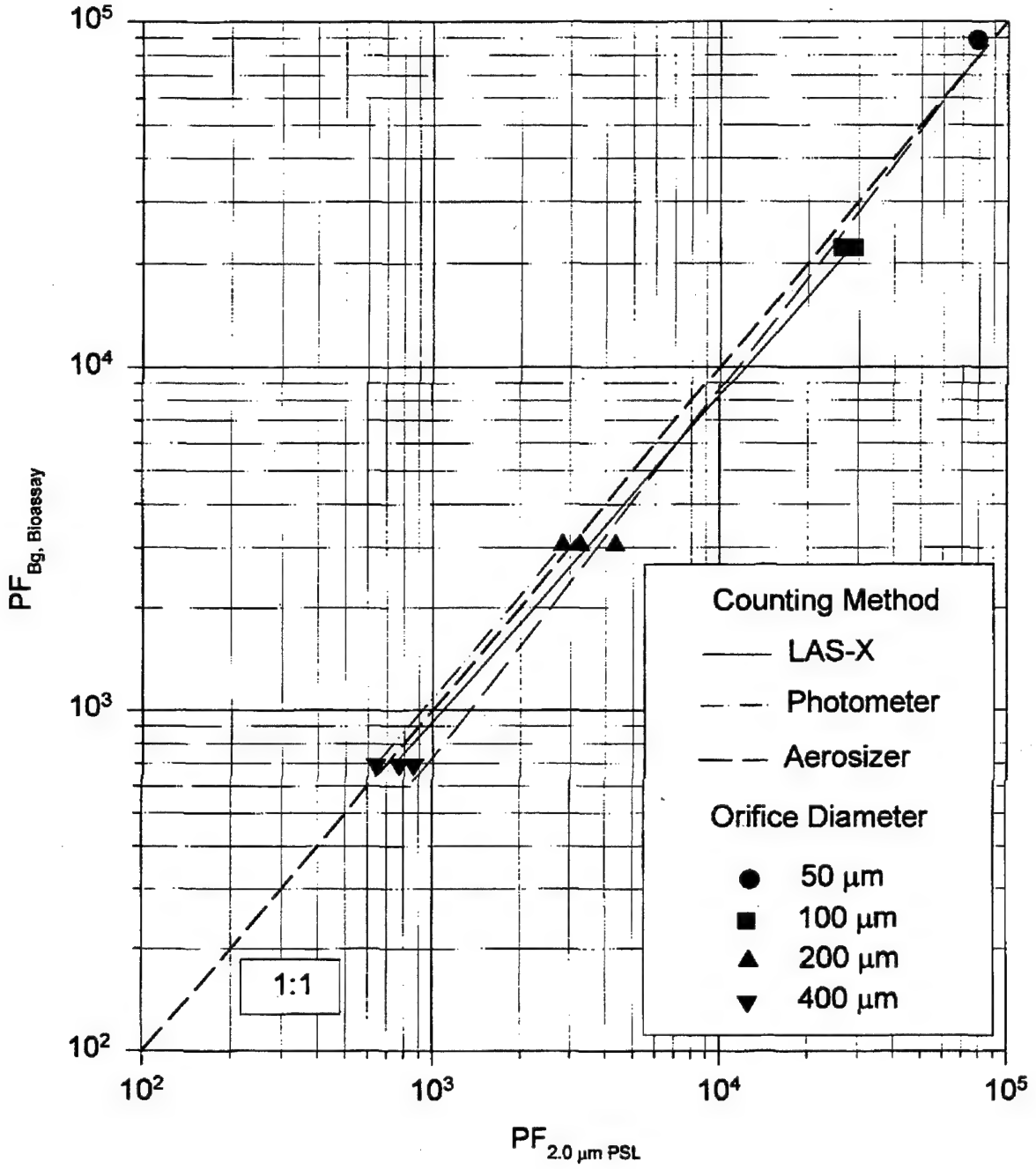

Figure D-4. Comparison of PFs Measured Using a Bioassay Counting Method and a Bg Spore Challenge to PFs Measured Using the LAS-X, Photometer, and Aerosizer and a 2.0 µm PSL Aerosol Challenge

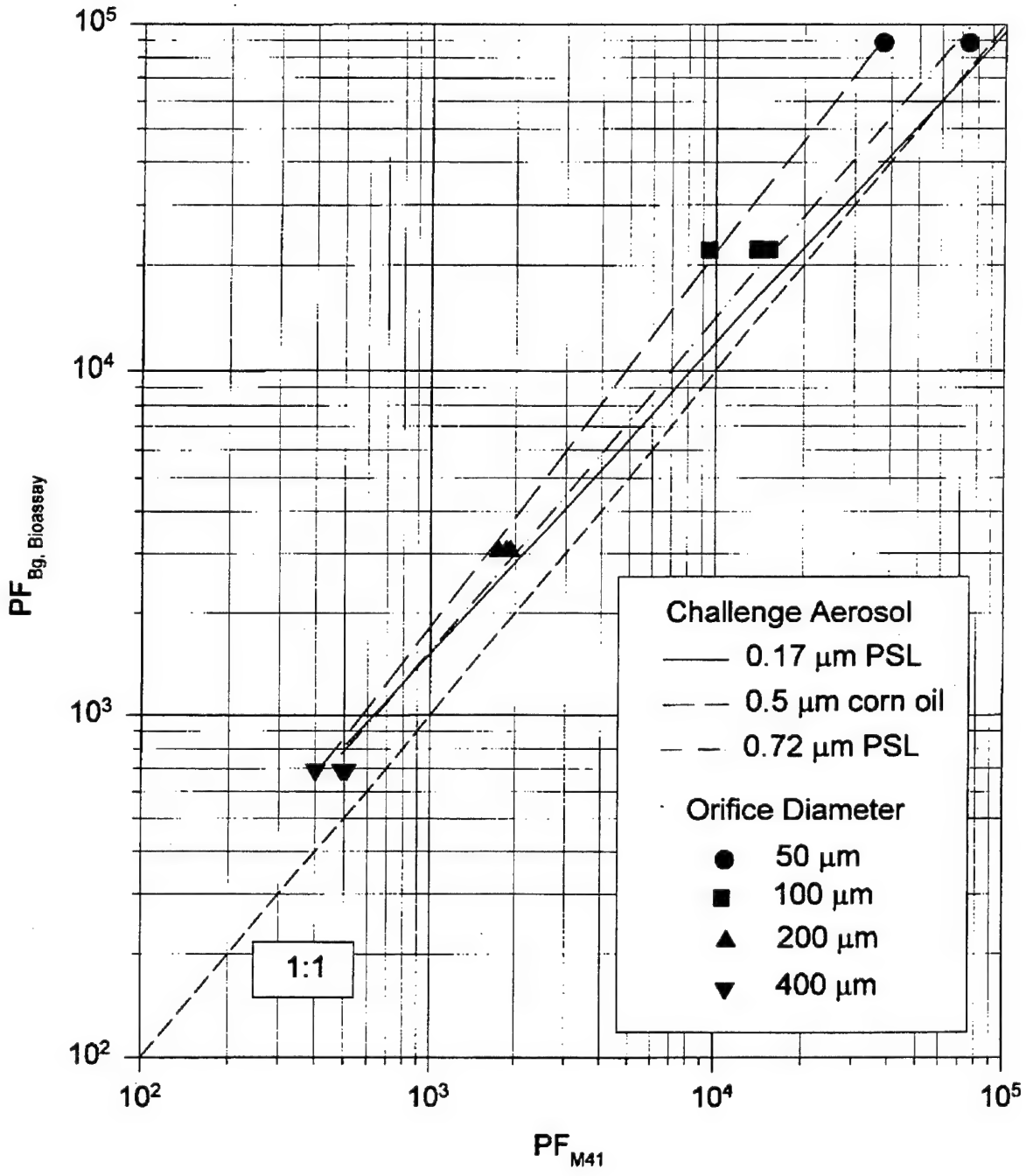

Figure D-5. Comparison of PFs Measured Using the Bioassay Counting Method and a Bg Spore Challenge to PFs Measured Using the M41 and 0.17 µm PSL, 0.5 µm CO, and 0.72 µm PSL Aerosol Challenges

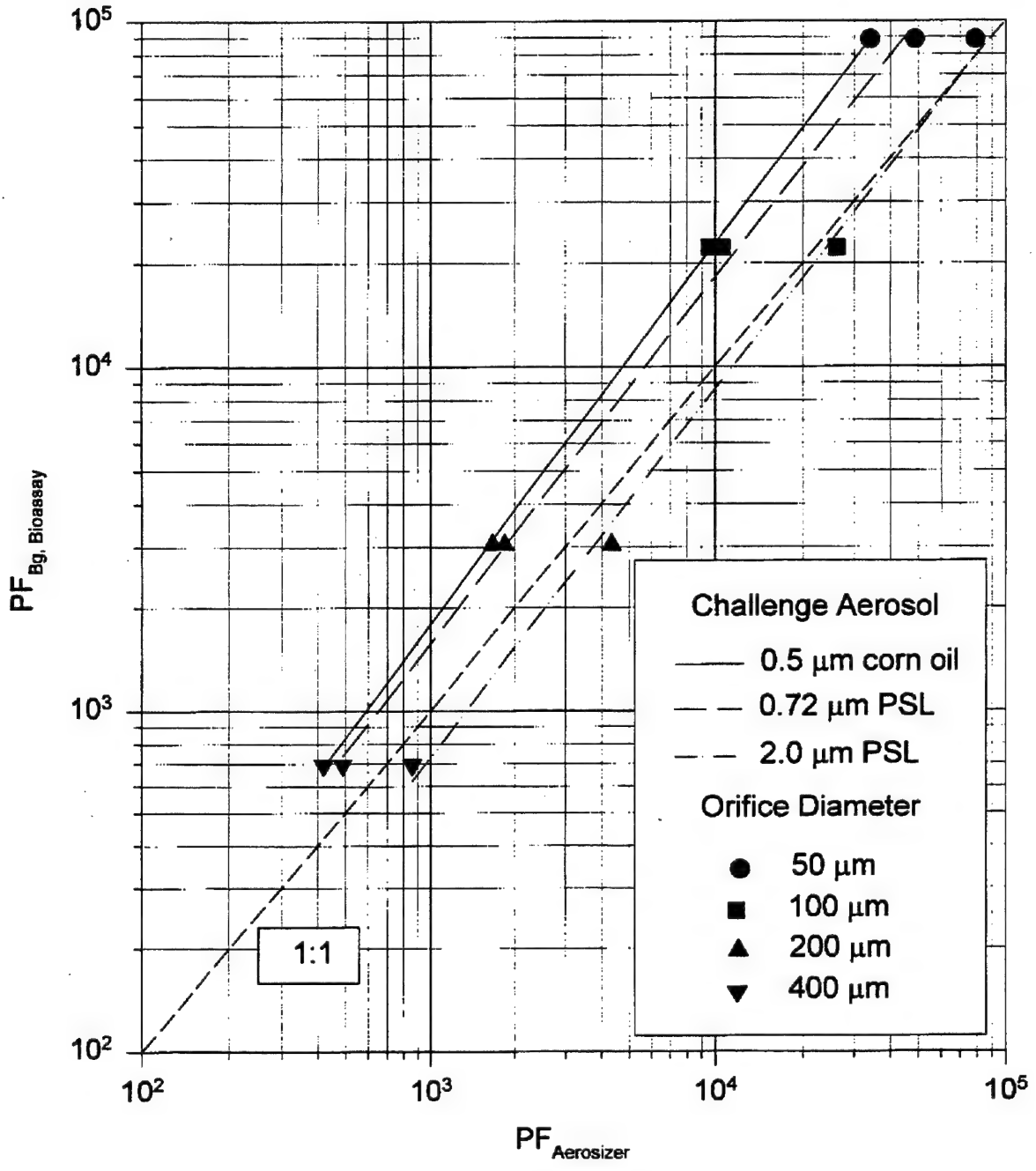

Figure D-6. Comparison of PFs Measured Using the Bioassay Counting Method and a Bg Spore Challenge to PFs Measured Using the Aerosizer and 0.5 µm CO, 0.72 µm PSL and 2.0 µm PSL Aerosol Challenges

Blank

APPENDIX E

MES PERMEATION TROUBLESHOOTING RESULTS

Preliminary Troubleshooting Results

PF measurements with a methyl salicylate (MeS) challenge were hindered due to penetration of MeS into the system. Prior to challenging the system with MeS, the mask was donned on the head form and sealed. A PF of greater than 50,000 was measured with the LAS-X using a 0.72 μm PSL challenge. This PF indicated a proper seal between the mask and head form interface. To ensure there were no leaks outside of the test chamber, the "throat" and breathing machine were exposed locally to 0.173 μm PSL. The LAS-X was used to monitor the in-mask concentration to determine whether leaks were present. No leaks were found.

With the mask sealed, an in-mask background was obtained prior to releasing MeS into the test system. MeS was not detected. A PF measurement was then performed with the mask sealed and an MeS challenge. The in-mask MeS concentration was 5 ng/L, with a challenge of approximately 450,000 ng/L, resulting in a PF of 90,000. A corresponding PF of >100,000 was measured with the LAS-X using a 0.72 μm challenge, and with the gas chromatograph using a sulfur hexaflouride (SF_6) challenge. Again, these high PFs indicated the mask was properly sealed to the headform.

The system was completely shut down for approximately 72 hours before another in-mask background sample was taken. This test was conducted to ensure there was no residual MeS in the system prior to performing the next PF measurement with MeS. This background indicated an MeS concentration of approximately 160 ng/L which far exceeded the amount of MeS seen in the mask while being challenged with MeS. A second background test was performed to verify the result. The system was allowed to flush for 1 hour prior to taking the sample, but the MeS concentration was still 170 ng/L. A blank was performed on the GC prior to each analysis demonstrated the GC was not contaminated with MeS prior to analyzing the samples.

Due to the high MeS backgrounds obtained, troubleshooting began to locate the point of permeation. Three possible sites of permeation were identified: (1) the hose connecting the filter canister and the mask, (2) the mask, and (3) the bladder of the headform, which is used to effect a seal with the mask.

The filter canister was placed directly on the mask to remove the hose as a possible source of penetration. It was noted that when the hose was removed (initially, an Aircrew Eye/Respiratory Protection [AERP] was used), a strong MeS odor was detected in the hose. The system was allowed to flush for 2 hours in this configuration and another background measurement was recorded. The MeS concentration was 220 ng/L.

The breathing machine was then removed from the system. A strong MeS odor was noted out of the polyethylene tubing to the breather and the "throat" of the headform. The fittings and sampling lines connected at the throat were rinsed with ethanol, air dried, and reconnected to the test system. A vacuum pump was connected to the test system and a constant flow of 25 lpm was pulled through the mask. The system was allowed to flush for 1 hour prior to collecting another background. This test eliminated the breathing machine, hose, and sampling lines as possible contamination sources. The MeS concentration was 230 ng/L, which indicated the system changes had no effect on the system background.

Although the MeS background concentration was considered high (a typical MeS background concentration was 200 ng/L and the challenge concentration was 400,000 ng/L), an attempt was made to measure PFs using the 200 and 400 μm orifices. It was predicted that the leakage of MeS into the mask would be at least twice that of the background, and therefore, PFs could be reliably measured. One PF test each with the 200 and 400 μm orifice did not yield useful results. In both tests, the background and in-mask MeS concentration were indistinguishable.

It was apparent that once MeS penetrated the system the entire system was contaminated. Therefore, the entire system was cleaned with a solvent flush and heat. When the mask was removed from the test head, a strong MeS smell was present in the mask. The headform and sampling lines were rinsed with ethanol and air dried. The

polyethylene tubing connecting the breathing machine and throat was replaced. A new mask was donned and sealed on the headform. The filter canister was moved to outside of the chamber. A breathing hose supplied by ERDEC was used to remotely connect the filter to the mask.

A PF of greater than 50,000, when challenged with aerosol, verified the mask/headform seal. A system background indicated the MeS background concentration was reduced 30 ng/L. A PF measurement with the sealed mask and an MeS challenge immediately followed the background. The in-mask concentration was 30 ng/L, indicating no leakage into the mask. A background test was performed 5 hours after the PF test to verify there was no permeation into the system. The breathing machine and pumps to sampling lines were operating the full 5 hours between the sealed test and the background. The subsequent MeS background concentration was 180 ng/L, indicating the system had been permeated with MeS. The polyethylene tube to the breathing simulator was detached and it was noted there was little to no MeS smell. Another PF measurement was performed with the MeS challenge and 100 μm orifice, which resulted in an in-mask concentration of 180 ng/L. Again, there was no measurable leakage into the mask.

To determine whether the MeS could be flushed from the system, the system operated overnight. This included the operation of the breathing machine and a 30 lpm flow of clean house air through the chamber. The MeS background sample was taken after the sampling pumps had flushed the sampling lines for 3 hours. The MeS background concentration was 568 ng/L. Active cleaning of the entire system would be needed to reduce the background concentration, which was not considered a practical approach. Therefore, the MeS background increased after the previous test and was not readily purged.

Portions of the test system were then isolated in an attempt to identify the source of contamination. First, a new mask was installed and the entire system background recorded. The background MeS concentration was 250 ng/L, indicating residual contamination in the system other than that of the mask. The breathing machine, throat fittings, and sampling lines were then isolated by connecting the filter canister directly to

the throat fittings. A significant background concentration of MeS was detected throughout all components of the system. It was therefore apparent that the site of MeS permeation could not be identified with the approach taken. A more systematic approach to identifying MeS permeation was developed and effected. A discussion of that approach and the results follow.

Isolation of MeS Permeation Problem

After challenging the mask with MeS (when the mask was sealed, PF > 50,000 using 0.72 μm aerosol challenge), a high MeS background concentration was measured in the mask; consequently, PFs could not be measured accurately in subsequent tests.

MeS Troubleshooting Results

The following represents a chronology of the results following efforts to isolate the site of MeS permeation and mitigate its effects. A summary of the results is also presented in Table 1.

1. The contaminated system was disassembled and all components were replaced or cleaned with an alcohol rinse. The stainless steel fittings from the "throat" of the headform and sampling lines were flushed with ethanol, air dried, and placed in an oven for 12 hours at 140°F to remove the MeS. The test head was rinsed with ethanol and air dried. The mask, filter canister, and hose were replaced with new components. The cylinder of the breathing machine was heated to thermally desorb any MeS contamination. The breathing machine was allowed to flush for 24 hours. The polyethylene tubing connecting the breathing machine to the "throat" was replaced.
2. The MeS background in the breathing simulator was measured to ensure it was clean. The system was set up to isolate the breathing machine and sampling lines. The resulting MeS concentration was 8 ng/L. Further heating and flushing of the breathing machine did not lower the MeS background concentration.

Table 1. Summary of MeS Background Concentration Within the Sealed Mask and Without a Challenge

Time (hrs)	Event	System Configuration	MeS Conc. (ng/L)	Notes
-19.25	Background	filter canister on mask second skin on mask	15	System cleaned, new mask and filter, breathing machine outside hood
0	In-mask	Unchanged	16	—
2.5	Background	Unchanged	32	Chamber flushed with 30 lpm clean house air and breathing machine, sampling lines flushed for 10 minutes prior to measuring background
5.5	Background	Unchanged	37	Chamber flushed with 30 lpm clean house air and breathing machine
5.75	In-mask	Unchanged	38	—
8.25	Background	Unchanged	63	Chamber flushed with 30 lpm clean house air and breathing machine, sampling lines flushed for 10 minutes prior to measuring background
23.75	Background	Unchanged	118	Chamber flushed with 30 lpm clean house air overnight, breathing machine shut down overnight, sampling lines flushed for 10 minutes prior to measuring background
25.75	Background	filter outside chamber	114	—
26.25	In-mask	Unchanged	111	—
30.25	Background	Unchanged	118	Chamber flushed with 30 lpm clean house air and breathing machine

3. The bladder on the test head was deflated and covered with duct tape. Using molding clay, a ridge was formed on the headform (this formed the mask interface and functionally replaced the bladder). This eliminated the bladder as a possible source of MeS penetration.
4. A new mask with a second skin made of butyl rubber was donned on the headform and sealed using additional molding clay.
5. The filter canister was placed directly onto the mask to eliminate the hose as a possible site of penetration.
6. The MeS background of the mask, headform, throat, and sampling lines was then measured. A pump was used to pull a constant flow of 25 lpm through the mask. This eliminated the breathing machine from the system. The resulting MeS concentration was 10 ng/L.
7. The breathing machine was removed from the hood. This eliminates the possibility of MeS leaking in through the breathing machine. The breathing machine was reconnected to the test system. A PF measurement was performed with the LAS-X and a 0.72 μm PSL challenge to ensure the mask was properly sealed. A PF of >100,000 resulted, indicating the mask was properly sealed. To ensure there were no leaks outside of the test system, the "throat" and breathing machine were locally exposed 0.173 μm PSL. The LAS-X was used to monitor in-mask concentration. No leaks were found.
8. Prior to releasing any MeS into the test system, a complete system background measurement was made. The resulting MeS concentration was 15 ng/L. Based on known MeS challenge concentrations that could be achieved (~400,000 ng/L) and expected PFs, this was adequately clean to allow accurate measurement of in-mask MeS concentrations during PF testing.
9. A PF measurement was performed with the mask sealed and using the MeS challenge. The resulting in-mask MeS concentration was 16 ng/L. When the background MeS concentration of 15 ng/L was subtracted, a PF of >100,000 resulted. This indicated no measurable leakage of MeS into the system.

10. MeS was flushed from the test chamber with 30 lpm of clean house air for 2 hours. The breathing machine was also in operation for 2 the hours after the MeS challenge. The background MeS concentration was 32 ng/L after the 2-hour system flush. This background concentration was double the background prior to releasing MeS into the test chamber.
11. Another MeS background measurement was performed 4 hours after the initial MeS challenge exposure. The MeS concentration was 37 ng/L. This indicated no significant increase between the 2-hour and 4-hour background MeS concentrations.
12. Since the background MeS concentration was still relatively low, another PF test was performed with the mask sealed and with the MeS challenge. The resulting in mask MeS concentration was 38 ng/L. When the background MeS concentration of 37 ng/L was subtracted, a PF of >100,000 resulted. This indicated no measurable leakage of MeS into the system.
13. Again, MeS was flushed from the system with 30 lpm of clean house air for 2 hours. The breathing machine was also in operation for 2 hours after the MeS challenge. The background MeS concentration after the 2 hours was 63 ng/L. This background concentration was approximately double the background prior to the second MeS exposure. The breathing machine was then turned off. Dilution air continued to flush the system.
14. Another MeS background was taken 17 hours after the second exposure to MeS. The MeS concentration was 118 ng/L, indicating large penetration into the mask. It was concluded MeS was penetrating the mask.
15. For completeness, the filter canister was removed from the mask and the hose inserted into the system. The filter was mounted outside of the test chamber. The hose connections were locally exposed to high concentrations of 0.173 μm PSL to determine if there was leakage. No leaks were located. The background MeS concentration in this configuration was 114 ng/L. This was consistent with the background taken without the hose in place.

16. With the mask sealed, a PF test was conducted using the MeS challenge. The resulting in-mask MeS concentration was 111 ng/L. This concentration could not be differentiated from the background concentration of 114 ng/L. The PF was >100,000 indicating no leakage of MeS into the system.
17. The test system was allowed to flush for 3 hours (breathing machine and dilution air) and the in-mask MeS background concentration was measured again. The MeS concentration was 118 ng/L. This is comparable to the 114 ng/L background prior to the third exposure to MeS. However, based on previous challenge concentrations and expected PFs, this background was too large to allow measurement of in-mask MeS concentrations during PF testing. This concluded PF measurements using the MeS challenge.

Conclusions

The above test approach was designed assuming there were three possible sites of MeS penetration into the system. These sites were: (1) the hose which connects the filter canister and the mask, (2) the mask facepiece, and (3) the bladder of the headform. The test results indicated that MeS was penetrating through the mask facepiece. (It should be noted that MeS permeation of the molding clay used to seal the mask to the headform cannot be discounted. However, MeS would have to permeate through an estimated 2.5 cm thick clay barrier before breaking through to the inside of the mask. Also, very little surface area is associated with the clay barrier.) Testing also demonstrated the system did not purge rapidly of MeS, and therefore active cleaning of the system would be needed to reduce background concentrations. It was concluded that MeS was not a practical challenge for PF measurement testing.